

Generalized R^2 Measures for a Mixture of Bivariate Linear Dependences

Jingyi Jessica Li^{1,4}, Xin Tong², and Peter J. Bickel³

¹Department of Statistics, University of California, Los Angeles, CA

²Department of Data Sciences and Operations, Marshall School of Business, University of Southern California, Los Angeles, CA

³Department of Statistics, University of California, Berkeley, CA

⁴To whom correspondence should be addressed. Email: jli@stat.ucla.edu

Abstract

Motivated by the pressing needs for capturing complex but interpretable variable relationships in scientific research, here we develop new mathematical foundation and statistical methodologies to generalize the squared Pearson correlation, i.e., the R^2 , to capture a mixture of linear dependences between two real-valued random variables. We define the population and sample generalized R^2 measures under the supervised and unsupervised scenarios, and we derive the asymptotic distributions of the sample measures to enable computationally efficient statistical inference of the population measures. To compute the sample generalized R^2 measure under the unsupervised scenario, we develop a K -lines clustering algorithm and investigate its connection to gradient descent and expectation-maximization algorithms. Our simulation results provide additional numerical verification of the theoretical results. Two real data genomic applications demonstrate the effectiveness of the generalized R^2 measures in capturing interpretable gene-gene relationships that are likely missed by existing association measures. The estimation and inference procedures are implemented in an R package `gR2`.

Keywords: generalized R square, dependence measures, non-functional relationship, asymptotic distribution, statistical inference, K -lines clustering

1. INTRODUCTION

The Pearson correlation coefficient is the most widely used similarity measure to describe the relationship between two random variables $X, Y \in \mathbb{R}$. The *population Pearson correlation coefficient*, often referred to as the *population Pearson correlation* or the *population correlation*, is defined as

$$\rho := \frac{\text{cov}(X, Y)}{\sqrt{\text{var}(X)}\sqrt{\text{var}(Y)}} \in [-1, 1], \quad (1)$$

where $\text{cov}(X, Y) := \mathbb{E}[(X - \mathbb{E}X)(Y - \mathbb{E}Y)]$, $\text{var}(X) := \mathbb{E}[(X - \mathbb{E}X)^2]$, and $\text{var}(Y) := \mathbb{E}[(Y - \mathbb{E}Y)^2]$ denote the covariance between X and Y , the variance of X , and the variance of Y , respectively. We say that X and Y are *uncorrelated* if $\rho = 0$ and *linearly dependent* if $\rho \neq 0$. Specifically, $\rho = 1$ or -1 indicates a perfect linear relationship with a positive or negative slope between X and Y . The *sample Pearson correlation coefficient*, often referred to as the *sample Pearson correlation* or the *sample correlation*, is defined based on a sample $(X_1, Y_1), \dots, (X_n, Y_n)$, usually assumed to be identically and independently distributed (i.i.d.) from the joint distribution of (X, Y) :

$$R := \frac{\sum_{i=1}^n (X_i - \bar{X})(Y_i - \bar{Y})}{\sqrt{\sum_{i=1}^n (X_i - \bar{X})^2} \sqrt{\sum_{i=1}^n (Y_i - \bar{Y})^2}}, \quad (2)$$

where $\bar{X} := \frac{1}{n} \sum_{i=1}^n X_i$ and $\bar{Y} := \frac{1}{n} \sum_{i=1}^n Y_i$. R is a plug-in estimator of ρ , because $\widehat{\text{cov}}(X, Y) = \frac{1}{n-1} \sum_{i=1}^n (X_i - \bar{X})(Y_i - \bar{Y})$, $\widehat{\text{var}}(X) = \frac{1}{n-1} \sum_{i=1}^n (X_i - \bar{X})^2$, and $\widehat{\text{var}}(Y) = \frac{1}{n-1} \sum_{i=1}^n (Y_i - \bar{Y})^2$ are unbiased estimators of $\text{cov}(X, Y)$, $\text{var}(X)$ and $\text{var}(Y)$, respectively.

When $(X_1, Y_1), \dots, (X_n, Y_n)$ is an independently and identically distributed (i.i.d.) sample, the asymptotic distribution of R has been derived under the condition that the bivariate distribution of (X, Y) has finite fourth moments. The asymptotic distribution has mean ρ and variance that depends on the (up to the fourth) moments of the distribution of (X, Y) (Ferguson, 1996; Lehmann, 2004). In the special case where (X, Y) follows a bivariate Gaussian distribution, the asymptotic variance of $\sqrt{n}(R - \rho)$ has the simple form of $(1 - \rho^2)^2$. Using the variance-stabilizing transformation, one can derive the Fisher's z -transformation (Fisher, 1915):

$$z := \frac{1}{2} \log \frac{1 + R}{1 - R}, \quad (3)$$

which is the test statistic for testing the null hypothesis $H_0 : \rho = \rho_0$ given a fixed constant $\rho_0 \in [0, 1]$. Under H_0 and when n is large, the distribution of $\sqrt{n} \left(z - \frac{1}{2} \log \frac{1 + \rho_0}{1 - \rho_0} \right)$ is approximately $\mathcal{N}(0, 1)$,

i.e., the standard Gaussian distribution. This test is widely used for statistical inference of ρ . The most common null hypothesis is $H_0 : \rho = 0$; in other words, practitioners are often interested in whether X and Y have a non-zero population correlation, a phenomenon we refer to as *linear dependence* in the following text.

In many applications, such as gene expression analysis in bioinformatic research, the linear dependence of two random variables of interest, e.g., the expression levels of two genes, is often dependent upon another hidden discrete random variable, e.g., the experimental condition or the cell state. In a motivating example, we observe a phenomenon from public gene expression data of *Arabidopsis thaliana* (Table A1), a widely-used plant model organism, that many genes exhibit different linear dependences between two tissue types: root and shoot. Fig. 1A shows the five genes that encode five isoforms of flavin-monooxygenase (FMO), a key enzyme in the biosynthesis of aliphatic glucosinolates (active compounds in *Arabidopsis thaliana*'s responses to tissue damages) (Li et al., 2008; Kim et al., 2012). Multiple pairs of those five FMO genes exhibit different linear dependences between root and shoot tissues. For example, in the second panel of the second row in Fig. 1A, *FMO GS-OX2* and *FMO GS-OX5* show a positive correlation in shoot tissues (blue dots) but a negative correlation in root tissues (red circles).

In an idealistic and extreme scenario (Fig. 1B), suppose that two real-valued random variables X and Y represent the expression levels of two genes. If X and Y have a positive correlation ρ in the shoot tissue but a negative correlation $-\rho$ in the root tissue, and that the two tissues are expected to have an equal representation in a study, then X and Y have a zero population Pearson correlation. Real scenarios are not in such an extreme case, but many of them show that two real-valued random variables exhibit a mixture relationship composed of more than one linear dependences (Li, 2002). Under the scenarios where ‘‘Simpson’s Paradox’’ occurs (Simpson, 1951; Pearson et al., 1899; Yule, 1903; Blyth, 1972), i.e., the overall correlation and the conditional correlations have opposite signs, the Pearson correlation may be a misleading measure for capturing the dependent relationship between two real-valued random variables, since the Pearson correlation specifically looks for a single linear dependence.

In the literature of scalar-valued association measures, also known as dependence measures, multiple measures have been developed to capture dependent relationships that are more general than

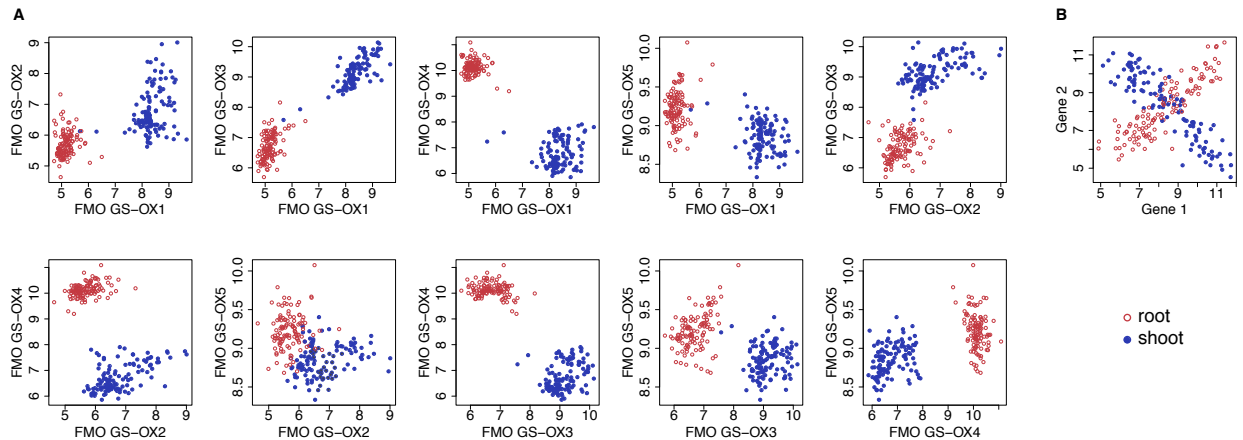


Figure 1: Motivating examples from gene expression analysis. **A**: Expression levels of five *Arabidopsis thaliana* genes (FMO GS-OX1, FMO GX-OX2, FMO GS-OX3, FMO GS-OX4, and FMO GS-OX5) in 232 public microarray datasets (Table A1 in the Appendix). **B**: A simulated toy example showing a gene-gene relationship as a mixture of two linear dependences, with a zero population correlation. The red circles and blue dots indicate the data from root and shoot tissues, respectively.

the linear dependence between two real-valued random variables. For monotone relationships, the most commonly-used measures are the two rank correlation coefficients: the Spearman’s rank correlation (Spearman, 1904) and the Kendall’s τ (Kendall, 1938). Regarding functional relationships that are more general than monotone ones, there exist measures such as the (Hirschfeld-Gebelein-Rényi) maximal correlation efficient (Hirschfeld, 1935; Gebelein, 1941; Rényi, 1959), the measures based on nonparametric estimation of correlation curves (Bjerve and Doksum, 1993) or principal curves (Delicado and Smrekar, 2009), a pair of generalized measures of correlation (GMC) that deals with asymmetries in explained variances, and linear or nonlinear relations between random variables (Zheng et al., 2012), the G^2 statistic derived from a regularized likelihood ratio test for piecewise-linear relationships (Wang et al., 2017), and gene co-expression measures for detecting local monotone patterns using count statistics (Wang et al., 2014). Furthermore, there is a large class of measures for capturing general dependence, as they give non-zero values to any pairs of non-independent random variables. Example measures include the maximal correlation coefficient, the Hoeffding’s D (Hoeffding, 1948), the mutual information (Shannon et al., 1951; Kraskov et al.,

2004; Cover and Thomas, 2012), kernel-based measures such as the Hilbert-Schmidt Independence Criterion (HSIC) (Gretton et al., 2005), the distance correlation (Székely et al., 2007, 2009), the maximal information coefficient (Reshef et al., 2011), and the Heller-Heller-Gorfine (HHG) association test statistic based on ranks of distances (Heller et al., 2012). It is worth noting that the Hoeffding’s D , the mutual information, the HSIC, the distance correlation, and the HHG test statistic are not restricted to comparing real-valued random variables, and the first four measures have the range $[0, \infty)$ as opposed to having absolute values no greater than one. Researchers have conducted comprehensive simulation studies to compare the statistical power of all those measures for various dependent relationships, i.e., the alternative hypotheses, with the null hypothesis as the independent relationship (Simon and Tibshirani, 2014; Gorfine et al., 2012).

Here we categorize the above existing measures into two types: the first type of measures were designed to describe functional (i.e., one-to-one) relationships, such as the Pearson correlation for linear relationships and the Spearman correlation for monotone relationships, between two real-valued random variables; the second type of measures, such as the maximal correlation, the mutual information, and the Hoeffding’s D , were developed to capture any deviation from an independent relationship. Both types have relative advantages and limitations. The first type of measures are generally interpretable but cannot capture non-functional (i.e., not one-to-one) relationships that are widespread in the real world, while the second type of measures, though being versatile and having desirable theoretic properties, do not convey an easy interpretation of their captured relationships to practitioners. In fact, as our motivating examples have shown (Fig. 1), there are widespread relationships that are decomposable into a small number of linear dependences. As the simplest and most interpretable relationship, linear dependence is often used to approximate general monotone relationships. Hence, a mixture of a small number of linear dependences is interpretable and often of great interest in scientific research. For example in cancer biology, if researchers observe that one gene positively regulates an important cancer gene in one cancer subtype but exhibits negative regulatory effects in another subtype, they may design different treatment strategies for the two cancer subtypes. In general, a mixture of linear dependences is often missed by the first type of measures and becomes indistinguishable from other “less interpretable” dependences by the second type of measures.

Therefore, a new measure is needed to capture this special type of non-functional relationships—a mixture of linear dependences. Although estimating a mixture of linear models has been a topic of wide interest in fields including statistics, economics, social sciences and machine learning for over 40 years (Quandt and Ramsey, 1978; De Veaux, 1989; Jacobs et al., 1991; Jones and McLachlan, 1992; Wedel and DeSarbo, 1994; Turner, 2000; Hawkins et al., 2001; Hurn et al., 2003; Leisch, 2008; Benaglia et al., 2009; Scharl et al., 2009), most existing studies have only focused on model parameter estimation and inference. In addition, there are algorithmic developments, such as Murtaph and Raftery (1984), which provides a stepwise clustering algorithm that considers both contiguity and linearity.

In this work we propose generalized R^2 measures, for which the squared Pearson correlation is a special case, to capture a mixture of linear dependences between two random variables. In Section 2, we define these measures, including their population and sample versions, under the supervised and unsupervised scenarios. We also introduce a K -lines clustering algorithm for the unsupervised scenario. In Section 3, we derive the asymptotic distributions of the sample generalized R^2 measures under these two scenarios. In Section 4, we discuss the convergence properties of the K -lines algorithm and its connection with the gradient descent algorithm and the Expectation-Maximization (EM) algorithm. In Section 5, we conduct simulation studies under various settings to verify the asymptotic distributions and evaluate the finite-sample statistical power of the sample generalized R^2 measures. In Section 6, we demonstrate the use of the generalized R^2 measures in two real data case studies, followed by discussions in Section 7. All the proofs of lemmas and theorems are in Appendix A. Appendix B includes the description of the real data sets used in this paper.

2. GENERALIZED R^2 MEASURES

We refer to the proposed measures that describe a mixture of linear dependences as *generalized R^2 measures*, motivated by the R^2 statistic, (i.e., the squared sample Pearson correlation defined in (2), also known as the coefficient of determination in linear regression), which is commonly used to describe the observed linear dependence in a bivariate sample.

2.1 Supervised and unsupervised scenarios

We consider two observable real-valued random variables X and Y and a discrete random variable $Z \in \{1, \dots, K\}$, where K is the number of linear dependences. Specifically, X and Y are the variables whose relationship is of our interest, and Z is an index variable of linear dependences. We define the *supervised scenario* as the case where X , Y and Z are all observable. In contrast, we define the *unsupervised scenario* as the case where only X and Y are observable but Z is not. In the special case of $K = 1$, we have $Z = 1$ as a constant, and only the supervised scenario exists. Please note that the “supervised scenario” in the following text does not refer to “supervised learning” or “prediction” commonly used in the machine learning field.

2.2 Supervised population generalized R^2

Under the supervised scenario (“ \mathcal{S} ”), we denote

$$p_{k(\mathcal{S})} := \mathbb{P}(Z = k), \quad k = 1, \dots, K. \quad \text{Then } \sum_{k=1}^K p_{k(\mathcal{S})} = 1. \quad (4)$$

Conditional on $Z = k$, the population Pearson correlation between X and Y is

$$\rho_{k(\mathcal{S})} = \frac{\text{cov}(X, Y|Z = k)}{\sqrt{\text{var}(X|Z = k)}\sqrt{\text{var}(Y|Z = k)}}, \quad (5)$$

if $\text{var}(X|Z = k) > 0$ and $\text{var}(Y|Z = k) > 0$, and $\rho_{k(\mathcal{S})} = 0$ otherwise.

In the special case of $K = 1$, $\rho_{1(\mathcal{S})}^2 = \rho^2$, the population version of the R^2 statistic. $\rho_{1(\mathcal{S})}^2$ indicates the population-level strength of a linear dependence, i.e., the similarity of the bivariate distribution of (X, Y) to the distribution on a line in \mathbb{R}^2 . Motivated by this, we propose to combine $\rho_{1(\mathcal{S})}^2, \dots, \rho_{K(\mathcal{S})}^2$ into a single measure, the *supervised population generalized R^2* , that indicates the overall strength of a K -component mixture of linear dependences, i.e., the similarity of the bivariate distribution of (X, Y) to the distribution on a mixture of K lines in \mathbb{R}^2 .

Definition 1. *The supervised population generalized R^2 is defined as*

$$\rho_{\mathcal{G}(\mathcal{S})}^2 := \mathbb{E}_Z \left[\rho_{Z(\mathcal{S})}^2 \right] = \mathbb{E}_Z \left[\frac{\text{cov}^2(X, Y|Z)}{\text{var}(X|Z)\text{var}(Y|Z)} \right] = \sum_{k=1}^K p_{k(\mathcal{S})} \cdot \rho_{k(\mathcal{S})}^2, \quad (6)$$

which is a weighted sum of $\rho_{1(\mathcal{S})}^2, \dots, \rho_{K(\mathcal{S})}^2$, i.e., the strengths of the K linear dependences, with weights as $p_{1(\mathcal{S})}, \dots, p_{K(\mathcal{S})}$, i.e., the probabilities of the K components.

In addition to this measure, we also provide a “ K -line interpretation” of the supervised scenario, so that we can investigate the extent to which the conditional distribution of $(X, Y)|(Z = k)$ in each k -th component concentrates on a line. How to define a *line center* of each component depends on how we measure the distance between a point $(x, y)^\top \in \mathbb{R}^2$ and a line

$$\left\{ (x, y)^\top : ax + by + c = 0, \text{ where } a, b, c \in \mathbb{R} \text{ with } a \neq 0 \text{ or } b \neq 0 \right\} \subset \mathbb{R}^2,$$

which we denote by $\beta = (a, b, c)^\top$. Because our proposed $\rho_{\mathcal{G}(S)}^2$ is symmetric in X and Y , a reasonable measure of the distance between $(x, y)^\top$ and β is the *perpendicular distance* $d_\perp : \mathbb{R}^2 \times \mathbb{R}^3 \mapsto \mathbb{R}$:

$$d_\perp \left((x, y)^\top, \beta \right) = \frac{|ax + by + c|}{\sqrt{a^2 + b^2}}. \quad (7)$$

Lemma 2.1. *Given two points $(x, y)^\top, (x', y')^\top \in \mathbb{R}^2$ and a line $\beta = (a, b, c)^\top$ where $a, b, c \in \mathbb{R}$ with $a \neq 0$ or $b \neq 0$, the following inequality holds.*

$$d_\perp \left((x, y)^\top, \beta \right) \leq \left\| (x, y)^\top - (x', y')^\top \right\| + d_\perp \left((x', y')^\top, \beta \right), \quad (8)$$

where $\|\cdot\|$ represents the ℓ_2 norm.

The proof of Lemma 2.1 is in Appendix A.1. Given the perpendicular distance $d_\perp(\cdot, *)$, the conditional means $\mu_{X,k(S)} := \mathbb{E}[X|Z = k]$ and $\mu_{Y,k(S)} := \mathbb{E}[Y|Z = k]$, and the conditional covariance matrix of $(X, Y)|(Z = k)$:

$$\Sigma_{k(S)} := \begin{bmatrix} \text{var}(X|Z = k) & \text{cov}(X, Y|Z = k) \\ \text{cov}(X, Y|Z = k) & \text{var}(Y|Z = k) \end{bmatrix},$$

below we define the *supervised population line center* for the k -th component.

Definition 2. *Under the supervised scenario, we denote by $\lambda_{1,k} \geq \lambda_{2,k} > 0$ the eigenvalues of $\Sigma_{k(S)}$. Let $\mathbf{u}_{1,k(S)} = (u_{11,k(S)}, u_{12,k(S)})^\top$ and $\mathbf{u}_{2,k(S)} = (u_{21,k(S)}, u_{22,k(S)})^\top$ represent the corresponding eigenvectors such that $\mathbf{u}_{1,k(S)}^\top \Sigma_{k(S)} \mathbf{u}_{1,k(S)} = \mathbf{u}_{2,k(S)}^\top \Sigma_{k(S)} \mathbf{u}_{2,k(S)} = 1$ and $\mathbf{u}_{1,k(S)}^\top \Sigma_{k(S)} \mathbf{u}_{2,k(S)} = 0$. The supervised population line center of the k -th component is defined as*

$$L_{k(S)} := \left\{ (x, y)^\top : u_{12,k(S)} (x - \mu_{X,k(S)}) - u_{11,k(S)} (y - \mu_{Y,k(S)}) = 0 \right\} \subset \mathbb{R}^2, \quad (9)$$

which corresponds to the first principal component of $\Sigma_{k(S)}$ and minimizes the conditional expectation of the squared perpendicular distance of (X, Y) to it given $Z = k$ (Jolliffe, 2011). We represent this line center $L_{k(S)}$ equivalently by $\beta_{k(S)} = (a_{k(S)}, b_{k(S)}, c_{k(S)})^\top$, where $a_{k(S)} = u_{12, k(S)}$, $b_{k(S)} = -u_{11, k(S)}$, and $c_{k(S)} = -u_{12, k(S)}\mu_{X, k(S)} + u_{11, k(S)}\mu_{Y, k(S)}$. That is,

$$\beta_{k(S)} = \arg \min_{\beta} \mathbb{E} \left[d_{\perp}^2 \left((X, Y)^\top, \beta \right) \middle| Z = k \right]. \quad (10)$$

Remark 1. When $\rho_{k(S)}^2 = 1$, the distribution of $(X, Y)|(Z = k)$ in the k -th component is totally concentrated on the k -th supervised population line center, i.e., $\text{support}((X, Y)^\top | Z = k) \subseteq L_{k(S)}$. The reason is that $\lambda_{1, k} = 1 + |\rho_{k(S)}| = 2$ and $\lambda_{2, k} = 0$, i.e., the first principal component of $\Sigma_{k(S)}$ explains all the variance of $(X, Y)|(Z = k)$.

2.3 Supervised sample generalized R^2

We consider a sample $(X_1, Y_1, Z_1), \dots, (X_n, Y_n, Z_n)$ from the joint distribution of $(X, Y, Z) \in \mathbb{R}^2 \times \{1, \dots, K\}$. Based on the definition of $\rho_{\mathcal{G}(S)}^2$ in (6) (Definition 1), we define the *supervised sample generalized R^2* as a plug-in estimator of $\rho_{\mathcal{G}(S)}^2$.

Definition 3. The supervised sample generalized R^2 is defined as

$$R_{\mathcal{G}(S)}^2 := \sum_{k=1}^K \hat{p}_{k(S)} \cdot \hat{\rho}_{k(S)}^2, \quad (11)$$

where

$$\hat{p}_{k(S)} = \frac{1}{n} \sum_{i=1}^n \mathbb{I}(Z_i = k), \quad (12)$$

$$\hat{\rho}_{k(S)}^2 = \frac{[\sum_{i=1}^n (X_i - \bar{X}_{k(S)})(Y_i - \bar{Y}_{k(S)})\mathbb{I}(Z_i = k)]^2}{[\sum_{i=1}^n (X_i - \bar{X}_{k(S)})^2\mathbb{I}(Z_i = k)] [\sum_{i=1}^n (Y_i - \bar{Y}_{k(S)})^2\mathbb{I}(Z_i = k)]}, \quad (13)$$

with $\bar{X}_{k(S)} = \frac{1}{n_{k(S)}} \sum_{i=1}^n X_i \mathbb{I}(Z_i = k)$, $\bar{Y}_{k(S)} = \frac{1}{n_{k(S)}} \sum_{i=1}^n Y_i \mathbb{I}(Z_i = k)$, and $n_{k(S)} = \sum_{i=1}^n \mathbb{I}(Z_i = k)$.

Motivated by the above definitions under the supervised scenario, we next define their counterpart concepts under the unsupervised scenario, where the index variable Z is unobservable.

2.4 Unsupervised population generalized R^2

Under the unsupervised scenario, we investigate a mixture of K linear dependences between two real-valued random variables X and Y without observing the index variable Z . Motivated by the

definition of the supervised population line centers (Definition 2), here we define the *unsupervised population line centers* as the K lines that minimize the expected squared perpendicular distance of (X, Y) to its closest line.

Definition 4. Under the unsupervised scenario, we denote a set containing K lines with possible repeats by $B_K = \{\beta_1, \dots, \beta_K\}$, where $\beta_k = (a_k, b_k, c_k)^\top \in \mathbb{R}^3$. That is, there may exist $\beta_k = \beta_r$ for $1 \leq k \neq r \leq K$. We define a set of unsupervised population line centers, $B_{K(\mathcal{U})} = \{\beta_{1(\mathcal{U})}, \dots, \beta_{K(\mathcal{U})}\}$, as

$$B_{K(\mathcal{U})} \in \arg \min_{B_K} \mathbb{E} \left[\min_{\beta \in B_K} d_\perp^2 \left((X, Y)^\top, \beta \right) \right]. \quad (14)$$

Specifically, we denote by $\beta_{k(\mathcal{U})} = (a_{k(\mathcal{U})}, b_{k(\mathcal{U})}, c_{k(\mathcal{U})})^\top$ the k -th unsupervised population line center, which is equivalently represented by

$$L_{k(\mathcal{U})} := \left\{ (x, y)^\top : a_{k(\mathcal{U})}x + b_{k(\mathcal{U})}y + c_{k(\mathcal{U})} = 0 \right\} \subset \mathbb{R}^2, \quad k = 1, \dots, K. \quad (15)$$

Remark 2. $B_{K(\mathcal{U})}$ in (14) exists when $f(B_K) := \mathbb{E} \left[\min_{\beta \in B_K} d_\perp^2 \left((X, Y)^\top, \beta \right) \right]$ is a continuous function of B_K , because $f(\cdot)$ is defined on the whole space of \mathbb{R}^{3K} and bounded from below by 0. If B_K contains $\beta_k = (0, 0, 0)^\top$, a degenerated line, we can always replace β_k by some $(a_k, b_k, 0)^\top$, where $a_k \neq 0$ or $b_k \neq 0$, so that β_k becomes a valid line while $f(B_K)$ stays the same.

Remark 3. By Definition 4, $B_{K(\mathcal{U})}$ is not unique in general. For example, suppose that (X, Y) has four possible values $\{(-1, -1), (-1, 1), (1, -1), (1, 1)\}$ with equal probabilities $1/4$. Then $B_{2(\mathcal{U})} = \{(1, -1, 0)^\top, (1, 1, 0)^\top\}$, $B_{2(\mathcal{U})} = \{(-1, 0, 1)^\top, (1, 0, 1)^\top\}$, and $B_{2(\mathcal{U})} = \{(0, -1, 1)^\top, (0, 1, 1)^\top\}$ all satisfy (14). Also note that unless (X, Y) concentrates on two perpendicular lines, there is no direct relation between the first two principal components of the covariance matrix of (X, Y) and the two unsupervised population line centers for $K = 2$.

Remark 4. By definition, $B_{K(\mathcal{U})} \neq B_{K(\mathcal{S})}$, i.e., the K population line centers are not the same under the unsupervised and supervised scenarios. The reason is that $B_{K(\mathcal{U})}$ and $B_{K(\mathcal{S})}$ are defined based on the distribution of (X, Y) and (X, Y, Z) , respectively. Figure 2 gives an example.

Provided that $B_{K(\mathcal{U})}$ is uniquely determined, we define a *random surrogate index* $\tilde{Z} \in \{1, \dots, K\}$ based on the K unsupervised population line centers $\beta_{1(\mathcal{U})}, \dots, \beta_{K(\mathcal{U})}$. Specifically, \tilde{Z} denotes the index of the line center to which (X, Y) is closest.

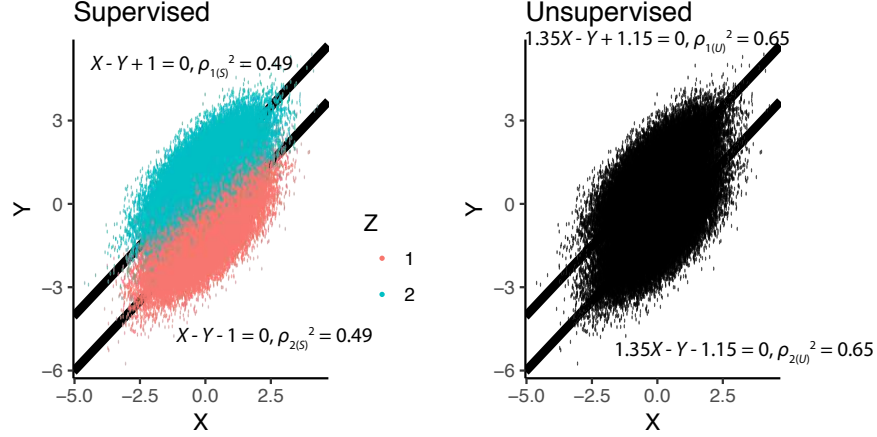


Figure 2: An example demonstrating the difference between $B_{K(S)}$ (Definition 2) and $B_{K(U)}$ (Definition 4). Under the supervised scenario, the distribution of (X, Y, Z) is specified by: $\mathbb{P}(Z = 1) = \mathbb{P}(Z = 2) = 0.5$ and $(X, Y)|(Z = k) \sim \mathcal{N}(\boldsymbol{\mu}_k, \boldsymbol{\Sigma}_k)$, $k = 1, 2$, where $\boldsymbol{\mu}_1 = (0, -1)^\top$, $\boldsymbol{\mu}_2 = (0, 1)^\top$, $\boldsymbol{\Sigma}_1 = \boldsymbol{\Sigma}_2 = \begin{bmatrix} 1 & 0.7 \\ 0.7 & 1 \end{bmatrix}$. Then $B_{K(S)} = \{(1, -1, 1)^\top, (1, -1, -1)^\top\}$ and $\rho_{1(S)}^2 = \rho_{2(S)}^2 = 0.49$ (Equation (5)). A large sample $\{(X_i, Y_i, Z_i)\}_{i=1}^{10,000}$ is simulated from the supervised population for illustration purpose (left panel). Under the unsupervised scenario, the distribution of (X, Y) is $\sum_{k=1}^2 0.5 \cdot \mathcal{N}(\boldsymbol{\mu}_k, \boldsymbol{\Sigma}_k)$. As the distribution of (X, Y) is the same under the two scenarios, the K -lines algorithm (Algorithm 1) is applied to $\{(X_i, Y_i)\}_{i=1}^{10,000}$ (right panel) to find the approximate $B_{K(U)} = \{(1.35, -1, 1.15)^\top, (1.35, -1, -1.15)^\top\}$ and $\rho_{1(U)}^2 = \rho_{2(U)}^2 = 0.65$ (Equation (19)).

Definition 5. Suppose that two real-valued random variables X and Y have uniquely determined K unsupervised population line centers $\boldsymbol{\beta}_{1(U)}, \dots, \boldsymbol{\beta}_{K(U)}$. Also suppose that the probability that (X, Y) is equally close to more than one line centers is zero. We define a random surrogate index \tilde{Z} as

$$\tilde{Z} := \arg \min_{k \in \{1, \dots, K\}} d_{\perp} \left((X, Y)^\top, \boldsymbol{\beta}_{k(U)} \right), \quad (16)$$

which is uniquely determined by (X, Y) except in a measure zero set. For example, if $d_{\perp} \left((X, Y)^\top, \boldsymbol{\beta}_{k(U)} \right) < \min_{r \neq k} d_{\perp} \left((X, Y)^\top, \boldsymbol{\beta}_{r(U)} \right)$, then $\tilde{Z} = k$.

Motivated by $\rho_{G(S)}^2$, we define the *unsupervised population generalized R^2* based on $\boldsymbol{\beta}_{1(U)}, \dots, \boldsymbol{\beta}_{K(U)}$ and \tilde{Z} .

Definition 6. The unsupervised population R^2 is defined as

$$\rho_{\mathcal{G}(\mathcal{U})}^2 := \sum_{k=1}^K p_{k(\mathcal{U})} \cdot \rho_{k(\mathcal{U})}^2, \quad (17)$$

where

$$p_{k(\mathcal{U})} := \mathbb{P}(\tilde{Z} = k), \quad (18)$$

$$\rho_{k(\mathcal{U})}^2 := \frac{\text{cov}^2(X, Y | \tilde{Z} = k)}{\text{var}(X | \tilde{Z} = k) \text{var}(Y | \tilde{Z} = k)}. \quad (19)$$

Remark 5. $\rho_{\mathcal{G}(\mathcal{U})}^2 \geq \rho_{\mathcal{G}(\mathcal{S})}^2$. The proof is in Appendix A.2.

2.5 Unsupervised sample generalized R^2

We consider a sample $(X_1, Y_1), \dots, (X_n, Y_n)$ from the joint distribution of (X, Y) . Based on the definitions of $\beta_{1(\mathcal{U})}, \dots, \beta_{K(\mathcal{U})}$ (Definition 4), \tilde{Z} (Definition 5) and $\rho_{\mathcal{G}(\mathcal{U})}^2$ (Definition 6), here we define the corresponding sample versions. First, we define the *unsupervised sample line centers* as the K lines that minimize the average squared perpendicular distance of (X_i, Y_i) , $i = 1, \dots, n$, to its closest line.

Definition 7. Under the same setting as in Definition 4, $B_K = \{\beta_1, \dots, \beta_K\}$ contains K lines with possible repeats. We define the set of *unsupervised sample line centers* as

$$\hat{B}_{K(\mathcal{U})} \in \arg \min_{B_K} \frac{1}{n} \sum_{i=1}^n \min_{\beta \in B_K} d_{\perp}^2 \left((X_i, Y_i)^{\top}, \beta \right). \quad (20)$$

We write each solution to (20) as $\hat{B}_{K(\mathcal{U})} = \{\hat{\beta}_{1(\mathcal{U})}, \dots, \hat{\beta}_{K(\mathcal{U})}\}$, where $\hat{\beta}_{k(\mathcal{U})} = (\hat{a}_{k(\mathcal{U})}, \hat{b}_{k(\mathcal{U})}, \hat{c}_{k(\mathcal{U})})^{\top}$ is the k -th unsupervised sample line center and equivalently represented by

$$\hat{L}_{k(\mathcal{U})} := \left\{ (x, y)^{\top} : \hat{a}_{k(\mathcal{U})}x + \hat{b}_{k(\mathcal{U})}y + \hat{c}_{k(\mathcal{U})} = 0 \right\} \subset \mathbb{R}^2, \quad k = 1, \dots, K. \quad (21)$$

Remark 6. Similar to Remark 3, by Definition 7, $\hat{B}_{K(\mathcal{U})}$ is not uniquely determined by the sample in general. For example, suppose $n = 4$, $(X_1, Y_1) = (-1, -1)$, $(X_2, Y_2) = (-1, 1)$, $(X_3, Y_3) = (1, -1)$, and $(X_4, Y_4) = (1, 1)$. Then $\hat{B}_{2(\mathcal{U})} = \{(1, -1, 0)^{\top}, (1, 1, 0)^{\top}\}$, $\hat{B}_{2(\mathcal{U})} = \{(-1, 0, 1)^{\top}, (1, 0, 1)^{\top}\}$, and $\hat{B}_{2(\mathcal{U})} = \{(0, -1, 1)^{\top}, (0, 1, 1)^{\top}\}$ all satisfy (20).

To find $\hat{B}_{K(\mathcal{U})}$, we propose a *K -lines clustering algorithm*, which is motivated by the Lloyd's K -means clustering algorithm widely used to partition data points into cloud-like clusters (Lloyd,

1982). In our K -lines clustering algorithm (Algorithm 1), the k -th cluster line center is represented by the k -th unsupervised sample line center $\widehat{\beta}_{k(\mathcal{U})} = \left(\widehat{a}_{k(\mathcal{U})}, \widehat{b}_{k(\mathcal{U})}, \widehat{c}_{k(\mathcal{U})}\right)^\top$, $k = 1, \dots, K$.

Algorithm 1 K -lines clustering algorithm

1: **input:**

Sample: $\{(X_i, Y_i)\}_{i=1}^n$

K : number of line centers

2: **procedure** K -LINES($\{(X_i, Y_i)\}_{i=1}^n, K$)

3: Initial cluster assignment: $\mathcal{C}_1^{(0)}, \dots, \mathcal{C}_K^{(0)}$, such that $\cup_{k=1}^K \mathcal{C}_k^{(0)} = \{1, \dots, n\}$

4: Given the initial cluster assignment, the algorithm proceeds by alternating between two steps in each iteration. In the t -th iteration, $t = 1, 2, \dots$

Recentering step: Calculate the cluster line centers $\widehat{\beta}_{1(\mathcal{U})}^{(t)}, \dots, \widehat{\beta}_{K(\mathcal{U})}^{(t)}$ based on the cluster assignment $\mathcal{C}_1^{(t-1)}, \dots, \mathcal{C}_K^{(t-1)}$ by (22).

Assignment step: Update the cluster assignment as

$$\mathcal{C}_k^{(t)} = \left\{ i : d_{\perp} \left((X_i, Y_i)^\top, \widehat{\beta}_{k(\mathcal{U})}^{(t)} \right) \leq d_{\perp} \left((X_i, Y_i)^\top, \widehat{\beta}_{s(\mathcal{U})}^{(t)} \right), \forall s = 1, \dots, K \right\}.$$

5: Stop the iteration when the cluster assignment no longer changes.

6: **output:**

Cluster assignment $\mathcal{C}_1, \dots, \mathcal{C}_K$

K unsupervised sample line centers $\widehat{\beta}_{1(\mathcal{U})}, \dots, \widehat{\beta}_{K(\mathcal{U})}$

As an iterative procedure, the K -lines clustering algorithm includes two alternating steps in each iteration. The *recentering step* uses the current cluster assignment to update each cluster line center, which minimizes the within-cluster sum of squared perpendicular distances from all the data points in that cluster to the cluster line center. The *assignment step* updates the cluster assignment based on the current cluster line centers: assign every data point to its closest cluster line center in the perpendicular distance. The two steps alternate until the algorithm converges, i.e., the cluster assignment stays unchanged as iterations proceed.

The recentering step updates each cluster center using the *major axis regression*, which minimizes the sums of squares of the perpendicular distance between each point and the regression

line (Samuelson, 1942; Jolliffe, 1982; Smith, 2009). Given the cluster assignment in the $(t-1)$ -th iteration, say $\mathcal{C}_1^{(t-1)}, \dots, \mathcal{C}_K^{(t-1)}$ (with $\cup_{k=1}^K \mathcal{C}_k^{(t-1)} = \{1, \dots, n\}$ and $\mathcal{C}_k^{(t-1)} \cap \mathcal{C}_r^{(t-1)} = \emptyset$ for all $1 \leq k \neq r \leq K$), the updated k -th cluster center, i.e., the k -th sample line center $\widehat{\beta}_{k(\mathcal{U})}^{(t)}$ that minimizes the within-cluster sum of squared perpendicular distances, is equal to the first principal component of the sample covariance matrix calculated based on the data points in $\mathcal{C}_k^{(t-1)}$. That is,

$$\widehat{\beta}_{k(\mathcal{U})}^{(t)} = \arg \min_{\beta} \sum_{i \in \mathcal{C}_k^{(t-1)}} d_{\perp}^2((X_i, Y_i)^{\top}, \beta) = (\widehat{u}_{12,k}, -\widehat{u}_{11,k}, -\widehat{u}_{12,k}\bar{X}_{k(\mathcal{U})} + \widehat{u}_{11,k}\bar{Y}_{k(\mathcal{U})})^{\top}, \quad (22)$$

where $(\widehat{u}_{11,k}, \widehat{u}_{12,k})^{\top}$ is the eigenvector corresponding to the largest eigenvalue of the sample covariance matrix

$$\begin{bmatrix} \sum_{i \in \mathcal{C}_k^{(t-1)}} (X_i - \bar{X}_{k(\mathcal{U})})^2 & \sum_{i \in \mathcal{C}_k^{(t-1)}} (X_i - \bar{X}_{k(\mathcal{U})})(Y_i - \bar{Y}_{k(\mathcal{U})}) \\ \sum_{i \in \mathcal{C}_k^{(t-1)}} (X_i - \bar{X}_{k(\mathcal{U})})(Y_i - \bar{Y}_{k(\mathcal{U})}) & \sum_{i \in \mathcal{C}_k^{(t-1)}} (Y_i - \bar{Y}_{k(\mathcal{U})})^2 \end{bmatrix} \quad (23)$$

with $\bar{X}_{k(\mathcal{U})} = \frac{1}{|\mathcal{C}_k^{(t-1)}|} \sum_{i \in \mathcal{C}_k^{(t-1)}} X_i$ and $\bar{Y}_{k(\mathcal{U})} = \frac{1}{|\mathcal{C}_k^{(t-1)}|} \sum_{i \in \mathcal{C}_k^{(t-1)}} Y_i$. The line fitted by the major axis regression exactly corresponds to $\widehat{\beta}_{k(\mathcal{U})}$ (Samuelson, 1942; Jolliffe, 1982; Smith, 2009).

After introducing the unsupervised sample line centers in Definition 7, we define the average within-cluster sum of perpendicular distances as

$$\begin{aligned} W(B_K, P_n) &:= \frac{1}{n} \sum_{i=1}^n \min_{\beta \in B_K} d_{\perp}^2((X_i, Y_i)^{\top}, \beta) \\ &= \int \min_{\beta \in B_K} d_{\perp}^2((x, y)^{\top}, \beta) P_n((dx, dy)^{\top}), \end{aligned} \quad (24)$$

where P_n is the empirical measure from the sample by placing mass n^{-1} at each of $(X_1, Y_1)^{\top}, \dots, (X_n, Y_n)^{\top}$.

Similar to the K -means clustering algorithm, the K -lines clustering algorithm is not guaranteed to find the global minimizer, $\arg \min_{B_K} W(B_K, P_n)$, but it may converge to a local minimizer. Heuristically, we can search for the global minimizer by running the K -lines clustering algorithm for M times with random initializations and obtain M sets of unsupervised sample line centers $B_K^{(1)}, \dots, B_K^{(M)}$. Then we set $\widehat{B}_{K(\mathcal{U})} \in \arg \min_{B_K \in \{B_K^{(1)}, \dots, B_K^{(M)}\}} W(B_K, P_n)$.

As in the population case, we introduce the *sample surrogate indices* $\widehat{Z}_i \in \{1, \dots, K\}$, $i = 1, \dots, n$, based on the K unsupervised sample line centers $\widehat{\beta}_{1(\mathcal{U})}, \dots, \widehat{\beta}_{K(\mathcal{U})}$.

Definition 8. Suppose that a sample $(X_1, Y_1), \dots, (X_n, Y_n)$ has uniquely determined K unsupervised sample line centers $\widehat{\beta}_{1(\mathcal{U})}, \dots, \widehat{\beta}_{K(\mathcal{U})}$. Also suppose that the probability that (X_i, Y_i) is equally

close to more than one sample line centers is zero. For each (X_i, Y_i) , we define its sample surrogate index

$$\widehat{Z}_i := \arg \min_{k \in \{1, \dots, K\}} d_{\perp} \left((X_i, Y_i)^{\top}, \widehat{\beta}_{k(\mathcal{U})} \right), \quad i = 1, \dots, n, \quad (25)$$

which is uniquely determined by the sample. That is, $\widehat{Z}_i = k$ is equivalent to $i \in \mathcal{C}_k$, where \mathcal{C}_k is the k -th cluster assignment output by the K -lines clustering algorithm (Algorithm 1), assuming that the algorithm finds the global minimum.

Then based on the definition of $\rho_{\mathcal{G}(\mathcal{U})}^2$ in (17) (Definition 6), we define the *unsupervised sample generalized R^2* as a plug-in estimator of $\rho_{\mathcal{G}(\mathcal{U})}^2$.

Definition 9. *The unsupervised sample generalized R^2 is defined as*

$$R_{\mathcal{G}(\mathcal{U})}^2 := \sum_{k=1}^K \widehat{p}_{k(\mathcal{U})} \cdot \widehat{\rho}_{k(\mathcal{U})}^2, \quad (26)$$

where

$$\widehat{p}_{k(\mathcal{U})} = \frac{1}{n} \sum_{i=1}^n \mathbb{I} \left(\widehat{Z}_i = k \right), \quad (27)$$

$$\widehat{\rho}_{k(\mathcal{U})}^2 = \frac{\left[\sum_{i=1}^n (X_i - \bar{X}_{k(\mathcal{U})}) (Y_i - \bar{Y}_{k(\mathcal{U})}) \mathbb{I} \left(\widehat{Z}_i = k \right) \right]^2}{\left[\sum_{i=1}^n (X_i - \bar{X}_{k(\mathcal{U})})^2 \mathbb{I} \left(\widehat{Z}_i = k \right) \right] \left[\sum_{i=1}^n (Y_i - \bar{Y}_{k(\mathcal{U})})^2 \mathbb{I} \left(\widehat{Z}_i = k \right) \right]}, \quad (28)$$

with $\bar{X}_{k(\mathcal{U})} = \frac{1}{n_{k(\mathcal{U})}} \sum_{i=1}^n X_i \mathbb{I} \left(\widehat{Z}_i = k \right)$, $\bar{Y}_{k(\mathcal{U})} = \frac{1}{n_{k(\mathcal{U})}} \sum_{i=1}^n Y_i \mathbb{I} \left(\widehat{Z}_i = k \right)$, and $n_{k(\mathcal{U})} = \sum_{i=1}^n \mathbb{I} \left(\widehat{Z}_i = k \right)$.

The choice of K When users do not have prior knowledge on the value of K , i.e., the number of lines in the K -lines algorithm, how to choose K becomes an important question in practice. Some methods for choosing K in K -means clustering can be easily adapted. For example, the elbow method, though not being theoretically principled, is visually appealing to practitioners and widely used. It employs a *scree plot*, whose horizontal axis displays a range of K values and vertical axis shows the average within-cluster sum of squared distances corresponding to each K . In the context of our K -lines algorithm, it is reasonable to modify the vertical axis of the scree plot to show the average within-cluster sums of squared perpendicular distances, i.e., $W(B_K, P_n)$ in (24), corresponding to varying values of K . We will demonstrate this graphical approach in Section 5.2.

Under the assumption that $(X, Y)|(Z = k)$ follows a bivariate Gaussian distribution for all $k = 1, \dots, K$, we may use the Akaike information criterion (AIC) to choose K (Akaike, 1998). Specifically, we define

$$\text{AIC}(K) := 12K - 2 \sum_{i=1}^n \log p \left(X_i, Y_i \mid \left\{ \hat{p}_k(\mathcal{U}), \hat{\boldsymbol{\mu}}_k(\mathcal{U}), \hat{\boldsymbol{\Sigma}}_k(\mathcal{U}) \right\}_{k=1}^K \right), \quad (29)$$

where

$$\begin{aligned} & p \left(X_i, Y_i \mid \left\{ \hat{p}_k(\mathcal{U}), \hat{\boldsymbol{\mu}}_k(\mathcal{U}), \hat{\boldsymbol{\Sigma}}_k(\mathcal{U}) \right\}_{k=1}^K \right) \\ &= \sum_{k=1}^K \hat{p}_k(\mathcal{U}) \frac{\exp \left\{ -\frac{1}{2} \left((X_i, Y_i)^\top - \hat{\boldsymbol{\mu}}_k(\mathcal{U}) \right)^\top \hat{\boldsymbol{\Sigma}}_k^{-1}(\mathcal{U}) \left((X_i, Y_i)^\top - \hat{\boldsymbol{\mu}}_k(\mathcal{U}) \right) \right\}}{2\pi \sqrt{|\hat{\boldsymbol{\Sigma}}_k(\mathcal{U})|}}. \end{aligned}$$

The first term $12K = 2 \times 6K$ because the number of parameters is 6 for each K . In the above equations, $\hat{p}_k(\mathcal{U}) = |\mathcal{C}_k|/n$, $\hat{\boldsymbol{\mu}}_k(\mathcal{U}) = (\bar{X}_{k(\mathcal{U})}, \bar{Y}_{k(\mathcal{U})})^\top$, and

$$\hat{\boldsymbol{\Sigma}}_k(\mathcal{U}) = \begin{bmatrix} \frac{\sum_{i \in \mathcal{C}_k} (X_i - \bar{X}_{k(\mathcal{U})})^2}{|\mathcal{C}_k|} & \frac{\sum_{i \in \mathcal{C}_k} (X_i - \bar{X}_{k(\mathcal{U})})(Y_i - \bar{Y}_{k(\mathcal{U})})}{|\mathcal{C}_k|} \\ \frac{\sum_{i \in \mathcal{C}_k} (X_i - \bar{X}_{k(\mathcal{U})})(Y_i - \bar{Y}_{k(\mathcal{U})})}{|\mathcal{C}_k|} & \frac{\sum_{i \in \mathcal{C}_k} (Y_i - \bar{Y}_{k(\mathcal{U})})^2}{|\mathcal{C}_k|} \end{bmatrix},$$

follow the notations used in Definitions 8 and 9 and are obtained from the K -lines clustering result. The K value that minimizes $\text{AIC}(K)$ will be chosen. We will demonstrate this AIC method in Section 5.2. In practice, we recommend users to visualize the K value chosen by the AIC in a scree plot, as a way to decide whether the chosen K value is reasonable.

3. ASYMPTOTIC THEORY OF THE GENERALIZED R^2 MEASURES

To enable statistical inference of the supervised and unsupervised population generalized R^2 measures, $\rho_{\mathcal{G}(S)}^2$ (6) and $\rho_{\mathcal{G}(\mathcal{U})}^2$ (17), here we derive the first-order asymptotic distributions of $R_{\mathcal{G}(S)}^2$ (11) and $R_{\mathcal{G}(\mathcal{U})}^2$ (26), respectively.

3.1 Asymptotic distribution of the supervised sample generalized R^2

We first derive the asymptotic distribution of $R_{\mathcal{G}(S)}^2$ by the Central Limit Theorem and the delta method, i.e., Cramér's Theorem (Ferguson, 1996), under mild conditions on the fourth conditional moments of X and Y .

Theorem 3.1. *Under the supervised scenario (Section 2.1), we define*

$$\mu_{X^c Y^d, k(\mathcal{S})} = \mathbb{E} \left[\left(\frac{X - \mathbb{E}[X|Z = k]}{\sqrt{\text{var}(X|Z = k)}} \right)^c \left(\frac{Y - \mathbb{E}[Y|Z = k]}{\sqrt{\text{var}(Y|Z = k)}} \right)^d \middle| Z = k \right], \quad c, d \in \mathbb{N},$$

Assume $\mu_{X^4, k(\mathcal{S})} < \infty$ and $\mu_{Y^4, k(\mathcal{S})} < \infty$ for all $k = 1, \dots, K$. Then

$$\sqrt{n} \left(R_{\mathcal{G}(\mathcal{S})}^2 - \rho_{\mathcal{G}(\mathcal{S})}^2 \right) \xrightarrow{d} \mathcal{N} \left(0, \gamma_{(\mathcal{S})}^2 \right), \quad (30)$$

where $\rho_{\mathcal{G}(\mathcal{S})}^2$ is the supervised population generalized R^2 defined in (6), and

$$\gamma_{(\mathcal{S})}^2 = \sum_{k=1}^K (A_{k(\mathcal{S})} + B_{k(\mathcal{S})}) + 2 \sum_{1 \leq k < r \leq K} C_{kr(\mathcal{S})}, \quad (31)$$

with

$$A_{k(\mathcal{S})} = p_{k(\mathcal{S})} \left[\rho_{k(\mathcal{S})}^4 \left(\mu_{X^4, k(\mathcal{S})} + 2\mu_{X^2 Y^2, k(\mathcal{S})} + \mu_{Y^4, k(\mathcal{S})} \right) - 4\rho_{k(\mathcal{S})}^3 \left(\mu_{X^3 Y, k(\mathcal{S})} + \mu_{X Y^3, k(\mathcal{S})} \right) + 4\rho_{k(\mathcal{S})}^2 \mu_{X^2 Y^2, k(\mathcal{S})} \right],$$

$$B_{k(\mathcal{S})} = p_{k(\mathcal{S})} (1 - p_{k(\mathcal{S})}) \rho_{k(\mathcal{S})}^4,$$

$$C_{kr(\mathcal{S})} = -p_{k(\mathcal{S})} p_{r(\mathcal{S})} \rho_{k(\mathcal{S})}^2 \rho_{r(\mathcal{S})}^2,$$

where $p_{k(\mathcal{S})}$ and $\rho_{k(\mathcal{S})}$ are defined in (4) and (5), respectively.

Applying Theorem 3.1 to the special case where $(X, Y)|Z$ follows a bivariate Gaussian distribution, we obtain a much simpler form of the first-order asymptotic distribution of $R_{\mathcal{G}(\mathcal{S})}^2$ in Corollary 3.2.

corollary 3.2. *In the special case of Theorem 3.1 where (X, Y) conditional on $Z = k$ follows a bivariate Gaussian distribution for all $k = 1, \dots, K$, the asymptotic variance of $\sqrt{n} \left(R_{\mathcal{G}(\mathcal{S})}^2 - \rho_{\mathcal{G}(\mathcal{S})}^2 \right)$, i.e., $\gamma_{(\mathcal{S})}^2$ in (31), becomes*

$$\begin{aligned} \gamma_{(\mathcal{S})}^2 = & \sum_{k=1}^K \left[4p_{k(\mathcal{S})} \rho_{k(\mathcal{S})}^2 \left(1 - \rho_{k(\mathcal{S})}^2 \right)^2 + p_{k(\mathcal{S})} (1 - p_{k(\mathcal{S})}) \rho_{k(\mathcal{S})}^4 \right] \\ & - 2 \sum_{1 \leq k < r \leq K} p_{k(\mathcal{S})} p_{r(\mathcal{S})} \rho_{k(\mathcal{S})}^2 \rho_{r(\mathcal{S})}^2, \end{aligned} \quad (32)$$

which only depends on $p_{k(\mathcal{S})}$ and $\rho_{k(\mathcal{S})}^2$, i.e., the probability of $Z = k$ and the squared Pearson correlation between X and Y conditional on $Z = k$, $k = 1, \dots, K$.

To derive an analog of Theorem 3.1 for the unsupervised scenario, we need to show that each sample surrogate index \tilde{Z}_i , $i = 1, \dots, n$, converges in distribution to the random surrogate index \tilde{Z} .

A sufficient condition is the strong consistency of the K unsupervised sample line centers $\widehat{B}_{K(\mathcal{U})} = \{\widehat{\beta}_{1(\mathcal{U})}, \dots, \widehat{\beta}_{K(\mathcal{U})}\}$ to the K unsupervised population line centers $B_{K(\mathcal{U})} = \{\beta_{1(\mathcal{U})}, \dots, \beta_{K(\mathcal{U})}\}$. Hence, we first prove this strong consistency.

3.2 Strong consistency of the K -lines clustering

Using Lemma 2.1 and the strong consistency result of the K -means clustering (Pollard et al., 1981), we derive the following theorem for the strong consistency of the K unsupervised sample line centers output by the K -lines clustering algorithm (Algorithm 1). We assume that the global optimal sample line centers $\widehat{B}_{K(\mathcal{U})} = \arg \min_{B_K} W(B_K, P_n)$ is attained and unique, where $W(B_K, P_n)$ is defined in (24).

Theorem 3.3. *Suppose that $\int \|(x, y)^\top\|^2 P((dx, dy)^\top) < \infty$ and that for each $k = 1, \dots, K$ there is a unique set $B_{k(\mathcal{U})} = \arg \min_{B_k} W(B_k, P)$. Then as the sample size $n \rightarrow \infty$, $\widehat{B}_{K(\mathcal{U})} \rightarrow B_{K(\mathcal{U})}$ almost surely, and $W(\widehat{B}_{K(\mathcal{U})}, P_n) \rightarrow W(B_{K(\mathcal{U})}, P)$ almost surely.*

The first statement of Theorem 3.3 means that there exists an ordering of the elements in $\widehat{B}_{K(\mathcal{U})} = \{\widehat{\beta}_{1(\mathcal{U})}, \dots, \widehat{\beta}_{K(\mathcal{U})}\}$ and $B_{K(\mathcal{U})} = \{\beta_{1(\mathcal{U})}, \dots, \beta_{K(\mathcal{U})}\}$ such that as the sample size $n \rightarrow \infty$,

$$\widehat{\beta}_{k(\mathcal{U})} \rightarrow \beta_{k(\mathcal{U})} \text{ almost surely, } k = 1, \dots, K. \quad (33)$$

Theorem 3.3 only hinges on two conditions. The first condition

$$\int \|(x, y)^\top\|^2 P((dx, dy)^\top) < \infty,$$

where $\|\cdot\|$ is the ℓ_2 norm in \mathbb{R}^2 , holds for many common probability measures P on \mathbb{R}^2 . This is to ensure that $W(B_k, P)$ is finite for every B_k , $k = 1, \dots, K$, because for each $\beta = (a, b, c)^\top \in \mathbb{R}^3$, where $a \neq 0$ or $b \neq 0$ (without loss of generality, we assume $a \neq 0$ and $|c| < \infty$ below),

$$\int d_{\perp}^2 \left((x, y)^{\top}, \boldsymbol{\beta} \right) P \left((dx, dy)^{\top} \right) \quad (34)$$

$$\begin{aligned} &\leq \int \left\| (x, y)^{\top} - (-c/a, 0)^{\top} \right\|^2 P \left((dx, dy)^{\top} \right) \\ &\leq \int \left(\left\| (x, y)^{\top} \right\| + \left\| (-c/a, 0)^{\top} \right\| \right)^2 P \left((dx, dy)^{\top} \right) \\ &\leq 4c^2/a^2 + 2 \int_{\left\| (x, y)^{\top} \right\| \geq |c/a|} \left\| (x, y)^{\top} \right\|^2 P \left((dx, dy)^{\top} \right) \\ &< \infty, \end{aligned} \quad (35)$$

where the first inequality holds by the definition of $d_{\perp} \left((x, y)^{\top}, \boldsymbol{\beta} \right)$ (7), because $(-c/a, 0)^{\top}$ is a point on the line $\{(x, y)^{\top} : ax + by + c = 0\}$ defined by $\boldsymbol{\beta}$. The second uniqueness condition on $B_{k(\mathcal{U})}$ is needed for the inductive argument in the proof.

Remark 7. *In a special case where the distribution of (X, Y) is concentrated on K lines $B_{K(S)}$ and contaminated by white Gaussian noise independently drawn from $\mathcal{N}(\mathbf{0}, \sigma^2 \mathbf{I}_2)$ under the supervised scenario, if $\sigma \rightarrow 0$ as $n \rightarrow \infty$, then $\widehat{B}_{K(\mathcal{U})} \rightarrow B_{K(S)}$ almost surely.*

3.3 Asymptotic distribution of the unsupervised sample generalized R^2

Based on Theorems 3.1 and 3.3, we derive the asymptotic distribution of $R_{\mathcal{G}(\mathcal{U})}^2$.

Theorem 3.4. *Under the unsupervised scenario (Section 2.1), we define*

$$\mu_{X^c Y^d, k(\mathcal{U})} = \mathbb{E} \left[\left(\frac{X - \mathbb{E}[X | \widetilde{Z} = k]}{\sqrt{\text{var}(X | \widetilde{Z} = k)}} \right)^c \left(\frac{Y - \mathbb{E}[Y | \widetilde{Z} = k]}{\sqrt{\text{var}(Y | \widetilde{Z} = k)}} \right)^d \middle| \widetilde{Z} = k \right], \quad c, d \in \mathbb{N},$$

where \widetilde{Z} is the random surrogate index defined in (16). Assume $\mu_{X^4, k(\mathcal{U})} < \infty$ and $\mu_{Y^4, k(\mathcal{U})} < \infty$ for all $k = 1, \dots, K$. Then

$$\sqrt{n} \left(R_{\mathcal{G}(\mathcal{U})}^2 - \rho_{\mathcal{G}(\mathcal{U})}^2 \right) \xrightarrow{d} \mathcal{N} \left(0, \gamma_{\mathcal{G}(\mathcal{U})}^2 \right), \quad (36)$$

where $\rho_{\mathcal{G}(\mathcal{U})}^2$ is the unsupervised population generalized R^2 defined in (17), and

$$\gamma_{\mathcal{G}(\mathcal{U})}^2 = \sum_{k=1}^K (A_{k(\mathcal{U})} + B_{k(\mathcal{U})}) + 2 \sum_{1 \leq k < r \leq K} C_{kr(\mathcal{U})}, \quad (37)$$

with

$$\begin{aligned} A_{k(\mathcal{U})} &= p_{k(\mathcal{U})} \left[\rho_{k(\mathcal{U})}^4 (\mu_{X^4, k(\mathcal{U})} + 2\mu_{X^2Y^2, k(\mathcal{U})} + \mu_{Y^4, k(\mathcal{U})}) - 4\rho_{k(\mathcal{U})}^3 (\mu_{X^3Y, k(\mathcal{U})} + \mu_{XY^3, k(\mathcal{U})}) + 4\rho_{k(\mathcal{U})}^2 \mu_{X^2Y^2, k(\mathcal{U})} \right], \\ B_{k(\mathcal{U})} &= p_{k(\mathcal{U})} (1 - p_{k(\mathcal{U})}) \rho_{k(\mathcal{U})}^4, \\ C_{kr(\mathcal{U})} &= -p_{k(\mathcal{U})} p_{r(\mathcal{U})} \rho_{k(\mathcal{U})}^2 \rho_{r(\mathcal{U})}^2, \end{aligned}$$

where $p_{k(\mathcal{U})}$ and $\rho_{k(\mathcal{U})}^2$ are defined in (18) and (19), respectively.

Applying Theorem 3.4 to the special case where $(X, Y)|\tilde{Z}$ follows a bivariate Gaussian distribution, we obtain a much simpler form of the first-order asymptotic distribution of $R_{\mathcal{G}(\mathcal{U})}^2$ in Corollary 3.5.

corollary 3.5. *In the special case of Theorem 3.4 where (X, Y) conditional on $\tilde{Z} = k$ follows a bivariate Gaussian distribution for all $k = 1, \dots, K$, the asymptotic variance of $\sqrt{n} \left(R_{\mathcal{G}(\mathcal{U})}^2 - \rho_{\mathcal{G}(\mathcal{U})}^2 \right)$, i.e., $\gamma_{\mathcal{U}}^2$ in (37), becomes*

$$\begin{aligned} \gamma_{\mathcal{U}}^2 &= \sum_{k=1}^K \left[4p_{k(\mathcal{U})} \rho_{k(\mathcal{U})}^2 \left(1 - \rho_{k(\mathcal{U})}^2 \right)^2 + p_{k(\mathcal{U})} (1 - p_{k(\mathcal{U})}) \rho_{k(\mathcal{U})}^4 \right] \\ &\quad - 2 \sum_{1 \leq k < r \leq K} p_{k(\mathcal{U})} p_{r(\mathcal{U})} \rho_{k(\mathcal{U})}^2 \rho_{r(\mathcal{U})}^2, \end{aligned} \quad (38)$$

which only depends on $p_{k(\mathcal{U})}$ and $\rho_{k(\mathcal{U})}^2$, i.e., the probability of $\tilde{Z} = k$ and the squared Pearson correlation between X and Y conditional on $\tilde{Z} = k$, $k = 1, \dots, K$.

Remark 8. *When $K = 1$, the asymptotic distributions of $R_{\mathcal{G}(\mathcal{S})}^2$ and $R_{\mathcal{G}(\mathcal{U})}^2$ in Theorems 3.1 and 3.4 both reduce to the asymptotic distribution of R^2 (Ferguson, 1996). In the special case that $K = 1$ and (X, Y) follows bivariate Gaussian distribution with correlation ρ , the asymptotic distributions of $R_{\mathcal{G}(\mathcal{S})}^2$ and $R_{\mathcal{G}(\mathcal{U})}^2$ in Corollaries 3.2 and 3.5 both reduce to $\sqrt{n}(R^2 - \rho^2) \xrightarrow{d} \mathcal{N} \left(0, 4\rho^2 (1 - \rho^2)^2 \right)$.*

4. CONVERGENCE PROPERTIES OF THE K -LINES ALGORITHM

Motivated by Bottou and Bengio (1995), we study the convergence properties of our proposed K -lines clustering algorithm (Algorithm 1). Below we show that the K -lines algorithm can be related to a gradient descent algorithm and an expectation-maximization (EM) style algorithm.

4.1 Relating K -lines to a gradient descent algorithm

Given a sample $\{(X_i, Y_i)\}_{i=1}^n$, the K -lines algorithm computes K sample line centers $\hat{B}_{K(\mathcal{U})} = \{\hat{\beta}_{1(\mathcal{U})}, \dots, \hat{\beta}_{K(\mathcal{U})}\}$, which minimize the loss function $W(B_K, P_n)$ defined in (24), the average

squared perpendicular distance between each data point and its closest sample line center. Denoting $B_K = \{\beta_1, \dots, \beta_K\}$, minimizing $W(B_K, P_n)$ is equivalent to minimizing

$$L(B_K) := \sum_{i=1}^n \frac{1}{2} \min_k d_{\perp}^2 \left((X_i, Y_i)^\top, \beta_k \right) = \sum_{i=1}^n \frac{1}{2} d_{\perp}^2 \left((X_i, Y_i)^\top, \beta_{s_i(B_K)} \right), \quad (39)$$

where $s_i(B_K)$ is the index of the closest line center to the i -th data point. Note that $W(B_K, P_n) = \frac{2}{n} L(B_K)$.

We can then derive a gradient descent algorithm based on $L(B_K)$ for $\beta_k = (a_k, b_k, c_k)^\top$:

$$\Delta \beta_k = \sum_{i=1}^n \begin{cases} -\epsilon_t \begin{pmatrix} \frac{(a_k X_i + b_k Y_i + c_k) X_i}{a_k^2 + b_k^2} - \frac{(a_k X_i + b_k Y_i + c_k)^2 a_k}{(a_k^2 + b_k^2)^2} \\ \frac{(a_k X_i + b_k Y_i + c_k) Y_i}{a_k^2 + b_k^2} - \frac{(a_k X_i + b_k Y_i + c_k)^2 b_k}{(a_k^2 + b_k^2)^2} \\ \frac{a_k X_i + b_k Y_i + c_k}{a_k^2 + b_k^2} \end{pmatrix} & \text{if } k = s_i(B_K) \\ (0, 0, 0)^\top & \text{otherwise} \end{cases}, \quad (40)$$

where ϵ_t is the learning rate is to be specified (Kohonen, 1989).

4.2 Relating K -lines to an EM algorithm

Although K -lines does not fit in a probabilistic framework, its derivation is similar to that of the EM algorithm, except that the soft-thresholding of EM is changed to hard-thresholding.

The EM algorithm has the principle of introducing additional hidden variables to simplify the optimization problem. Since these hidden variables are unobservable, the maximization step (i.e., the M step) maximizes an auxiliary function calculated in the expectation step (i.e., the E step), which averages over the possible values of the hidden variables given the parameter estimates from the previous iteration. In our unsupervised scenario, the hidden variables are the assignments $s_1(B_K), \dots, s_n(B_K)$ of the data points to the sample line centers. Instead of considering the expectation of $L(B_K)$ over the distribution on these hidden variables as in the EM algorithm, the K -lines algorithm calculates the values of the hidden variables that maximize the negative loss given the parameter estimates from the previous iteration. That is, the “ Q function” to be maximized in the M step after $(t-1)$ ($t = 1, 2, \dots$) iterations becomes:

$$Q(B_K, B_K^{(t-1)}) := - \sum_{i=1}^n \frac{1}{2} d_{\perp}^2 \left((X_i, Y_i)^\top, \beta_{s_i(B_K^{(t-1)})} \right). \quad (41)$$

The next step is to find

$$B_K^{(t)} := \arg \max_{B_K} Q \left(B_K, B_K^{(t-1)} \right). \quad (42)$$

The solution $B_K^{(t)} = \{\beta_1^{(t)}, \dots, \beta_K^{(t)}\}$ consists of $\beta_k^{(t)}$ calculated by (22), where $\mathcal{C}_k^{(k-1)}$ represents the index set of data points that are closer to $\beta_k^{(t-1)}$ than other sample line centers in perpendicular distance. The K -lines algorithm iterates by replacing $B_K^{(t-1)}$ by $B_K^{(t)}$ using the update equation (42) until convergence. Since $s_i \left(B_K^{(t-1)} \right)$ is by definition the best assignment of the i -th data point to the closet line center in $B_K^{(t-1)}$, we have the following inequality:

$$-L \left(B_K^{(t)} \right) - Q \left(B_K^{(t)}, B_K^{(t-1)} \right) = \frac{1}{2} \sum_{i=1}^n d_{\perp}^2 \left((X_i, Y_i)^{\top}, \beta_{s_i(B_K^{(t-1)})}^{(t)} \right) - d_{\perp}^2 \left((X_i, Y_i)^{\top}, \beta_{s_i(B_K^{(t)})}^{(t)} \right) \geq 0.$$

Using this result, the identity $-L \left(B_K^{(t-1)} \right) = Q \left(B_K^{(t-1)}, B_K^{(t-1)} \right)$, and the definition of $B_K^{(t)}$ in (42), we have the following inequality:

$$\begin{aligned} L \left(B_K^{(t)} \right) - L \left(B_K^{(t-1)} \right) &= L \left(B_K^{(t)} \right) + Q \left(B_K^{(t)}, B_K^{(t-1)} \right) - Q \left(B_K^{(t)}, B_K^{(t-1)} \right) - L \left(B_K^{(t-1)} \right) \\ &\leq -Q \left(B_K^{(t)}, B_K^{(t-1)} \right) + Q \left(B_K^{(t-1)}, B_K^{(t-1)} \right) \stackrel{(42)}{\leq} 0. \end{aligned} \quad (43)$$

Hence, each iteration decreases the loss function until $B_K^{(t)} = B_K^{(t-1)}$, denoted by B_K^* . Since the assignments $s_1(B_K), \dots, s_n(B_K)$ are discrete, there is an open neighborhood of B_K^* in which the assignments are constant. Based on their definitions, the functions $-L(\cdot)$ and $Q(\cdot, B_K^*)$ are equal in this neighborhood. Therefore, B_K^* , the maximum of the function $Q(\cdot, B_K^*)$, is also a local minimum of the loss function $L(\cdot)$.

We can further show that the M step of an EM algorithm under a bivariate Gaussian mixture model is the same as the M step of the K -lines algorithm in (42). We assume that $(X_i, Y_i) \stackrel{\text{i.i.d.}}{\sim} \sum_{k=1}^K p_k \mathcal{N}(\mu_k, \Sigma_k)$ with mean vectors μ_k and covariance matrices Σ_k , $k = 1, \dots, K$, and we denote $\Theta = \{p_k, \mu_k, \Sigma_k\}_{k=1}^K$. The hidden variables are $Z_i \stackrel{\text{i.i.d.}}{\sim} \text{Multinomial}(K, (p_1, \dots, p_K)^{\top})$. Suppose that in the t -th iteration of the EM algorithm, the E step computes $\delta_{ik}^{(t)} := \mathbb{P}(Z_i = k \mid (X_i, Y_i), \Theta^{(t-1)})$. The next M step would then update the value of Σ_k as

$$\Sigma_k^{(t)} = \begin{bmatrix} \frac{\sum_{i=1}^n \delta_{ik}^{(t)} (X_i - \bar{X}_k^{(t)})^2}{\sum_{i=1}^n \delta_{ik}^{(t)}} & \frac{\sum_{i=1}^n \delta_{ik}^{(t)} (X_i - \bar{X}_k^{(t)}) (Y_i - \bar{Y}_k^{(t)})}{\sum_{i=1}^n \delta_{ik}^{(t)}} \\ \frac{\sum_{i=1}^n \delta_{ik}^{(t)} (X_i - \bar{X}_k^{(t)}) (Y_i - \bar{Y}_k^{(t)})}{\sum_{i=1}^n \delta_{ik}^{(t)}} & \frac{\sum_{i=1}^n \delta_{ik}^{(t)} (Y_i - \bar{Y}_k^{(t)})^2}{\sum_{i=1}^n \delta_{ik}^{(t)}} \end{bmatrix}, \quad (44)$$

where $\bar{X}_k^{(t)} = \frac{\sum_{i=1}^n \delta_{ik}^{(t)} X_i}{\sum_{i=1}^n \delta_{ik}^{(t)}}$ and $\bar{Y}_k^{(t)} = \frac{\sum_{i=1}^n \delta_{ik}^{(t)} Y_i}{\sum_{i=1}^n \delta_{ik}^{(t)}}$.

If we modify the EM algorithm by replacing the E step in every iteration by that of the K -lines algorithm, i.e., define

$$\delta_{ik}^{(t)} := \mathbb{I} \left\{ d_{\perp} \left((X_i, Y_i)^{\top}, \beta_k^{(t-1)} \right) < d_{\perp} \left((X_i, Y_i)^{\top}, \beta_r^{(t-1)} \right), \forall r \neq k \right\} \quad (45)$$

in a hard-thresholding way (assuming that every data point is closest to only one sample line center in perpendicular distance), the M step still updates $\Sigma_k^{(t)}$ as in (44). Then by (22), $\beta_k^{(t)} = \left(\hat{u}_{12,k}^{(t)}, -\hat{u}_{11,k}^{(t)}, -\hat{u}_{12,k}^{(t)} \bar{X}_k^{(t)} + \hat{u}_{11,k}^{(t)} \bar{Y}_k^{(t)} \right)^{\top}$, where $\left(\hat{u}_{11,k}^{(t)}, \hat{u}_{12,k}^{(t)} \right)^{\top}$ is the eigenvector corresponding to the largest eigenvalue of $\Sigma_k^{(t)}$, minimizes the function $\sum_{i=1}^n \delta_{ik}^{(t)} d_{\perp}^2 \left((X_i, Y_i)^{\top}, * \right)$. Hence, $B_K^{(t)} = \left\{ \beta_1^{(t)}, \dots, \beta_K^{(t)} \right\}$ is the same solution as in (42).

5. SIMULATIONS

In this section, we perform simulations under various distributional settings to numerically verify the theoretical results in Section 3 and to compare the statistical power of our generalized R^2 measures with that of multiple association measures.

5.1 Numerical verification of theoretical results

We first compare the asymptotic distributions in Section 3 with numerically simulated finite-sample distributions under eight settings (Table 1), where $(X, Y)|Z$ follows a bivariate Gaussian distribution under the first four settings and a bivariate t distribution under the latter four settings. Under each setting, we generate $B = 1000$ samples with sizes $n = 50$ or 100 , calculate the supervised and unsupervised sample generalized R^2 measures ($R_{\mathcal{G}(S)}^2$ and $R_{\mathcal{G}(U)}^2$) of each sample, and compare the simulated finite-sample distributions of those sample measures to the corresponding asymptotic distributions. In the first four settings, the asymptotic distributions of $R_{\mathcal{G}(S)}^2$ and $R_{\mathcal{G}(U)}^2$ are from Corollaries 3.2 and 3.5 (the bivariate Gaussian results), respectively. In the latter four settings, the asymptotic distributions of $R_{\mathcal{G}(S)}^2$ and $R_{\mathcal{G}(U)}^2$ are from Theorems 3.1 and 3.4 (the general results), respectively. Figure 3 illustrates the comparison results, which show that the finite-sample distributions and the asymptotic results have good agreement. These results justify the use of the asymptotic distributions for statistical inference of $\rho_{\mathcal{G}(S)}^2$ or $\rho_{\mathcal{G}(U)}^2$ based on a finite-sized sample.

However, as the asymptotic distributions in Section 3 involve unobservable parameters in the asymptotic variances, they cannot be directly used for statistical inference of $\rho_{\mathcal{G}(S)}^2$ or $\rho_{\mathcal{G}(U)}^2$. A classical solution is to plug in the parameter estimates into the asymptotic variances. Another popular solution is to use the bootstrap, which is computationally more intensive than the plug-in approach. Here we numerically verify whether the plug-in approach works reasonably well for statistical inference of $\rho_{\mathcal{G}(S)}^2$ and $\rho_{\mathcal{G}(U)}^2$. Under each of the eight settings (Table 1), we simulate two samples with sizes $n = 50$ and $n = 100$, respectively. We then use each sample to construct a 95% confidence interval (CI) of $\rho_{\mathcal{G}(S)}^2$ and $\rho_{\mathcal{G}(U)}^2$ as $R_{\mathcal{G}(S)}^2 \pm 1.96\sqrt{\widehat{\text{var}}(R_{\mathcal{G}(S)}^2)}$ and $R_{\mathcal{G}(U)}^2 \pm 1.96\sqrt{\widehat{\text{var}}(R_{\mathcal{G}(U)}^2)}$, respectively. We construct the variance estimates $\widehat{\text{var}}(R_{\mathcal{G}(S)}^2)$ and $\widehat{\text{var}}(R_{\mathcal{G}(U)}^2)$ in two ways: using (1) the plug-in estimates of the asymptotic variances of $R_{\mathcal{G}(S)}^2$ and $R_{\mathcal{G}(U)}^2$, or (2) the bootstrap estimates of $\text{var}(R_{\mathcal{G}(S)}^2)$ and $\text{var}(R_{\mathcal{G}(U)}^2)$. We also calculate the true asymptotic variances of $R_{\mathcal{G}(S)}^2$ and $R_{\mathcal{G}(U)}^2$ and use them as the standard. In the calculation of the true asymptotic variances, whenever an exact closed form is not attainable, we generate a large sample with size 100,000 from the population and use the plug-in estimate to approximate the true asymptotic variance. In the first four settings as mixtures of bivariate Gaussians, we use the asymptotic variances from Corollaries 3.2 and 3.5, and we perform the parametric bootstrap to obtain the bootstrap estimates. In the latter four settings as mixtures of bivariate t distributions, we compare the non-parametric bootstrap approach with two plug-in options: the first is to plug in the asymptotic variances of the special bivariate Gaussian forms in Corollaries 3.2 and 3.5, and the second is to plug in the asymptotic variances of the general forms in Theorems 3.1 and 3.4. The results in Figure 4 show that the CIs constructed from the same sample by the plug-in and bootstrap approaches have similar lengths. When n increases from 50 to 100, the CIs constructed by both approaches agree better with the theoretical CIs based on the true asymptotic variances, as expected. In addition, under Settings 5-8, where the bivariate Gaussian assumption does not hold, the two plug-in options result in similar CIs.

We also evaluate the coverage probabilities of the 95% CIs constructed by the plug-in approach and compare them with those of the theoretical CIs based on the true asymptotic variances. Table 2 summarizes the results. The theoretical CIs have coverage probabilities close to 95% under all the eight settings in both scenarios, providing additional verification of the asymptotic distributions de-

rived in Section 3. The plug-in confidence intervals have coverage probabilities increasingly similar to 95% as n increases. Their coverage probabilities are in general closer to 95% under Settings 1-4 (mixtures of bivariate Gaussians) than under Settings 5-8 (mixtures of bivariate t -distributions). The reason is that the former four settings have distributions more concentrated on K lines and allow the K -lines algorithm to find the sample line centers more easily, thus reducing the unwanted variance caused by the failed convergence of the algorithm and making the actual variance of the resulting $R_{\mathcal{G}(U)}^2$ more similar to its plug-in variance estimate. Comparing the supervised and unsupervised scenarios, the plugin-confidence intervals, as expected, have better coverage probabilities when supervised. Overall the plug-in confidence intervals have good coverage probabilities; even under the most difficult cases, i.e., Settings 5-8 under the unsupervised scenarios, the plug-in CIs still have coverage probabilities greater than 87% when $n = 100$. Table 2 also shows that the two plug-in options do not have obvious differences, suggesting that the first plug-in option, i.e., plugging into the asymptotic variances in the special bivariate Gaussian forms (Corollaries 3.2 and 3.5), is robust and can be used in practice for its simplicity. Given these results and the consideration of computational efficiency, we recommend using the first plug-in option for statistical inference of $\rho_{\mathcal{G}(S)}^2$ and $\rho_{\mathcal{G}(U)}^2$.

5.2 Use of the scree plot and AIC to choose K

Following Section 2.5, here we demonstrate the results of using the scree plot or AIC to choose K in the eight simulation settings (Table 1). Under each setting, we simulate a sample of size $n = 100$ and evaluate $W(B_K, P_n)$ (24), the average within-cluster squared perpendicular distance, and $\text{AIC}(K)$ (29) on this sample for K ranging from 1 to 10. Figure 5 shows the results. For all the eight settings, the scree plots and the AIC suggest K values that agree with the true K values. Even though Settings 4 to 8 violate the bivariate Gaussian assumption required by the AIC, the AIC results are still reasonable. In practice, users may use the scree plot together with the AIC to decide a reasonable choice of K .

5.3 Power analysis

Recall that the motivation of this study is to develop powerful association measures for capturing a mixture of linear dependences between two real-valued random variables, a relationship that

is complex but interpretable. To confirm that the proposed unsupervised sample generalized R^2 measure, i.e., $R_{\mathcal{G}(\mathcal{U})}^2$ with $K = 2$, is indeed a powerful measure, we conduct a simulation study to compare it with four existing association measures: the squared Pearson correlation (R^2), the maximal correlation (Hirschfeld, 1935; Gebelein, 1941; Rényi, 1959) estimated by the alternating condition expectation algorithm Breiman and Friedman (1985), the distance correlation (Székely et al., 2007, 2009), and the maximal information coefficient (MIC) (Reshef et al., 2011). For MIC, we use the implementation in R package `minerva` (version 1.4.7). All the five measures have values in $[0, 1]$. Our simulation procedure follows the study of Simon and Tibshirani (2014), where each relationship between two real-valued random variables X and Y is composed of a marginal distribution of $X \sim \mathcal{N}(0, 5^2)$, a noiseless pattern representing a noiseless relationship between X and Y , and a random error from $\mathcal{N}(0, \sigma^2)$ added to Y . Given a noiseless pattern and σ , the corresponding relationship is the alternative hypothesis, while the null hypothesis is that X and Y are independent. Given a sample size $n = 30, 50, \text{ or } 200$, we simulate $B = 1000$ samples from the alternative hypothesis. For each sample, we randomly permute the Y observations to create a sample from the null hypothesis. Then we calculate the values of the five association measures on the 1000 samples from the null, and decide a rejection threshold for each measure as the $(1 - \alpha)$ quantile among its 1000 values, where $\alpha = 0.05$ is the pre-specified significance level. Next we calculate the values of the five association measures on the 1000 samples from the alternative hypothesis, compare each measure’s 1000 values with its rejection threshold, and estimate the measures’s power as the proportion of values above the threshold.

Figure 6 summarizes the power analysis results for four patterns. When the noiseless pattern is linear, the squared Pearson correlation is the most powerful measure, while the other four measures also have the perfect power at $n = 30$ up to $\sigma = 3$. When the noiseless pattern is a parabola, the maximal correlation is the most powerful measure, while R^2 has low power as expected. Since the parabola pattern can be approximated by two intersecting lines, $R_{\mathcal{G}(\mathcal{U})}^2$ is also demonstrated to have good power, which is comparable to the power of the three measures (maxCor, dCor, and MIC) that aim to capture the general dependence. When the noiseless pattern is a mixture of positive and negative linear dependences, $R_{\mathcal{G}(\mathcal{U})}^2$ is clearly the most powerful measure as it is designed to be. Moreover, when the noiseless pattern is two tangent arcs plus some outliers, a pattern that

can be approximated by a mixture of positive and negative linear dependences, $R_{\mathcal{G}(\mathcal{U})}^2$ is still the most powerful measure. These results confirm the application potential of $R_{\mathcal{G}(\mathcal{U})}^2$ in capturing relationships as mixtures of linear dependences.

In addition, Figure A4 illustrates each measures’s 1000 values at each n and σ . As expected, all the measures exhibit decreasing variances as n increases. Except MIC, the other four measures show a monotone trend of increasing variances as σ increases, which is reasonable. As expected, R^2 gives low values except for the linear pattern. Among the five measures, $R_{\mathcal{G}(\mathcal{U})}^2$ has the smallest variances when the noiseless pattern is a mixture of positive and negative linear dependences.

6. REAL DATA APPLICATIONS

6.1 Gene expression analysis in Arabidopsis

Back to our motivating example in *Arabidopsis thaliana*, we would like to use its gene expression data to demonstrate the use of our generalized R^2 measures in capturing biologically meaningful gene-gene relationships. The glucosinolate (GSL) biosynthesis pathway has been well studied in *Arabidopsis thaliana*, and 31 genes have been experimentally verified in this pathway (Kim et al., 2012). Given that genes in the same pathway are known to be functionally related, those 31 genes should have pairwise gene expression relationships distinct from their relationships with other genes outside of the GSL pathway. Hence, a powerful association measure should be able to distinguish the pairwise gene-gene relationships within the GSL pathway from the relationship of two randomly paired GSL and non-GSL genes.

It is worth noting that the gene expression data (Table A1 in Appendix B) contain four index variables: `condition` (oxidation, wounding, UV-B light, and drought), `treatment` (yes and no), `replicate` (1 and 2), and `tissue` (root and shoot). From our exploratory data analysis, we observe that only the `tissue` variable is a good indicator of linear dependences, as demonstrated in Figure 1 and Figures A1-A3 in the Appendix. Therefore, we expect that our supervised sample generalized R^2 , i.e., $R_{\mathcal{G}(S)}^2$ is only meaningful when it uses the `tissue` variable as the index variable Z . For our unsupervised sample generalized R^2 , i.e., $R_{\mathcal{G}(\mathcal{U})}^2$, we set $K = 2$.

The results in Figure 7A show the comparison of five unsupervised measures (the squared Pearson correlation R^2 , the maximal correlation “maxCor,” the distance correlation “dCor,” the

maximal information coefficient “MIC,” and our $R_{\mathcal{G}(\mathcal{U})}^2(K = 2)$) and four supervised measures ($R_{\mathcal{G}(\mathcal{S})}^2$ with the index variable as `condition`, `treatment`, `replicate`, or `tissue`). As expected, $R_{\mathcal{G}(\mathcal{S})}^2$ (tissue) is the only supervised measure that shows stronger relationships between the GSL gene pairs than the random GSL-nonGSL gene pairs. Among the five unsupervised measures, $R_{\mathcal{G}(\mathcal{U})}^2(K = 2)$ is the only one that shows the same trend between the two groups of gene pairs as does $R_{\mathcal{G}(\mathcal{S})}^2$ (tissue). These results demonstrate that $R_{\mathcal{G}(\mathcal{S})}^2$ is a useful and powerful measure when users have prior knowledge on the index variable. Moreover, these results show the advantage of $R_{\mathcal{G}(\mathcal{U})}^2$ in capturing complex but interpretable gene-gene relationships even in the lack of prior knowledge.

6.2 Cell-cycle gene expression analysis based on single-cell RNA sequencing data

In the second real data application, we apply the same five unsupervised measures (R^2 , `maxCor`, `dCor`, `MIC`, and $R_{\mathcal{G}(\mathcal{U})}^2$ with $K = 2$) used in the last application to studying pairwise relationships among 625 mouse cell-cycle genes. The data are from a single-cell RNA-sequencing (scRNA-seq) dataset including gene expression levels in 182 mouse cells, which span three stages (G1, G2M, and S) in a cell cycle (Buettner et al., 2015). Our exploratory data analysis suggests that the cell stage variable is not a good index variable for linear dependences, so we does not include the supervised $R_{\mathcal{G}(\mathcal{S})}^2$ in this study. For information on the data accession and preprocessing, please refer to Section B.2 in the Appendix.

We randomly select 614 gene pairs from all the $\binom{625}{2} = 195,000$ cell-cycle gene pairs, compute the five measures on each pair, and summarize the empirical distributions of the five measures’ 614 values in Figure 7B. In the results, $R_{\mathcal{G}(\mathcal{U})}^2(K = 2)$ is the only measure that demonstrates a two-mode distribution, revealing that certain cell-cycle gene pairs have strong relationships that are distinct from the rest pairs. This result is biologically reasonable, because some cell cycle genes are known to function together, while others do not. In contrast, the squared Pearson correlation R^2 has dominantly low values, indicating its low power in detecting complex gene-gene relationships from a mix of cells in multiple cell cycle stages. The other three measures, `maxCor`, `dCor`, and `MIC`, although having overall larger values than R^2 , do not show a clear division of cell-cycle gene pairs into the strongly related ones and others. Hence, from a scientific discovery perspective,

$R_{\mathcal{G}(\mathcal{U})}^2(K = 2)$ reveals the most information among the five measures.

Although experimental validation is required to verify and understand the strongly related genes found by $R_{\mathcal{G}(\mathcal{U})}^2(K = 2)$, as a preliminary check, we search the literature to confirm the biological functional relatedness of the gene pairs that have top $R_{\mathcal{G}(\mathcal{U})}^2$ values. The results are promising. For example, the gene pair *Cdc25b-Lats2* receive the highest $R_{\mathcal{G}(\mathcal{U})}^2$ value, and their physical interaction has been previously reported (Mukai et al., 2015). Moreover, *Lats2* appears in 17 out of the randomly sampled 614 gene pairs, and 11 of those 17 gene pairs are among the top 25% pairs that have the highest $R_{\mathcal{G}(\mathcal{U})}^2$ values. This result is consistent with a known fact that *Lats2* is an essential regulator gene that interacts with many cell-cycle genes (Yabuta et al., 2007).

7. DISCUSSIONS

In the application of the unsupervised sample generalized R^2 , i.e., $R_{\mathcal{G}(\mathcal{U})}^2$, the closed-form asymptotic distribution of $R_{\mathcal{G}(\mathcal{U})}^2$ (Section 3) and the plug-in approach (Section 5) together allow a fast computation of the p -value associated with an observed $R_{\mathcal{G}(\mathcal{U})}^2$ value given K , i.e., the number of linear dependences. A practical question is how to set the value of K . To detect the relationship between X and Y without a pre-specified K , a reasonable approach is to design a sequential test for $K = 1, 2, \dots, K_{\max}$, where K_{\max} is the maximum number of linear dependences a user would like to consider, often 2 or 3. Specifically, one starts with $K = 1$, that is, testing the hypotheses $H_0 : \rho = 0$ vs. $H_1 : \rho \neq 0$, and the test statistic is R^2 . If the test is rejected at a given significance level (e.g., 0.05), the sequential test stops; otherwise, the sequential test will continue to test $H_0 : \rho_{\mathcal{G}(\mathcal{U})}^2 = 0$ vs. $H_1 : \rho_{\mathcal{G}(\mathcal{U})}^2 \neq 0$ for $K = 2$. The sequential test will stop whenever it encounters a rejection, or after it finishes the test at K_{\max} . A future research question is how to design the significance level at each step of the sequential test, so that the overall type I error is controlled under a user-specified threshold.

In gene expression analysis, for example, this sequential test will allow users to detect gene-gene interactions up to a mixture of K_{\max} linear dependences based on their scientific interests. The detected gene-gene interactions can be used to construct a gene co-expression network, whose nodes and edges represent individual genes and the pairwise gene-gene interactions. A valid gene co-expression network allows researchers to leverage existing knowledge on the functions of hundreds of

key genes, which have been well studied by experimentalists, so that the functions of those key genes can be used to infer the functions of the less-studied genes based on the network information. Gene co-expression networks have been widely used to study gene regulatory mechanisms in diseases such as cancers (Stuart et al., 2003; Aggarwal et al., 2006; Horvath et al., 2006; Zhao et al., 2010). A key challenge in the state-of-the-art gene co-expression network analysis is how to find good biological interpretation of the complex network structure (Serin et al., 2016). Pearson correlation, the most widely used similarity measure for network construction, provides an easy interpretation on the network edges but lacks a good power to capture widespread gene-gene relationships that are more complex than the linear relationship. Our proposed generalized R^2 measures and the sequential test will provide a powerful alternative way for network construction, as they can capture more complex relationships than the Pearson correlation does, and meanwhile they still maintain good interpretability of the resulting network edges.

In many applications such as our *Arabidopsis* study in Section 6.1, discrete variables are observable and may serve as candidates for the index variable Z . A key question is, do any of the discrete variables provide useful information for capturing interpretable relationships among the real-valued variables of interest, and if yes, what these variables are. In this regard, the unsupervised measure $R_{\mathcal{G}(\mathcal{U})}^2$, as a powerful measure for capturing a mixture of linear dependences without knowing the index variable, provides useful guidance for users. Given the observed $R_{\mathcal{G}(\mathcal{U})}^2$ values, users can select the discrete variables, which, if existing and used as the index variable, lead to supervised measures $R_{\mathcal{G}(\mathcal{S})}^2$ that give values with a similar trend as the $R_{\mathcal{G}(\mathcal{U})}^2$ values. Those selected variables will serve as an informative basis for understanding the captured relationships. If none of the discrete variables are informative, the unsupervised measure and its accompanying K -lines clustering algorithm still provide users with a way to investigate the hidden factor that drive the captured relationships.

As a future direction, we can further extend the generalized R^2 measures to be rank-based measures, similar to the idea behind the Spearman’s rank correlation (Spearman, 1904). Specifically, we can first convert the sample $(X_1, Y_1), \dots, (X_n, Y_n)$ into $(R_1, T_1), \dots, (R_n, T_n)$, where R_i and T_i are the ranks of X_i among X_1, \dots, X_n and Y_i among Y_1, \dots, Y_n , respectively. Then we can calculate $R_{\mathcal{G}(\mathcal{S})}^2$ and $R_{\mathcal{G}(\mathcal{U})}^2$ based on $(R_1, T_1), \dots, (R_n, T_n)$, and the resulting sample measures can be

defined as the *ranked-based sample generalized R^2 measures*. Advantages of this extension include the increased robustness to outliers and the ability to capture a mixture of monotone relationships. However, there are of course limitations. The prominent one is the lack of population versions for the rank-based measures, making statistical inference impossible.

To elevate our generalized R^2 measures to more abstract statistical thinking, we think of the new measures as interpretable additive structures of fundamental elements. The additive structures are predominant in statistics, both due to their good interpretability and the universal finite sample constraint of statistical problems. In the most-commonly used linear regression, features are combined additively to make prediction. Other examples include the well-known additive models (Hastie and Tibshirani, 1986) for regression and a more recent FANS model (Fan et al., 2016) for classification. Here we elaborate the parallel between the proposed generalized R^2 measures and the additive models. Seemingly two drastically different topics, the generalized R^2 measures and the additive models share similar philosophical flavors. From the model complexity perspective, the additive models are more flexible than the linear model and can capture more complex relationships between the response variable and the predictors; the generalized R^2 measures are more flexible than the Pearson correlation and can capture relationships more complex than the linear relationship between two real-valued variables. From the model interpretability perspective, the additive model still keeps good interpretability from its additive nature, i.e., each additive component exactly corresponds to the effects of that individual feature; the generalized R^2 measures have good interpretability also from its “additive nature,” i.e., the target relationship is composed of linear dependences, each of which is well interpretable.

SOFTWARE

We have implemented the inference of the supervised and unsupervised generalized R^2 measures, the K -lines algorithm, as well as the choice of K , in an R package `gR2` available at GitHub: <https://github.com/lijy03/gR2>.

REFERENCES

- Aggarwal, A., D. L. Guo, Y. Hoshida, S. T. Yuen, K.-M. Chu, S. So, A. Boussioutas, X. Chen, D. Bowtell, H. Aburatani, et al. (2006). Topological and functional discovery in a gene coexpression meta-network of gastric cancer. *Cancer research* 66(1), 232–241.
- Akaike, H. (1998). Information theory and an extension of the maximum likelihood principle. In *Selected papers of hirotugu akaike*, pp. 199–213. Springer.
- Benaglia, T., D. Chauveau, D. Hunter, and D. Young (2009). mixtools: An r package for analyzing finite mixture models. *Journal of Statistical Software* 32(6), 1–29.
- Bjerve, S. and K. Doksum (1993). Correlation curves: measures of association as functions of covariate values. *The Annals of Statistics*, 890–902.
- Blyth, C. R. (1972). On simpson’s paradox and the sure-thing principle. *Journal of the American Statistical Association* 67(338), 364–366.
- Bottou, L. and Y. Bengio (1995). Convergence properties of the k-means algorithms. In *Advances in neural information processing systems*, pp. 585–592.
- Breiman, L. and J. H. Friedman (1985). Estimating optimal transformations for multiple regression and correlation. *Journal of the American statistical Association* 80(391), 580–598.
- Buettner, F., K. N. Natarajan, F. P. Casale, V. Proserpio, A. Scialdone, F. J. Theis, S. A. Teichmann, J. C. Marioni, and O. Stegle (2015). Computational analysis of cell-to-cell heterogeneity in single-cell rna-sequencing data reveals hidden subpopulations of cells. *Nature biotechnology* 33(2), 155.
- Cover, T. M. and J. A. Thomas (2012). *Elements of information theory*. John Wiley & Sons.
- De Veaux, R. D. (1989). Mixtures of linear regressions. *Computational Statistics & Data Analysis* 8(3), 227–245.
- Delicado, P. and M. Smrekar (2009). Measuring non-linear dependence for two random variables distributed along a curve. *Statistics and Computing* 19(3), 255.

- Fan, J., Y. Feng, J. Jiang, and X. Tong (2016). Feature augmentation via nonparametrics and selection (fans) in high-dimensional classification. *Journal of the American Statistical Association* 111(513), 275–287. PMID: 27185970.
- Ferguson, T. S. (1996). *A course in large sample theory*. Chapman & Hall.
- Fisher, R. A. (1915). Frequency distribution of the values of the correlation coefficient in samples from an indefinitely large population. *Biometrika* 10(4), 507–521.
- Gebelein, H. (1941). Das statistische problem der korrelation als variations-und eigenwertproblem und sein zusammenhang mit der ausgleichsrechnung. *ZAMM-Journal of Applied Mathematics and Mechanics/Zeitschrift für Angewandte Mathematik und Mechanik* 21(6), 364–379.
- Gorfine, M., R. Heller, and Y. Heller (2012). Comment on detecting novel associations in large data sets. *Unpublished (available at <http://emotion.technion.ac.il/~gorfinm/files/science6.pdf> on 11 Nov. 2012)*.
- Gretton, A., O. Bousquet, A. Smola, and B. Schölkopf (2005). Measuring statistical dependence with hilbert-schmidt norms. In *International conference on algorithmic learning theory*, pp. 63–77. Springer.
- Hastie, T. and R. Tibshirani (1986). Generalized additive models. *Statistical Science* 1(3), 297–318.
- Hawkins, D. S., D. M. Allen, and A. J. Stromberg (2001). Determining the number of components in mixtures of linear models. *Computational Statistics & Data Analysis* 38(1), 15–48.
- Heller, R., Y. Heller, and M. Gorfine (2012). A consistent multivariate test of association based on ranks of distances. *Biometrika* 100(2), 503–510.
- Hirschfeld, H. O. (1935). A connection between correlation and contingency. In *Mathematical Proceedings of the Cambridge Philosophical Society*, Volume 31, pp. 520–524. Cambridge University Press.
- Hoeffding, W. (1948). A non-parametric test of independence. *The annals of mathematical statistics*, 546–557.

- Horvath, S., B. Zhang, M. Carlson, K. Lu, S. Zhu, R. Felciano, M. Laurance, W. Zhao, S. Qi, Z. Chen, et al. (2006). Analysis of oncogenic signaling networks in glioblastoma identifies aspm as a molecular target. *Proceedings of the National Academy of Sciences* 103(46), 17402–17407.
- Hurn, M., A. Justel, and C. P. Robert (2003). Estimating mixtures of regressions. *Journal of computational and graphical statistics* 12(1), 55–79.
- Jacobs, R. A., M. I. Jordan, S. J. Nowlan, and G. E. Hinton (1991). Adaptive mixtures of local experts. *Neural computation* 3(1), 79–87.
- Jolliffe, I. (2011). Principal component analysis. In *International encyclopedia of statistical science*, pp. 1094–1096. Springer.
- Jolliffe, I. T. (1982). A note on the use of principal components in regression. *Applied Statistics*, 300–303.
- Jones, P. and G. McLachlan (1992). Fitting finite mixture models in a regression context. *Australian & New Zealand Journal of Statistics* 34(2), 233–240.
- Kendall, M. G. (1938). A new measure of rank correlation. *Biometrika* 30(1/2), 81–93.
- Kim, K., K. Jiang, S. L. Teng, L. J. Feldman, and H. Huang (2012). Using biologically interrelated experiments to identify pathway genes in arabidopsis. *Bioinformatics* 28(6), 815–822.
- Kohonen, T. (1989). *Self-organization and associative memory*, Volume 3rd edition. Springer-Verlag, Berlin.
- Kraskov, A., H. Stögbauer, and P. Grassberger (2004). Estimating mutual information. *Physical review E* 69(6), 066138.
- Lehmann, E. L. (2004). *Elements of large-sample theory*. Springer Science & Business Media.
- Leisch, F. (2008). Modelling background noise in finite mixtures of generalized linear regression models. In *COMPSTAT 2008*, pp. 385–396. Springer.

- Li, J., B. G. Hansen, J. A. Ober, D. J. Kliebenstein, and B. A. Halkier (2008). Subclade of flavin-monooxygenases involved in aliphatic glucosinolate biosynthesis. *Plant Physiology* 148(3), 1721–1733.
- Li, K.-C. (2002). Genome-wide coexpression dynamics: theory and application. *Proceedings of the National Academy of Sciences* 99(26), 16875–16880.
- Li, W. V. and J. J. Li (2018). An accurate and robust imputation method scimpute for single-cell rna-seq data. *Nature communications* 9(1), 997.
- Lloyd, S. (1982). Least squares quantization in pcm. *IEEE transactions on information theory* 28(2), 129–137.
- Morrison, D. F. (1967). *Multivariate statistical methods*. McGraw Hill, New York.
- Mukai, S., N. Yabuta, K. Yoshida, A. Okamoto, D. Miura, Y. Furuta, T. Abe, and H. Nojima (2015). Lats1 suppresses centrosome overduplication by modulating the stability of cdc25b. *Scientific reports* 5, 16173.
- Murtagh, F. and A. Raftery (1984). Fitting straight lines to point patterns. *Pattern recognition* 17, 479–483.
- Pearson, K., A. Lee, and L. Bramley-Moore (1899). Mathematical contributions to the theory of evolution. vi. genetic (reproductive) selection: Inheritance of fertility in man, and of fecundity in thoroughbred racehorses. *Philosophical Transactions of the Royal Society of London. Series A, Containing Papers of a Mathematical or Physical Character* 192, 257–330.
- Pollard, D. et al. (1981). Strong consistency of k -means clustering. *The Annals of Statistics* 9(1), 135–140.
- Quandt, R. E. and J. B. Ramsey (1978). Estimating mixtures of normal distributions and switching regressions. *Journal of the American statistical Association* 73(364), 730–738.
- Rényi, A. (1959). On measures of dependence. *Acta mathematica hungarica* 10(3-4), 441–451.

- Reshef, D. N., Y. A. Reshef, H. K. Finucane, S. R. Grossman, G. McVean, P. J. Turnbaugh, E. S. Lander, M. Mitzenmacher, and P. C. Sabeti (2011). Detecting novel associations in large data sets. *science* 334(6062), 1518–1524.
- Samuelson, P. A. (1942). A note on alternative regressions. *Econometrica: Journal of the Econometric Society*, 80–83.
- Scharl, T., B. Grün, and F. Leisch (2009). Mixtures of regression models for time course gene expression data: evaluation of initialization and random effects. *Bioinformatics* 26(3), 370–377.
- Serin, E. A., H. Nijveen, H. W. Hilhorst, and W. Ligterink (2016). Learning from co-expression networks: possibilities and challenges. *Frontiers in plant science* 7, 444.
- Shannon, C. E., W. Weaver, and A. W. Burks (1951). The mathematical theory of communication.
- Simon, N. and R. Tibshirani (2014). Comment on” detecting novel associations in large data sets” by reshef et al, science dec 16, 2011. *arXiv preprint arXiv:1401.7645*.
- Simpson, E. H. (1951). The interpretation of interaction in contingency tables. *Journal of the Royal Statistical Society. Series B (Methodological)*, 238–241.
- Smith, R. J. (2009). Use and misuse of the reduced major axis for line-fitting. *American Journal of Physical Anthropology: The Official Publication of the American Association of Physical Anthropologists* 140(3), 476–486.
- Spearman, C. (1904). The proof and measurement of association between two things. *The American journal of psychology* 15(1), 72–101.
- Stuart, J. M., E. Segal, D. Koller, and S. K. Kim (2003). A gene-coexpression network for global discovery of conserved genetic modules. *science* 302(5643), 249–255.
- Székely, G. J., M. L. Rizzo, et al. (2009). Brownian distance covariance. *The annals of applied statistics* 3(4), 1236–1265.
- Székely, G. J., M. L. Rizzo, and N. K. Bakirov (2007). Measuring and testing dependence by correlation of distances. *The annals of statistics*, 2769–2794.

- Turner, T. R. (2000). Estimating the propagation rate of a viral infection of potato plants via mixtures of regressions. *Journal of the Royal Statistical Society: Series C (Applied Statistics)* 49(3), 371–384.
- Wang, X., B. Jiang, and J. S. Liu (2017). Generalized r-squared for detecting dependence. *Biometrika* 104(1), 129–139.
- Wang, Y. R., M. S. Waterman, and H. Huang (2014). Gene coexpression measures in large heterogeneous samples using count statistics. *Proceedings of the National Academy of Sciences* 111(46), 16371–16376.
- Wedel, M. and W. S. DeSarbo (1994). A review of recent developments in latent class regression models.
- Yabuta, N., N. Okada, A. Ito, T. Hosomi, S. Nishihara, Y. Sasayama, A. Fujimori, D. Okuzaki, H. Zhao, M. Ikawa, et al. (2007). Lats2 is an essential mitotic regulator required for the coordination of cell division. *Journal of Biological Chemistry* 282(26), 19259–19271.
- Yule, G. U. (1903). Notes on the theory of association of attributes in statistics. *Biometrika* 2(2), 121–134.
- Zhao, W., P. Langfelder, T. Fuller, J. Dong, A. Li, and S. Hovarth (2010). Weighted gene co-expression network analysis: state of the art. *Journal of biopharmaceutical statistics* 20(2), 281–300.
- Zheng, S., N.-Z. Shi, and Z. Zhang (2012). Generalized measures of correlation for asymmetry, nonlinearity, and beyond. *Journal of the American Statistical Association* 107(499), 1239–1252.

Setting	K	Population	Parameters
1	$K = 2$		$p_1 = p_2 = 0.5$ $\boldsymbol{\mu}_1 = (0, -2)^\top, \boldsymbol{\mu}_2 = (0, 2)^\top$ $\boldsymbol{\Sigma}_1 = \boldsymbol{\Sigma}_2 = \begin{bmatrix} 1 & 0.8 \\ 0.8 & 1 \end{bmatrix}$
2	$K = 2$	Supervised: $\mathbb{P}(Z = k) = p_k$ $(X, Y) (Z = k) \sim \mathcal{N}(\boldsymbol{\mu}_k, \boldsymbol{\Sigma}_k)$ $k = 1, \dots, K$	$p_1 = p_2 = 0.5$ $\boldsymbol{\mu}_1 = \boldsymbol{\mu}_2 = (0, 0)^\top$ $\boldsymbol{\Sigma}_1 = \begin{bmatrix} 1 & 0.8 \\ 0.8 & 1 \end{bmatrix}, \boldsymbol{\Sigma}_2 = \begin{bmatrix} 1 & -0.8 \\ -0.8 & 1 \end{bmatrix}$
3	$K = 2$	Unsupervised: $\sum_{k=1}^K p_k \mathcal{N}(\boldsymbol{\mu}_k, \boldsymbol{\Sigma}_k)$	$p_1 = 0.3, p_2 = 0.7$ $\boldsymbol{\mu}_1 = (0, -2)^\top, \boldsymbol{\mu}_2 = (0, 2)^\top$ $\boldsymbol{\Sigma}_1 = \begin{bmatrix} 1 & 0.8 \\ 0.8 & 1 \end{bmatrix}, \boldsymbol{\Sigma}_2 = \begin{bmatrix} 1 & -0.8 \\ -0.8 & 1 \end{bmatrix}$
4	$K = 3$		$p_1 = 0.25, p_2 = 0.5, p_3 = 0.25$ $\boldsymbol{\mu}_1 = (0, -2)^\top, \boldsymbol{\mu}_2 = (0, 6)^\top, \boldsymbol{\mu}_3 = (-2, 2)^\top$ $\boldsymbol{\Sigma}_1 = \begin{bmatrix} 1 & 0.8 \\ 0.8 & 1 \end{bmatrix}, \boldsymbol{\Sigma}_2 = \begin{bmatrix} 1 & -0.7 \\ -0.7 & 1 \end{bmatrix}, \boldsymbol{\Sigma}_3 = \begin{bmatrix} 1 & 0.9 \\ 0.9 & 1 \end{bmatrix}$
5	$K = 2$		$p_1 = p_2 = 0.5, \nu_1 = \nu_2 = 8$ $\boldsymbol{\mu}_1 = (0, -2)^\top, \boldsymbol{\mu}_2 = (0, 2)^\top$ $\boldsymbol{\Sigma}_1 = \boldsymbol{\Sigma}_2 = \begin{bmatrix} 1 & 0.8 \\ 0.8 & 1 \end{bmatrix}$
6	$K = 2$	Supervised: $\mathbb{P}(Z = k) = p_k$ $(X, Y) (Z = k) \sim t_{\nu_k}(\boldsymbol{\mu}_k, \boldsymbol{\Sigma}_k)$ $k = 1, \dots, K$	$p_1 = p_2 = 0.5, \nu_1 = \nu_2 = 8$ $\boldsymbol{\mu}_1 = \boldsymbol{\mu}_2 = (0, 0)^\top$ $\boldsymbol{\Sigma}_1 = \begin{bmatrix} 1 & 0.8 \\ 0.8 & 1 \end{bmatrix}, \boldsymbol{\Sigma}_2 = \begin{bmatrix} 1 & -0.8 \\ -0.8 & 1 \end{bmatrix}$
7	$K = 2$	Unsupervised: $\sum_{k=1}^K p_k t_{\nu_k}(\boldsymbol{\mu}_k, \boldsymbol{\Sigma}_k)$	$p_1 = 0.3, p_2 = 0.7, \nu_1 = \nu_2 = 8$ $\boldsymbol{\mu}_1 = (0, -2)^\top, \boldsymbol{\mu}_2 = (0, 2)^\top$ $\boldsymbol{\Sigma}_1 = \begin{bmatrix} 1 & 0.8 \\ 0.8 & 1 \end{bmatrix}, \boldsymbol{\Sigma}_2 = \begin{bmatrix} 1 & -0.8 \\ -0.8 & 1 \end{bmatrix}$
8	$K = 3$		$p_1 = 0.25, p_2 = 0.5, p_3 = 0.25$ $\nu_1 = \nu_2 = \nu_3 = 8$ $\boldsymbol{\mu}_1 = (0, -2)^\top, \boldsymbol{\mu}_2 = (0, 6)^\top, \boldsymbol{\mu}_3 = (-2, 2)^\top$ $\boldsymbol{\Sigma}_1 = \begin{bmatrix} 1 & 0.8 \\ 0.8 & 1 \end{bmatrix}, \boldsymbol{\Sigma}_2 = \begin{bmatrix} 1 & -0.7 \\ -0.7 & 1 \end{bmatrix}, \boldsymbol{\Sigma}_3 = \begin{bmatrix} 1 & 0.9 \\ 0.9 & 1 \end{bmatrix}$

Table 1: Eight settings in simulation studies (Section 5). In the settings 1-4, $\mathcal{N}(\boldsymbol{\mu}_k, \boldsymbol{\Sigma}_k)$ represents a bivariate Gaussian distribution with the mean vector $\boldsymbol{\mu}_k$ and the covariance matrix $\boldsymbol{\Sigma}_k$. In the settings 5-8, $t_{\nu_k}(\boldsymbol{\mu}_k, \boldsymbol{\Sigma}_k)$ represents a bivariate t distribution with the degrees of freedom ν_k , the location vector $\boldsymbol{\mu}_k$ and the shape matrix $\boldsymbol{\Sigma}_k$.

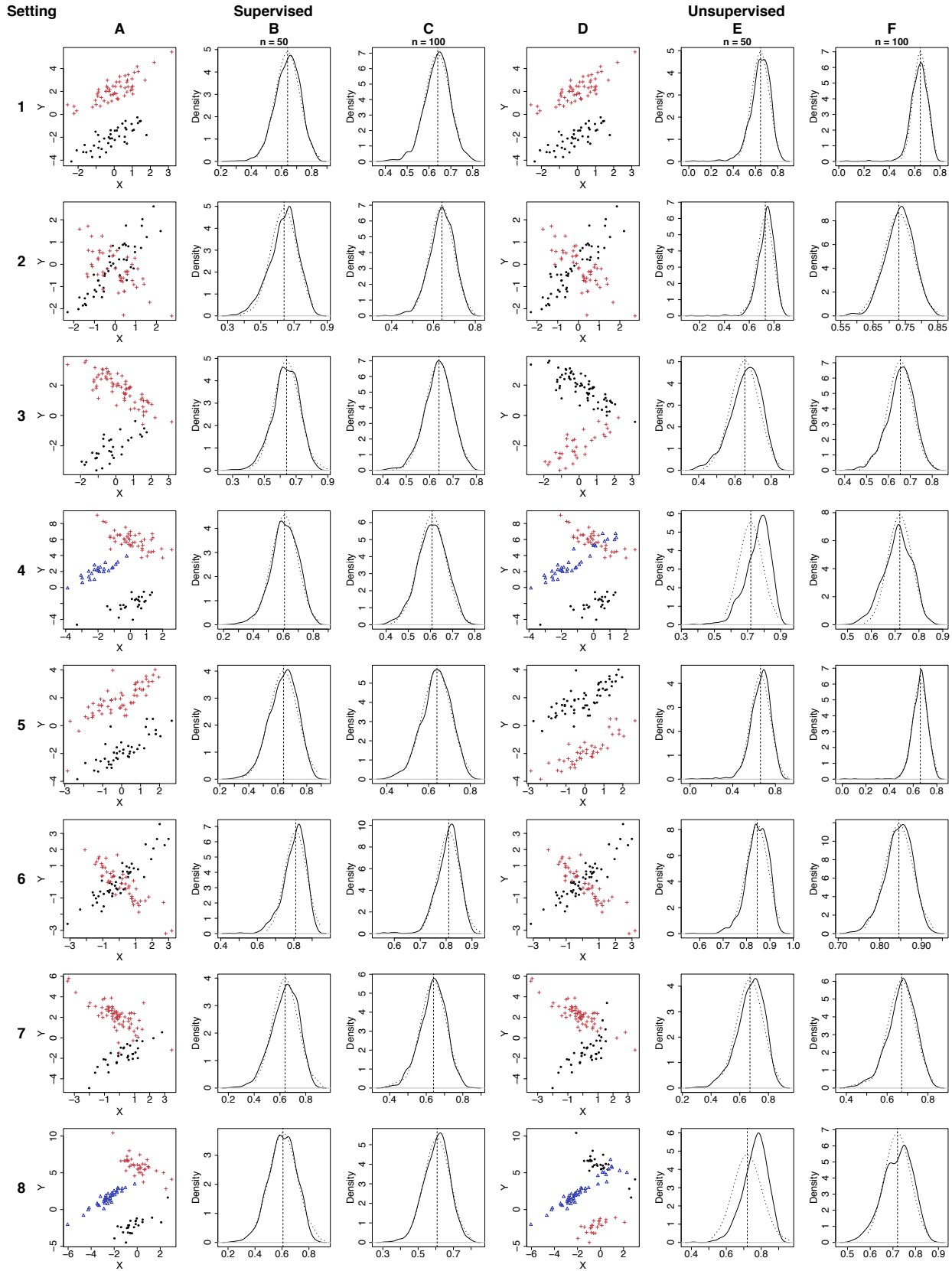


Figure 3: (Continued on the following page.)

Figure 3: Comparison of the asymptotic distributions and the finite-sample distributions of the supervised and unsupervised sample generalized R^2 measures ($R_{\mathcal{G}(\mathcal{S})}^2$ and $R_{\mathcal{G}(\mathcal{U})}^2$) under the eight simulation settings in Table 1. A: For each setting, a scatterplot shows a sample with $n = 100$ under the supervised scenario; different colors and symbols represent different values of Z . B-C: Finite-sample distributions ($n = 50$ or 100 , black solid curves) vs. the asymptotic distribution (black dotted curves) of $R_{\mathcal{G}(\mathcal{S})}^2$ in Corollary 3.2 (Settings 1-4) or Theorem 3.1 (Settings 5-8); the vertical dashed lines mark the values of $\rho_{\mathcal{G}(\mathcal{S})}^2$. D: For each setting, a scatterplot shows a sample with $n = 100$ under the unsupervised scenario; different colors and symbols represent different values of \tilde{Z} inferred by the K -lines algorithm (Algorithm 1). E-F: Finite-sample distributions of ($n = 50$ or 100 , black solid curves) vs. the asymptotic distribution (black dotted curves) of $R_{\mathcal{G}(\mathcal{U})}^2$ in Corollary 3.5 (Settings 1-4) or Theorem 3.4 (Settings 5-8); the vertical dashed lines mark the values of $\rho_{\mathcal{G}(\mathcal{U})}^2$.

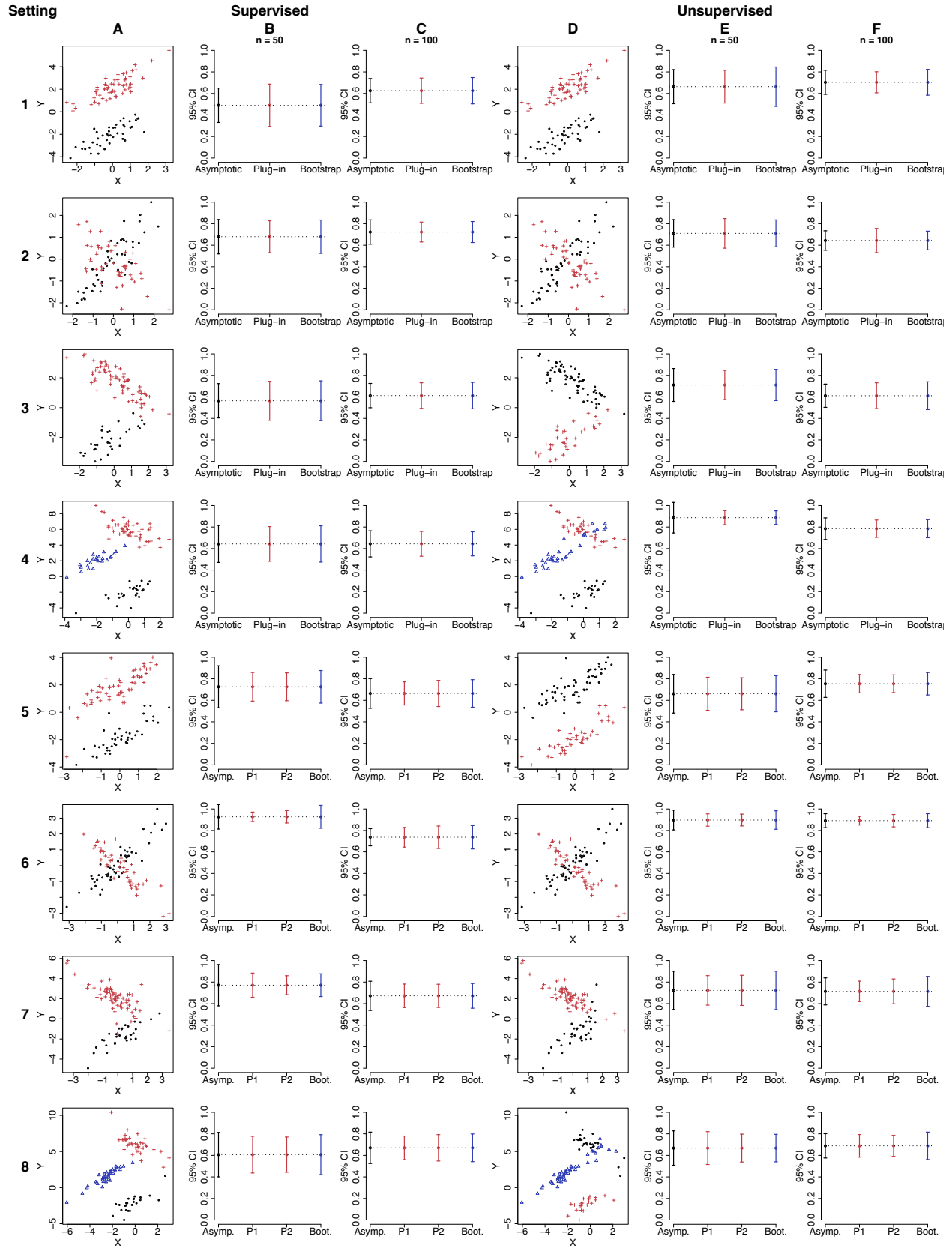


Figure 4: (Continued on the following page.)

Figure 4: Comparison of the 95% confidence intervals of $\rho_{\mathcal{G}(\mathcal{S})}^2$ and $\rho_{\mathcal{G}(\mathcal{U})}^2$ under the eight simulation settings (Table 1). A: For each setting, a scatterplot shows a sample with $n = 100$ under the supervised scenario; different colors and symbols represent different values of Z . B-C: Confidence intervals of $\rho_{\mathcal{G}(\mathcal{S})}^2$ based one sample ($n = 50$ or 100) using one of the three distributions: (1) black: the asymptotic distribution using the true asymptotic variance of $R_{\mathcal{G}(\mathcal{S})}^2$ in Corollary 3.2 (Settings 1-4) or Theorem 3.1 (Settings 5-8), (2) red: the asymptotic distribution using the plug-in asymptotic variance of $R_{\mathcal{G}(\mathcal{S})}^2$ in Corollary 3.2 (Settings 1-4 and “P1” under Settings 5-8) or Theorem 3.1 (“P2” under Settings 5-8), (3) blue: the parametric (Settings 1-4) or non-parametric (Settings 5-8) bootstrap based on 1000 simulations. D: For each setting, a scatterplot shows a sample with $n = 100$ under the unsupervised scenario; different colors and symbols represent different values of \tilde{Z} inferred by the K -lines algorithm (Algorithm 1). E-F: Confidence intervals of $\rho_{\mathcal{G}(\mathcal{U})}^2$ based one sample ($n = 50$ or 100) using one of the three distributions: (1) black: the asymptotic distribution using the true asymptotic variance of $R_{\mathcal{G}(\mathcal{U})}^2$ in Corollary 3.5 (Settings 1-4) or Theorem 3.4 (Settings 5-8), (2) red: the asymptotic distribution using the plug-in asymptotic variance of $R_{\mathcal{G}(\mathcal{U})}^2$ in Corollary 3.5 (Settings 1-4 and “P1” under Settings 5-8) or Theorem 3.4 (“P2” under Settings 5-8), (3) blue: the parametric (Settings 1-4) or non-parametric (Settings 5-8) bootstrap based on 1000 simulations.

Setting	n	95% CI Coverage Probability					
		Supervised			Unsupervised		
		Asymp.	P1	P2	Asymp.	P1	P2
1	50	.947	.933		.954	.916	
	100	.959	.947		.934	.926	
2	50	.959	.930		.959	.924	
	100	.939	.932		.958	.927	
3	50	.941	.924		.929	.881	
	100	.952	.951		.945	.916	
4	50	.956	.916		.921	.775	
	100	.944	.937		.888	.878	
5	50	.960	.868	.863	.953	.884	.852
	100	.957	.896	.903	.961	.912	.915
6	50	.942	.906	.897	.948	.888	.869
	100	.949	.900	.917	.965	.900	.898
7	50	.958	.876	.869	.957	.855	.857
	100	.969	.884	.900	.944	.870	.905
8	50	.955	.882	.861	.981	.753	.692
	100	.961	.906	.917	.945	.871	.866

Table 2: Coverage probabilities of the 95% confidence intervals (CIs) of $\rho_{\mathcal{G}(S)}^2$ or $\rho_{\mathcal{G}(U)}^2$ constructed by the plug-in approach or based on the true asymptotic variances. Under the unsupervised scenario, $\rho_{\mathcal{G}(U)}^2$ is approximated by $R_{\mathcal{G}(U)}^2$ calculated from a large sample with size 10,000. “Asymp,” “P1,” and “P2” represent the CIs constructed based on the true asymptotic variances, the plug-in estimates of the asymptotic variances in the special bivariate Gaussian forms (Corollaries 3.2 and 3.5), and the plug-in estimates of the asymptotic variances in the general forms (Theorems 3.1 and 3.4), respectively. The coverage probabilities are estimated as the percentages of CIs that cover $\rho_{\mathcal{G}(S)}^2$ or $\rho_{\mathcal{G}(U)}^2$ in 1000 simulations. For Settings 1-4 as mixtures of bivariate Gaussians, we only consider the plug-in option 1 (“P1”).

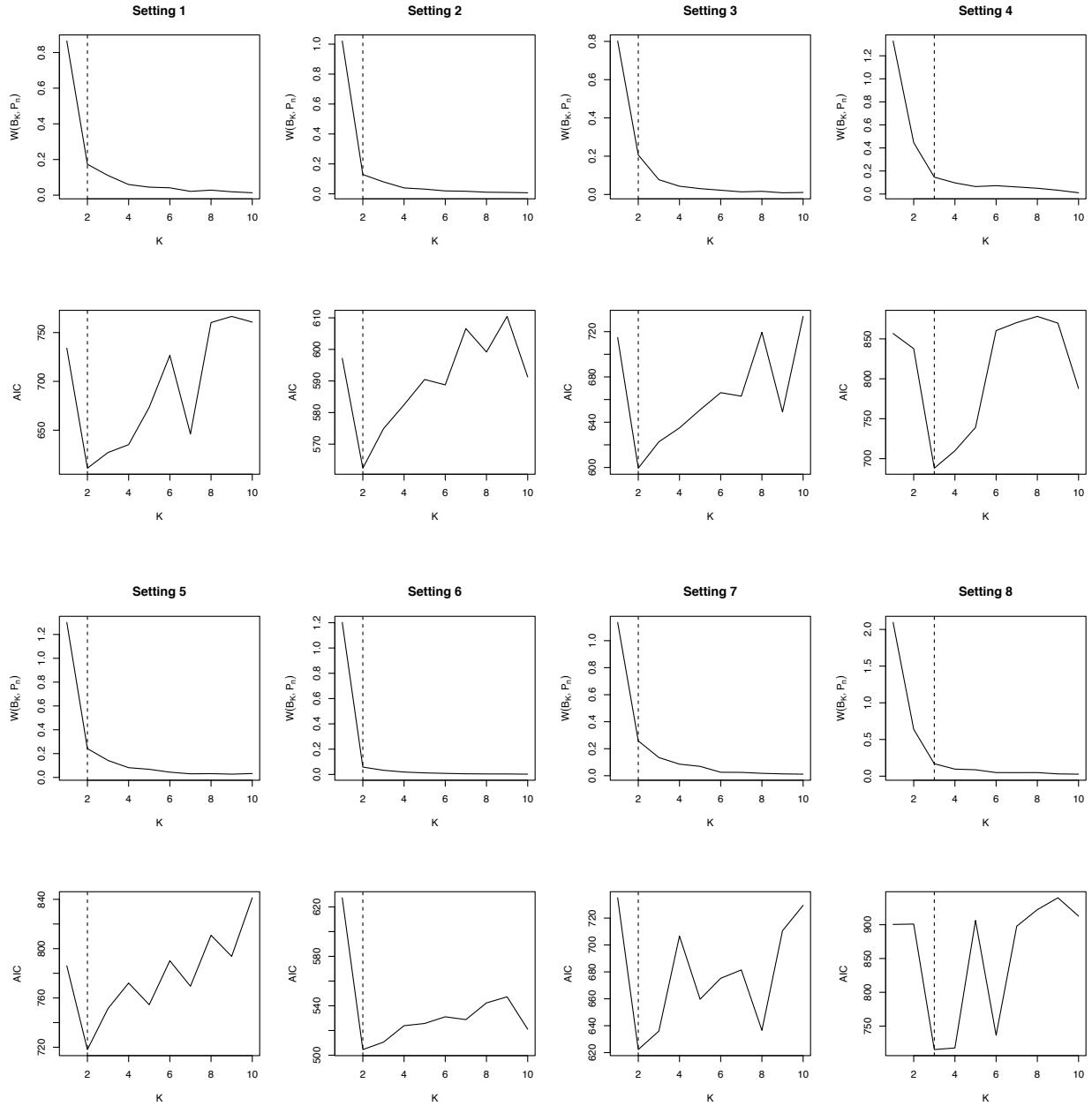


Figure 5: The choice of K . Under each of the eight simulation settings (Table 1), we simulate a sample of size $n = 100$ and calculate $W(B_K, P_n)$ and $AIC(K)$. The dashed vertical lines indicate the true K values used in the simulations.

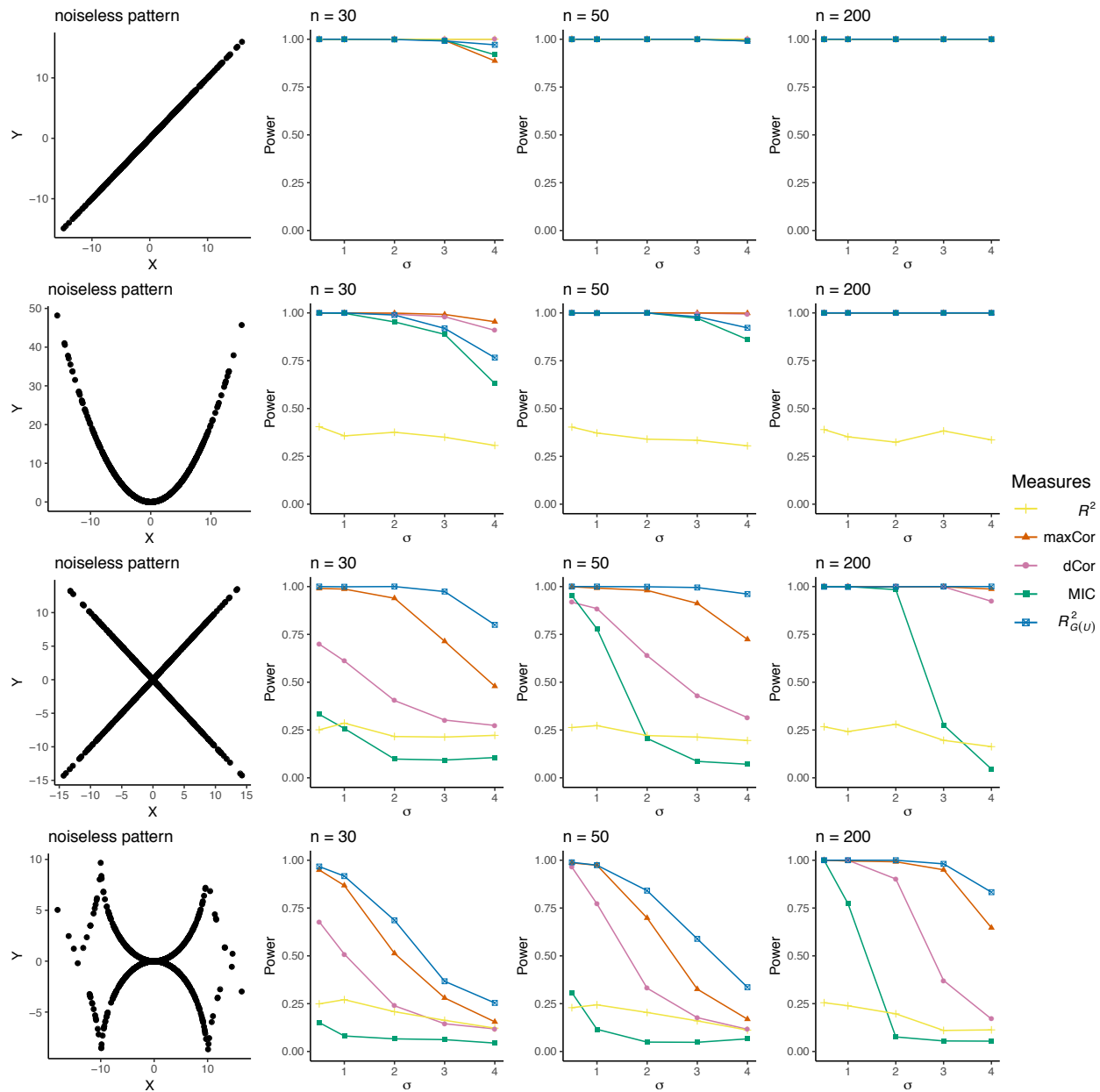


Figure 6: Power analysis. Simulation studies that compare the statistical power of five measures: $R_{\mathcal{G}(U)}^2$ with $K = 2$, the squared Pearson correlation (R^2), the maximal correlation (maxCor), the distance correlation (dCor), and the maximal information coefficient (MIC). Each noiseless pattern illustrates a relationship between two real-valued random variables X and Y when no noise is added. Under the null hypothesis, the two variables X and Y are independent. Varying alternative hypotheses are formed by the noiseless pattern with noise $\sim \mathcal{N}(0, \sigma^2)$ added to Y for varying σ . Under each alternative corresponding to one σ , we use a permutation test procedure to estimate the power of the five measures given each sample size n .

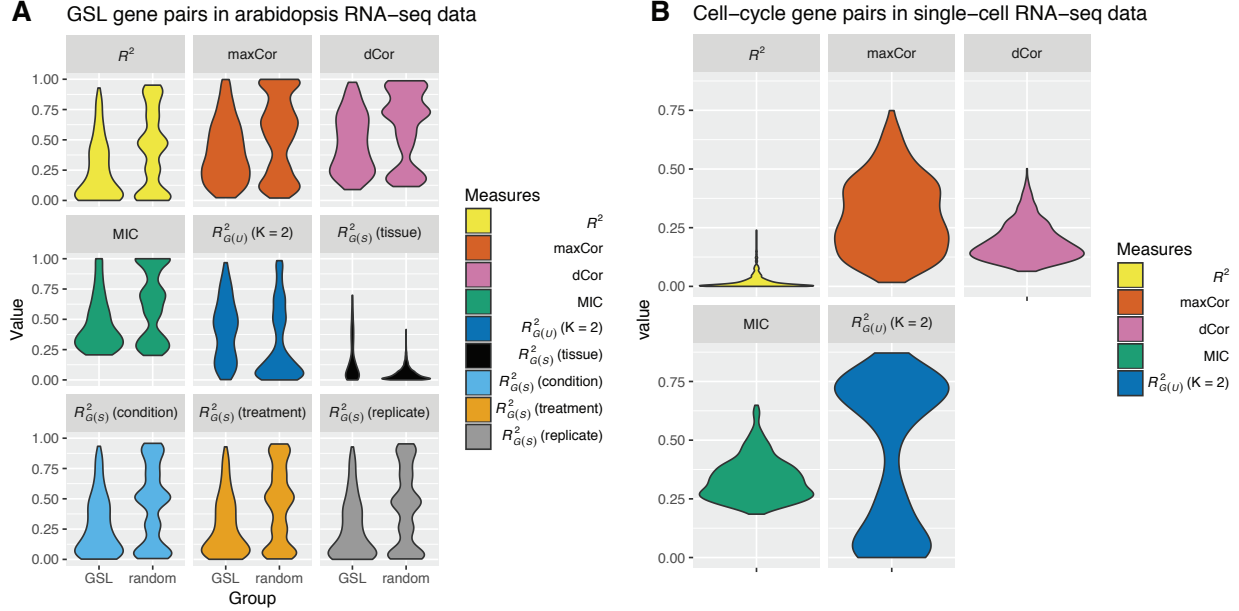


Figure 7: Real data applications of $R^2_{G(S)}$ and $R^2_{G(U)}$ to capturing gene-gene relationships. A: Gene expression analysis in Arabidopsis. We compare nine measures, including five unsupervised measures (R^2 , maxCor, dCor, MIC, and $R^2_{G(U)}$ with $K = 2$) and four $R^2_{G(S)}$ measures with different index variables, in terms of measuring pairwise gene relationships within the GSL pathway (“GSL”) vs. relationships between a GSL gene and a randomly paired non-GSL gene (“random”). $R^2_{G(U)}(K = 2)$ and $R^2_{G(S)}(\text{tissue})$ are the only two measures indicating that the gene pairs within the GSL pathway have stronger relationships than the random GSL-nonGSL gene pairs do. B: Cell-cycle gene expression analysis based on single-cell RNA sequencing data. The five unsupervised measures used in A are applied to capture the relationships of 1000 known cell-cycle gene pairs. $R^2_{G(U)}(K = 2)$ shows that some pairs of cell-cycle genes have strong relationships, which would likely be missed by the other four measures.

A. PROOFS

A.1 Proof of Lemma 2.1

Proof. By the definition of the perpendicular distance $d_{\perp}(\cdot, *)$ in Equation (7), we have for $\beta = (a, b, c)^{\top}$, where $a, b, c \in \mathbb{R}$ with $a \neq 0$ or $b \neq 0$, that

$$d_{\perp} \left((x, y)^{\top}, \beta \right) \leq \left\| (x, y)^{\top} - (x_0, y_0)^{\top} \right\|, \quad \forall (x_0, y_0)^{\top} \text{ s.t. } ax_0 + by_0 + c = 0,$$

and

$$d_{\perp} \left((x', y')^{\top}, \beta \right) = \left\| (x', y')^{\top} - \left(\frac{b(bx' - ay') - ac}{a^2 + b^2}, \frac{a(-bx' + ay') - bc}{a^2 + b^2} \right)^{\top} \right\|,$$

where $\left(\frac{b(bx' - ay') - ac}{a^2 + b^2}, \frac{a(-bx' + ay') - bc}{a^2 + b^2} \right)^{\top}$ is a point on the line corresponding to β . Therefore,

$$\begin{aligned} d_{\perp} \left((x, y)^{\top}, \beta \right) &\leq \left\| (x, y)^{\top} - \left(\frac{b(bx' - ay') - ac}{a^2 + b^2}, \frac{a(-bx' + ay') - bc}{a^2 + b^2} \right)^{\top} \right\| \\ &\leq \left\| (x, y)^{\top} - (x', y')^{\top} \right\| + \left\| (x', y')^{\top} - \left(\frac{b(bx' - ay') - ac}{a^2 + b^2}, \frac{a(-bx' + ay') - bc}{a^2 + b^2} \right)^{\top} \right\| \\ &\leq \left\| (x, y)^{\top} - (x', y')^{\top} \right\| + d_{\perp} \left((x', y')^{\top}, \beta \right). \end{aligned}$$

□

A.2 Proof of Remark 5

Proof. Denote by Z the index variable under the supervised scenario and by \tilde{Z} the surrogate index variable under the unsupervised scenario. Both $Z, \tilde{Z} \in \{1, \dots, K\}$. Given Definition 1 of $\rho_{\mathcal{G}(S)}^2$ and Definition 6 of $\rho_{\mathcal{G}(U)}^2$, if we denote

$$\rho^2(Z) = \frac{\text{cov}^2(X, Y|Z)}{\text{var}(X|Z)\text{var}(Y|Z)},$$

then

$$\rho_{\mathcal{G}(S)}^2 = \mathbb{E}_Z [\rho^2(Z)] \quad \text{and} \quad \rho_{\mathcal{G}(U)}^2 = \mathbb{E}_{\tilde{Z}} [\rho^2(\tilde{Z})]. \quad (\text{A.1})$$

Without loss of generality, we assume $\rho(Z), \rho(\tilde{Z}) \geq 0$, $\text{var}(X|Z) = \text{var}(Y|Z) = \text{var}(X|\tilde{Z}) = \text{var}(Y|\tilde{Z}) = 1$ for all Z, \tilde{Z} .

Denote by $\lambda_1(Z)$ and $\lambda_2(Z)$ the first and second eigenvalues of the correlation matrix of $(X, Y)|Z$, denoted by $\Sigma(Z)$. An important property about the two eigenvalues is

$$\lambda_1(Z) + \lambda_2(Z) = 2 \quad \text{and} \quad \lambda_1(Z) = 1 + \rho(Z),$$

where the second equation was proved in (Morrison, 1967). Hence

$$\lambda_2(Z) = 1 - \rho(Z) \in [0, 1]. \quad (\text{A.2})$$

$\lambda_2(Z)$ is equal to the variance of the projection of $(X, Y)|Z$ onto its second principal component, which is perpendicular to its first principal component, i.e., the line center defined in Definition 2 and denoted by $\beta(Z)$ here. Hence,

$$\lambda_2(Z) = \mathbb{E} \left[d_{\perp}^2 \left((X, Y)^{\top}, \beta(Z) \right) \middle| Z \right].$$

Denote by $B_K(Z)$ the set of K population line centers corresponding to (X, Y, Z) . Then

$$\begin{aligned} \mathbb{E}_Z[\lambda_2(Z)] &\geq \mathbb{E}_{(X, Y, Z)} \left[\min_{\beta \in B_K(Z)} d_{\perp}^2 \left((X, Y)^{\top}, \beta \right) \right] \\ &\geq \mathbb{E}_{(X, Y, \tilde{Z})} \left[\min_{\beta \in B_K(\tilde{Z})} d_{\perp}^2 \left((X, Y)^{\top}, \beta \right) \right] = \mathbb{E}_{\tilde{Z}}[\lambda_2(\tilde{Z})], \end{aligned} \quad (\text{A.3})$$

where the second inequality and the last equality hold by Definition 4 of the unsupervised population line centers and Definition 5 of \tilde{Z} .

By (A.1), (A.2) and (A.3),

$$\begin{aligned} \rho_{\mathcal{G}(S)}^2 - \rho_{\mathcal{G}(U)}^2 &= \mathbb{E}_Z[\rho^2(Z)] - \mathbb{E}_{\tilde{Z}}[\rho^2(\tilde{Z})] \\ &= \mathbb{E}_Z[(1 - \lambda_2(Z))^2] - \mathbb{E}_{\tilde{Z}}[(1 - \lambda_2(\tilde{Z}))^2] \\ &= \mathbb{E}_{(Z, \tilde{Z})} \left[\left(\lambda_2(\tilde{Z}) - \lambda_2(Z) \right) \left(2 - \lambda_2(Z) - \lambda_2(\tilde{Z}) \right) \right] \\ &\leq 2\mathbb{E}_{(Z, \tilde{Z})} \left[\lambda_2(\tilde{Z}) - \lambda_2(Z) \right] \\ &\leq 0. \end{aligned}$$

□

A.3 Proof of Theorem 3.1

Proof. We derive the asymptotic distribution of the supervised sample generalized R^2 , $R_{\mathcal{G}(S)}^2$, in this proof. For notation simplicity, we drop the subscript “(S)” in $p_{k(S)}$ in (4), $\rho_{k(S)}$ in (5), and $\hat{p}_{k(S)}$, $\hat{\rho}_{k(S)}^2$, $\bar{X}_{k(S)}$, and $\bar{Y}_{k(S)}$ in Definition 3, following which we have

$$R_{\mathcal{G}(S)}^2 = \sum_{k=1}^K \hat{p}_k \hat{\rho}_k^2 = \sum_{k=1}^K \hat{p}_k \frac{\hat{\sigma}_{XY,k}^2}{\hat{\sigma}_{X,k}^2 \hat{\sigma}_{Y,k}^2},$$

where

$$\begin{aligned}\widehat{p}_k &= \frac{1}{n} \sum_{i=1}^n \mathbb{I}(Z_i = k), \\ \widehat{\sigma}_{XY,k} &= \frac{1}{n\widehat{p}_k} \sum_{i=1}^n (X_i - \bar{X}_k)(Y_i - \bar{Y}_k) \mathbb{I}(Z_i = k), \\ \widehat{\sigma}_{X,k}^2 &= \frac{1}{n\widehat{p}_k} \sum_{i=1}^n (X_i - \bar{X}_k)^2 \mathbb{I}(Z_i = k), \\ \widehat{\sigma}_{Y,k}^2 &= \frac{1}{n\widehat{p}_k} \sum_{i=1}^n (Y_i - \bar{Y}_k)^2 \mathbb{I}(Z_i = k),\end{aligned}$$

with $\bar{X}_k = \frac{1}{n\widehat{p}_k} \sum_{i=1}^n X_i \mathbb{I}(Z_i = k)$ and $\bar{Y}_k = \frac{1}{n\widehat{p}_k} \sum_{i=1}^n Y_i \mathbb{I}(Z_i = k)$.

To derive the asymptotic distribution of $R_{\mathcal{G}(S)}^2$, we need to first derive the joint asymptotic distribution of

$$\widehat{\boldsymbol{\theta}} = (\widehat{p}_1, \widehat{\sigma}_{XY,1}, \widehat{\sigma}_{X,1}^2, \widehat{\sigma}_{Y,1}^2, \dots, \widehat{p}_K, \widehat{\sigma}_{XY,K}, \widehat{\sigma}_{X,K}^2, \widehat{\sigma}_{Y,K}^2)^\top \in \mathbb{R}^{4K}.$$

Without loss of generality, we assume

$$\begin{aligned}\mu_{X,k} &= \mathbb{E}[X|Z = k] = 0, & \mu_{Y,k} &= \mathbb{E}[Y|Z = k] = 0, \\ \sigma_{X,k}^2 &= \text{var}[X|Z = k] = 1, & \sigma_{Y,k}^2 &= \text{var}[Y|Z = k] = 1.\end{aligned}$$

Hence,

$$\begin{aligned}\mathbb{E}[X] &= 0, & \mathbb{E}[Y] &= 0, \\ \mu_{X^2,k} &= \mathbb{E}[X^2|Z = k] = 1, & \mu_{Y^2,k} &= \mathbb{E}[Y^2|Z = k] = 1, \\ \sigma_{XY,k} &= \text{cov}[X, Y|Z = k] = \rho_k, & \mu_{XY,k} &= \mathbb{E}[XY|Z = k] = \rho_k,\end{aligned}$$

where $\rho_k = \rho_{k(S)}$ defined in Equation (5).

To facilitate the rest of the proof, we define the following sample moments.

$$\begin{aligned}M_k &:= \frac{1}{n} \sum_{i=1}^n \mathbb{I}(Z_i = k), & M_{XY,k} &:= \frac{1}{n} \sum_{i=1}^n X_i Y_i \mathbb{I}(Z_i = k), \\ M_{X,k} &:= \frac{1}{n} \sum_{i=1}^n X_i \mathbb{I}(Z_i = k), & M_{X^2,k} &:= \frac{1}{n} \sum_{i=1}^n X_i^2 \mathbb{I}(Z_i = k), \\ M_{Y,k} &:= \frac{1}{n} \sum_{i=1}^n Y_i \mathbb{I}(Z_i = k), & M_{Y^2,k} &:= \frac{1}{n} \sum_{i=1}^n Y_i^2 \mathbb{I}(Z_i = k),\end{aligned}$$

for $k = 1, \dots, K$. Then

$$\begin{aligned}
\hat{p}_k &= M_k, \quad \bar{X}_k = M_{X,k}/M_k, \quad \bar{Y}_k = M_{Y,k}/M_k \\
\hat{\sigma}_{XY,k} &= \frac{1}{n\hat{p}_k} \sum_{i=1}^n (X_i - \bar{X}_k)(Y_i - \bar{Y}_k) \mathbb{I}(Z_i = k) \\
&= \frac{1}{n\hat{p}_k} \sum_{i=1}^n (X_i Y_i - X_i \bar{Y}_k - \bar{X}_k Y_i + \bar{X}_k \bar{Y}_k) \mathbb{I}(Z_i = k) \\
&= \left(\frac{1}{n\hat{p}_k} \sum_{i=1}^n X_i Y_i \mathbb{I}(Z_i = k) \right) - \bar{Y}_k \left(\frac{1}{n\hat{p}_k} \sum_{i=1}^n X_i \mathbb{I}(Z_i = k) \right) \\
&\quad - \bar{X}_k \left(\frac{1}{n\hat{p}_k} \sum_{i=1}^n Y_i \mathbb{I}(Z_i = k) \right) + \bar{X}_k \bar{Y}_k \left(\frac{1}{n\hat{p}_k} \sum_{i=1}^n \mathbb{I}(Z_i = k) \right) \\
&= M_{XY,k}/M_k - M_{X,k} M_{Y,k}/M_k^2, \\
\hat{\sigma}_{X,k}^2 &= \frac{1}{n\hat{p}_k} \sum_{i=1}^n (X_i - \bar{X}_k)^2 \mathbb{I}(Z_i = k) \\
&= \frac{1}{n\hat{p}_k} \sum_{i=1}^n (X_i^2 - 2X_i \bar{X}_k + (\bar{X}_k)^2) \mathbb{I}(Z_i = k) \\
&= \left(\frac{1}{n\hat{p}_k} \sum_{i=1}^n X_i^2 \mathbb{I}(Z_i = k) \right) - 2\bar{X}_k \left(\frac{1}{n\hat{p}_k} \sum_{i=1}^n X_i \mathbb{I}(Z_i = k) \right) + (\bar{X}_k)^2 \left(\frac{1}{n\hat{p}_k} \sum_{i=1}^n \mathbb{I}(Z_i = k) \right) \\
&= M_{X^2,k}/M_k - (M_{X,k})^2/M_k^2.
\end{aligned}$$

Similarly,

$$\hat{\sigma}_{Y,k}^2 = M_{Y^2,k}/M_k - (M_{Y,k})^2/M_k^2.$$

Hence,

$$\hat{\boldsymbol{\theta}} = \begin{pmatrix} \hat{p}_1 \\ \hat{\sigma}_{XY,1} \\ \hat{\sigma}_{X,1}^2 \\ \hat{\sigma}_{Y,1}^2 \\ \vdots \\ \hat{p}_K \\ \hat{\sigma}_{XY,K} \\ \hat{\sigma}_{X,K}^2 \\ \hat{\sigma}_{Y,K}^2 \end{pmatrix} = \begin{pmatrix} M_1 \\ M_{XY,1}/M_1 - M_{X,1}M_{Y,1}/M_1^2 \\ M_{X^2,1}/M_1 - (M_{X,1})^2/M_1^2 \\ M_{Y^2,1}/M_1 - (M_{Y,1})^2/M_1^2 \\ \vdots \\ M_K \\ M_{XY,K}/M_k - M_{X,K}M_{Y,K}/M_K^2 \\ M_{X^2,K}/M_k - (M_{X,K})^2/M_K^2 \\ M_{Y^2,K}/M_k - (M_{Y,K})^2/M_K^2 \end{pmatrix} = g \begin{pmatrix} M_1 \\ M_{X,1} \\ M_{Y,1} \\ M_{X^2,1} \\ M_{Y^2,1} \\ M_{XY,1} \\ \vdots \\ M_K \\ M_{X,K} \\ M_{Y,K} \\ M_{X^2,K} \\ M_{Y^2,K} \\ M_{XY,K} \end{pmatrix}.$$

Given any $\boldsymbol{\xi} = (x_1, y_1, z_1, u_1, v_1, w_1, \dots, x_K, y_K, z_K, u_K, v_K, w_K)^\top \in \mathbb{R}^{6K}$, the function $g : \mathbb{R}^{6K} \rightarrow \mathbb{R}^{4K}$ is

$$g(\boldsymbol{\xi}) = g \begin{pmatrix} x_1 \\ y_1 \\ z_1 \\ u_1 \\ v_1 \\ w_1 \\ \vdots \\ x_K \\ y_K \\ z_K \\ u_K \\ v_K \\ w_K \end{pmatrix} = \begin{pmatrix} x_1 \\ w_1/x_1 - y_1z_1/x_1^2 \\ u_1/x_1 - y_1^2/x_1^2 \\ v_1/x_1 - z_1^2/x_1^2 \\ \vdots \\ x_K \\ w_K/x_K - y_Kz_K/x_K^2 \\ u_K/x_K - y_K^2/x_K^2 \\ v_K/x_K - z_K^2/x_K^2 \end{pmatrix}, \quad (\text{A.4})$$

with Jacobian

$$Dg(\boldsymbol{\xi}) = \begin{bmatrix} Dg(\boldsymbol{\xi})_1 & & & & & & \\ & \ddots & & & & & \\ & & & & & & \\ & & & Dg(\boldsymbol{\xi})_K & & & \end{bmatrix}_{(4K) \times (6K)},$$

where

$$Dg(\boldsymbol{\xi})_k = \begin{bmatrix} 1 & 0 & 0 & 0 & 0 & 0 \\ -w_k/x_k^2 + 2y_k z_k/x_k^3 & -z_k/x_k^2 & -y_k/x_k^2 & 0 & 0 & 1/x_k \\ -u_k/x_k^2 + 2y_k^2/x_k^3 & -2y_k/x_k^2 & 0 & 1/x_k & 0 & 0 \\ -v_k/x_k^2 + 2z_k^2/x_k^3 & 0 & -2z_k/x_k^2 & 0 & 1/x_k & 0 \end{bmatrix}, \quad k = 1, \dots, K.$$

To derive the joint asymptotic distribution of $\widehat{\boldsymbol{\theta}}$, we need the joint asymptotic distribution of

$$\begin{aligned} \widehat{\boldsymbol{\mu}} &= (M_1, M_{X,1}, M_{Y,1}, M_{X^2,1}, M_{Y^2,1}, M_{XY,1}, \dots, M_K, M_{X,K}, M_{Y,K}, M_{X^2,K}, M_{Y^2,K}, M_{XY,K})^\top \\ &= (\widehat{\boldsymbol{\mu}}_1^\top, \dots, \widehat{\boldsymbol{\mu}}_K^\top)^\top, \end{aligned}$$

where

$$\widehat{\boldsymbol{\mu}}_k = (M_k, M_{X,k}, M_{Y,k}, M_{X^2,k}, M_{Y^2,k}, M_{XY,k})^\top,$$

because $\widehat{\boldsymbol{\theta}} = g(\widehat{\boldsymbol{\mu}})$.

For notation simplicity, we denote $Z_{[k]} = \mathbb{I}(Z = k)$ and $Z_{[k]i} = \mathbb{I}(Z_i = k)$, and thus $\widehat{\boldsymbol{\mu}}_k$ can be expressed as

$$\widehat{\boldsymbol{\mu}}_k = \left(\frac{1}{n} \sum_{i=1}^n Z_{[k]i}, \frac{1}{n} \sum_{i=1}^n X_i Z_{[k]i}, \frac{1}{n} \sum_{i=1}^n Y_i Z_{[k]i}, \frac{1}{n} \sum_{i=1}^n X_i^2 Z_{[k]i}, \frac{1}{n} \sum_{i=1}^n Y_i^2 Z_{[k]i}, \frac{1}{n} \sum_{i=1}^n X_i Y_i Z_{[k]i} \right)^\top.$$

Hence, the joint asymptotic distribution of $\widehat{\boldsymbol{\mu}}$ can be derived based on the Central Limit Theorem.

Before applying the Central Limit Theorem, we note that the joint moments satisfy

$$\begin{aligned} \mathbb{E} \left[X^a Y^b Z_{[k]} \right] &= \mathbb{P}(Z_{[k]} = 1) \mathbb{E} \left[X^a Y^b Z_{[k]} \mid Z_{[k]} = 1 \right] + \mathbb{P}(Z_{[k]} = 0) \mathbb{E} \left[X^a Y^b Z_{[k]} \mid Z_{[k]} = 0 \right] \\ &= p_k \mu_{X^a Y^b, k} + (1 - p_k) \cdot 0 \\ &= p_k \mu_{X^a Y^b, k}, \quad a, b \in \mathbb{R}, \end{aligned}$$

and thus specifically,

$$\begin{aligned}
\mathbb{E} [XZ_{[k]}] &= p_k \mu_{X,k} = 0, & \mathbb{E} [YZ_{[k]}] &= p_k \mu_{Y,k} = 0, \\
\mathbb{E} [X^2Z_{[k]}] &= p_k \mu_{X^2,k} = p_k, & \mathbb{E} [Y^2Z_{[k]}] &= p_k \mu_{Y^2,k} = p_k, \\
\mathbb{E} [XYZ_{[k]}] &= p_k \mu_{XY,k} = p_k \rho_k, \\
\mathbb{E} [X^3Z_{[k]}] &= p_k \mu_{X^3,k}, & \mathbb{E} [Y^3Z_{[k]}] &= p_k \mu_{Y^3,k}, \\
\mathbb{E} [X^2YZ_{[k]}] &= p_k \mu_{X^2Y,k}, & \mathbb{E} [XY^2Z_{[k]}] &= p_k \mu_{XY^2,k}, \\
\mathbb{E} [X^4Z_{[k]}] &= p_k \mu_{X^4,k}, & \mathbb{E} [Y^4Z_{[k]}] &= p_k \mu_{Y^4,k}, \\
\mathbb{E} [X^3YZ_{[k]}] &= p_k \mu_{X^3Y,k}, & \mathbb{E} [XY^3Z_{[k]}] &= p_k \mu_{XY^3,k}, \\
\mathbb{E} [X^2Y^2Z_{[k]}] &= p_k \mu_{X^2Y^2,k}.
\end{aligned}$$

By the Central Limit Theorem, the joint asymptotic distribution of $\hat{\boldsymbol{\mu}}$ is

$$\sqrt{n}(\hat{\boldsymbol{\mu}} - \boldsymbol{\mu}) \xrightarrow{d} \mathcal{N}(0, \boldsymbol{\Sigma}), \quad (\text{A.5})$$

where

$$\boldsymbol{\mu} = (\boldsymbol{\mu}_1, \dots, \boldsymbol{\mu}_K)^\top,$$

with

$$\begin{aligned}
\boldsymbol{\mu}_k &= (\mathbb{E} [Z_{[k]}], \mathbb{E} [XZ_{[k]}], \mathbb{E} [YZ_{[k]}], \mathbb{E} [X^2Z_{[k]}], \mathbb{E} [Y^2Z_{[k]}], \mathbb{E} [XYZ_{[k]}])^\top \\
&= (p_k, 0, 0, p_k, p_k, p_k \rho_k)^\top,
\end{aligned}$$

and

$$\boldsymbol{\Sigma} = \begin{bmatrix} \boldsymbol{\Sigma}_{11} & \cdots & \boldsymbol{\Sigma}_{1K} \\ \vdots & \ddots & \vdots \\ \boldsymbol{\Sigma}_{K1} & \cdots & \boldsymbol{\Sigma}_{KK} \end{bmatrix}_{(6K) \times (6K)}.$$

For $k = 1, \dots, K$, $\boldsymbol{\Sigma}_{kk}$ is the variance-covariance matrix of $(Z_{[k]}, XZ_{[k]}, YZ_{[k]}, X^2Z_{[k]}, Y^2Z_{[k]}, XYZ_{[k]})^\top$:

$$\Sigma_{kk} = \begin{bmatrix} \text{var}(Z_{[k]}) & \text{cov}(Z_{[k]}, XZ_{[k]}) & \text{cov}(Z_{[k]}, YZ_{[k]}) & \text{cov}(Z_{[k]}, X^2Z_{[k]}) & \text{cov}(Z_{[k]}, Y^2Z_{[k]}) & \text{cov}(Z_{[k]}, XYZ_{[k]}) \\ \text{cov}(XZ_{[k]}, Z_{[k]}) & \text{var}(XZ_{[k]}) & \text{cov}(XZ_{[k]}, YZ_{[k]}) & \text{cov}(XZ_{[k]}, X^2Z_{[k]}) & \text{cov}(XZ_{[k]}, Y^2Z_{[k]}) & \text{cov}(XZ_{[k]}, XYZ_{[k]}) \\ \text{cov}(YZ_{[k]}, Z_{[k]}) & \text{cov}(YZ_{[k]}, XZ_{[k]}) & \text{var}(YZ_{[k]}) & \text{cov}(YZ_{[k]}, X^2Z_{[k]}) & \text{cov}(YZ_{[k]}, Y^2Z_{[k]}) & \text{cov}(YZ_{[k]}, XYZ_{[k]}) \\ \text{cov}(X^2Z_{[k]}, Z_{[k]}) & \text{cov}(X^2Z_{[k]}, XZ_{[k]}) & \text{cov}(X^2Z_{[k]}, YZ_{[k]}) & \text{var}(X^2Z_{[k]}) & \text{cov}(X^2Z_{[k]}, Y^2Z_{[k]}) & \text{cov}(X^2Z_{[k]}, XYZ_{[k]}) \\ \text{cov}(Y^2Z_{[k]}, Z_{[k]}) & \text{cov}(Y^2Z_{[k]}, XZ_{[k]}) & \text{cov}(Y^2Z_{[k]}, YZ_{[k]}) & \text{cov}(Y^2Z_{[k]}, X^2Z_{[k]}) & \text{var}(Y^2Z_{[k]}) & \text{cov}(Y^2Z_{[k]}, XYZ_{[k]}) \\ \text{cov}(XYZ_{[k]}, Z_{[k]}) & \text{cov}(XYZ_{[k]}, XZ_{[k]}) & \text{cov}(XYZ_{[k]}, YZ_{[k]}) & \text{cov}(XYZ_{[k]}, X^2Z_{[k]}) & \text{cov}(XYZ_{[k]}, Y^2Z_{[k]}) & \text{var}(XYZ_{[k]}) \end{bmatrix},$$

where

$$\text{var} (Z_{[k]}) = p_k (1 - p_k) ,$$

$$\text{cov} (Z_{[k]}, XZ_{[k]}) = \mathbb{E} [XZ_{[k]}^2] - \mathbb{E} [Z_{[k]}] \mathbb{E} [XZ_{[k]}] = p_k ,$$

$$\text{cov} (Z_{[k]}, YZ_{[k]}) = p_k ,$$

$$\text{cov} (Z_{[k]}, X^2Z_{[k]}) = \mathbb{E} [X^2Z_{[k]}^2] - \mathbb{E} [Z_{[k]}] \mathbb{E} [X^2Z_{[k]}] = \mathbb{E} [X^2Z_{[k]}] - p_k^2 = p_k (1 - p_k) ,$$

$$\text{cov} (Z_{[k]}, Y^2Z_{[k]}) = p_k (1 - p_k) ,$$

$$\text{cov} (Z_{[k]}, XYZ_{[k]}) = \mathbb{E} [XYZ_{[k]}^2] - \mathbb{E} [Z_{[k]}] \mathbb{E} [XYZ_{[k]}] = \mathbb{E} [XYZ_{[k]}] - p_k^2 \rho_k = p_k (1 - p_k) \rho_k ,$$

$$\text{var} (XZ_{[k]}) = \mathbb{E} [X^2Z_{[k]}^2] - (\mathbb{E} [XZ_{[k]}])^2 = \mathbb{E} [X^2Z_{[k]}] - 0 = p_k ,$$

$$\text{cov} (XZ_{[k]}, YZ_{[k]}) = \mathbb{E} [XYZ_{[k]}^2] - \mathbb{E} [XZ_{[k]}] \mathbb{E} [YZ_{[k]}] = \mathbb{E} [XYZ_{[k]}] - 0 = p_k \rho_k ,$$

$$\text{cov} (XZ_{[k]}, X^2Z_{[k]}) = \mathbb{E} [X^3Z_{[k]}^2] - \mathbb{E} [XZ_{[k]}] \mathbb{E} [X^2Z_{[k]}] = \mathbb{E} [X^3Z_{[k]}] - 0 = p_k \mu_{X^3,k} ,$$

$$\text{cov} (XZ_{[k]}, Y^2Z_{[k]}) = \mathbb{E} [XY^2Z_{[k]}^2] - \mathbb{E} [XZ_{[k]}] \mathbb{E} [Y^2Z_{[k]}] = \mathbb{E} [XY^2Z_{[k]}] - 0 = p_k \mu_{XY^2,k} ,$$

$$\text{cov} (XZ_{[k]}, XYZ_{[k]}) = \mathbb{E} [X^2YZ_{[k]}^2] - \mathbb{E} [XZ_{[k]}] \mathbb{E} [XYZ_{[k]}] = \mathbb{E} [X^2YZ_{[k]}] - 0 = p_k \mu_{X^2Y,k} ,$$

$$\text{var} (YZ_{[k]}) = \mathbb{E} [Y^2Z_{[k]}^2] - (\mathbb{E} [YZ_{[k]}])^2 = \mathbb{E} [Y^2Z_{[k]}] - 0 = p_k ,$$

$$\text{cov} (YZ_{[k]}, X^2Z_{[k]}) = \mathbb{E} [X^2YZ_{[k]}^2] - \mathbb{E} [YZ_{[k]}] \mathbb{E} [X^2Z_{[k]}] = \mathbb{E} [X^2YZ_{[k]}] - 0 = p_k \mu_{X^2Y,k} ,$$

$$\text{cov} (YZ_{[k]}, Y^2Z_{[k]}) = \mathbb{E} [Y^3Z_{[k]}^2] - \mathbb{E} [YZ_{[k]}] \mathbb{E} [Y^2Z_{[k]}] = \mathbb{E} [Y^3Z_{[k]}] - 0 = p_k \mu_{Y^3,k} ,$$

$$\text{cov} (YZ_{[k]}, XYZ_{[k]}) = \mathbb{E} [XY^2Z_{[k]}^2] - \mathbb{E} [YZ_{[k]}] \mathbb{E} [XYZ_{[k]}] = \mathbb{E} [XY^2Z_{[k]}] - 0 = p_k \mu_{XY^2,k} ,$$

$$\text{var} (X^2Z_{[k]}) = \mathbb{E} [X^4Z_{[k]}^2] - (\mathbb{E} [X^2Z_{[k]}])^2 = \mathbb{E} [X^4Z_{[k]}] - p_k^2 = p_k \mu_{X^4,k} - p_k^2 ,$$

$$\text{cov} (X^2Z_{[k]}, Y^2Z_{[k]}) = \mathbb{E} [X^2Y^2Z_{[k]}^2] - \mathbb{E} [X^2Z_{[k]}] \mathbb{E} [Y^2Z_{[k]}] = \mathbb{E} [X^2Y^2Z_{[k]}] - p_k^2$$

$$= p_k \mu_{X^2Y^2,k} - p_k^2 ,$$

$$\text{cov} (X^2Z_{[k]}, XYZ_{[k]}) = \mathbb{E} [X^3YZ_{[k]}^2] - \mathbb{E} [X^2Z_{[k]}] \mathbb{E} [XYZ_{[k]}] = \mathbb{E} [X^3YZ_{[k]}] - p_k^2 \rho_k$$

$$= p_k \mu_{X^3Y,k} - p_k^2 \rho_k ,$$

$$\text{var} (Y^2Z_{[k]}) = \mathbb{E} [Y^4Z_{[k]}^2] - (\mathbb{E} [Y^2Z_{[k]}])^2 = \mathbb{E} [Y^4Z_{[k]}] - p_k^2 = p_k \mu_{Y^4,k} - p_k^2 ,$$

$$\text{cov} (Y^2Z_{[k]}, XYZ_{[k]}) = \mathbb{E} [XY^3Z_{[k]}^2] - \mathbb{E} [Y^2Z_{[k]}] \mathbb{E} [XYZ_{[k]}] = \mathbb{E} [XY^3Z_{[k]}] - p_k^2 \rho_k$$

$$= p_k \mu_{XY^3,k} - p_k^2 \rho_k ,$$

$$\text{var} (XYZ_{[k]}) = \mathbb{E} [X^2Y^2Z_{[k]}^2] - (\mathbb{E} [XYZ_{[k]}])^2 = \mathbb{E} [X^2Y^2Z_{[k]}] - p_k^2 \rho_k^2 = p_k \mu_{X^2Y^2,k} - p_k^2 \rho_k^2 .$$

That is,

$$\begin{aligned} & \Sigma_{kk} \\ = & \begin{bmatrix} p_k(1-p_k) & p_k & p_k & p_k(1-p_k) & p_k(1-p_k) & p_k(1-p_k)\rho_k \\ p_k & p_k & p_k\rho_k & p_k\mu_{X^3,k} & p_k\mu_{XY^2,k} & p_k\mu_{X^2Y,k} \\ p_k & p_k\rho_k & p_k & p_k\mu_{X^2Y,k} & p_k\mu_{Y^3,k} & p_k\mu_{XY^2,k} \\ p_k(1-p_k) & p_k\mu_{X^3,k} & p_k\mu_{X^2Y,k} & p_k\mu_{X^4,k} - p_k^2 & p_k\mu_{X^2Y^2,k} - p_k^2 & p_k\mu_{X^3Y,k} - p_k^2\rho_k \\ p_k(1-p_k) & p_k\mu_{XY^2,k} & p_k\mu_{Y^3,k} & p_k\mu_{X^2Y^2,k} - p_k^2 & p_k\mu_{Y^4,k} - p_k^2 & p_k\mu_{XY^3,k} - p_k^2\rho_k \\ p_k(1-p_k)\rho_k & p_k\mu_{X^2Y,k} & p_k\mu_{XY^2,k} & p_k\mu_{X^3Y,k} - p_k^2\rho_k & p_k\mu_{XY^3,k} - p_k^2\rho_k & p_k\mu_{X^2Y^2,k} - p_k^2\rho_k^2 \end{bmatrix}. \end{aligned}$$

For $1 \leq k \neq r \leq K$, Σ_{ks} is the covariance matrix of $(Z_{[k]}, XZ_{[k]}, YZ_{[k]}, X^2Z_{[k]}, Y^2Z_{[k]}, XYZ_{[k]})^\top$ and $(Z_{[r]}, XZ_{[r]}, YZ_{[r]}, X^2Z_{[r]}, Y^2Z_{[r]}, XYZ_{[r]})^\top$:

$$\Sigma_{ks} = \begin{bmatrix} \text{cov}(Z_{[k]}, Z_{[r]}) & \text{cov}(Z_{[k]}, XZ_{[r]}) & \text{cov}(Z_{[k]}, YZ_{[r]}) & \text{cov}(Z_{[k]}, X^2Z_{[r]}) & \text{cov}(Z_{[k]}, Y^2Z_{[r]}) & \text{cov}(Z_{[k]}, XYZ_{[r]}) \\ \text{cov}(XZ_{[k]}, Z_{[r]}) & \text{cov}(XZ_{[k]}, XZ_{[r]}) & \text{cov}(XZ_{[k]}, YZ_{[r]}) & \text{cov}(XZ_{[k]}, X^2Z_{[r]}) & \text{cov}(XZ_{[k]}, Y^2Z_{[r]}) & \text{cov}(XZ_{[k]}, XYZ_{[r]}) \\ \text{cov}(YZ_{[k]}, Z_{[r]}) & \text{cov}(YZ_{[k]}, XZ_{[r]}) & \text{cov}(YZ_{[k]}, YZ_{[r]}) & \text{cov}(YZ_{[k]}, X^2Z_{[r]}) & \text{cov}(YZ_{[k]}, Y^2Z_{[r]}) & \text{cov}(YZ_{[k]}, XYZ_{[r]}) \\ \text{cov}(X^2Z_{[k]}, Z_{[r]}) & \text{cov}(X^2Z_{[k]}, XZ_{[r]}) & \text{cov}(X^2Z_{[k]}, YZ_{[r]}) & \text{cov}(X^2Z_{[k]}, X^2Z_{[r]}) & \text{cov}(X^2Z_{[k]}, Y^2Z_{[r]}) & \text{cov}(X^2Z_{[k]}, XYZ_{[r]}) \\ \text{cov}(Y^2Z_{[k]}, Z_{[r]}) & \text{cov}(Y^2Z_{[k]}, XZ_{[r]}) & \text{cov}(Y^2Z_{[k]}, YZ_{[r]}) & \text{cov}(Y^2Z_{[k]}, X^2Z_{[r]}) & \text{cov}(Y^2Z_{[k]}, Y^2Z_{[r]}) & \text{cov}(Y^2Z_{[k]}, XYZ_{[r]}) \\ \text{cov}(XYZ_{[k]}, Z_{[r]}) & \text{cov}(XYZ_{[k]}, XZ_{[r]}) & \text{cov}(XYZ_{[k]}, YZ_{[r]}) & \text{cov}(XYZ_{[k]}, X^2Z_{[r]}) & \text{cov}(XYZ_{[k]}, Y^2Z_{[r]}) & \text{var}(XYZ_{[k]}, XYZ_{[r]}) \end{bmatrix},$$

where

$$\text{cov}(Z_{[k]}, Z_{[r]}) = \mathbb{E}[Z_{[k]}Z_{[r]}] - \mathbb{E}[Z_{[k]}]\mathbb{E}[Z_{[r]}] = 0 - p_k p_r = -p_k p_r,$$

$$\text{cov}(Z_{[k]}, XZ_{[r]}) = \mathbb{E}[XZ_{[k]}Z_{[r]}] - \mathbb{E}[Z_{[k]})\mathbb{E}[XZ_{[r]}] = 0 - p_k \cdot 0 = 0,$$

$$\text{cov}(Z_{[k]}, YZ_{[r]}) = 0,$$

$$\text{cov}(Z_{[k]}, X^2Z_{[r]}) = \mathbb{E}[X^2Z_{[k]}Z_{[r]}] - \mathbb{E}[Z_{[k]})\mathbb{E}[X^2Z_{[r]}] = 0 - p_k p_r = -p_k p_r,$$

$$\text{cov}(Z_{[k]}, Y^2Z_{[r]}) = -p_k p_r,$$

$$\text{cov}(Z_{[k]}, XYZ_{[r]}) = \mathbb{E}[XYZ_{[k]}Z_{[r]}] - \mathbb{E}[Z_{[k]})\mathbb{E}[XYZ_{[r]}] = 0 - p_k p_r \rho_r = -p_k p_r \rho_r,$$

$$\text{cov}(XZ_{[k]}, Z_{[r]}) = \mathbb{E}[XZ_{[k]}Z_{[r]}] - \mathbb{E}[XZ_{[k]})\mathbb{E}[Z_{[r]}] = 0 - 0 = 0,$$

$$\text{cov}(XZ_{[k]}, XZ_{[r]}) = \mathbb{E}[X^2Z_{[k]}Z_{[r]}] - \mathbb{E}[XZ_{[k]})\mathbb{E}[XZ_{[r]}] = 0 - 0 = 0,$$

$$\text{cov}(XZ_{[k]}, YZ_{[r]}) = \mathbb{E}[XYZ_{[k]}Z_{[r]}] - \mathbb{E}[XZ_{[k]})\mathbb{E}[YZ_{[r]}] = 0 - 0 = 0,$$

$$\text{cov}(XZ_{[k]}, X^2Z_{[r]}) = \mathbb{E}[X^3Z_{[k]}Z_{[r]}] - \mathbb{E}[XZ_{[k]})\mathbb{E}[X^2Z_{[r]}] = 0 - 0 = 0,$$

$$\text{cov}(XZ_{[k]}, Y^2Z_{[r]}) = \mathbb{E}[XY^2Z_{[k]}Z_{[r]}] - \mathbb{E}[XZ_{[k]})\mathbb{E}[Y^2Z_{[r]}] = 0 - 0 = 0,$$

$$\text{cov}(XZ_{[k]}, XYZ_{[r]}) = \mathbb{E}[X^2YZ_{[k]}Z_{[r]}] - \mathbb{E}[XZ_{[k]})\mathbb{E}[XYZ_{[r]}] = 0 - 0 = 0,$$

$$\text{cov}(YZ_{[k]}, Z_{[r]}) = \mathbb{E}[YZ_{[k]}Z_{[r]}] - \mathbb{E}[YZ_{[k]})\mathbb{E}[Z_{[r]}] = 0 - 0 = 0,$$

$$\text{cov}(YZ_{[k]}, XZ_{[r]}) = \mathbb{E}[XYZ_{[k]}Z_{[r]}] - \mathbb{E}[YZ_{[k]})\mathbb{E}[XZ_{[r]}] = 0 - 0 = 0,$$

$$\text{cov}(YZ_{[k]}, YZ_{[r]}) = \mathbb{E}[Y^2Z_{[k]}Z_{[r]}] - \mathbb{E}[YZ_{[k]})\mathbb{E}[YZ_{[r]}] = 0 - 0 = 0,$$

$$\text{cov}(YZ_{[k]}, X^2Z_{[r]}) = \mathbb{E}[X^2YZ_{[k]}Z_{[r]}] - \mathbb{E}[YZ_{[k]})\mathbb{E}[X^2Z_{[r]}] = 0 - 0 = 0,$$

$$\text{cov}(YZ_{[k]}, Y^2Z_{[r]}) = \mathbb{E}[Y^3Z_{[k]}Z_{[r]}] - \mathbb{E}[YZ_{[k]})\mathbb{E}[Y^2Z_{[r]}] = 0 - 0 = 0,$$

$$\text{cov}(YZ_{[k]}, XYZ_{[r]}) = \mathbb{E}[XY^2Z_{[k]}Z_{[r]}] - \mathbb{E}[YZ_{[k]})\mathbb{E}[XYZ_{[r]}] = 0 - 0 = 0,$$

$$\text{cov}(X^2Z_{[k]}, Z_{[r]}) = \mathbb{E}[X^2Z_{[k]}Z_{[r]}] - \mathbb{E}[X^2Z_{[k]})\mathbb{E}[Z_{[r]}] = 0 - p_k p_r = -p_k p_r,$$

$$\text{cov}(X^2Z_{[k]}, XZ_{[r]}) = \mathbb{E}[X^3Z_{[k]}Z_{[r]}] - \mathbb{E}[X^2Z_{[k]})\mathbb{E}[XZ_{[r]}] = 0 - 0 = 0,$$

$$\text{cov}(X^2Z_{[k]}, YZ_{[r]}) = \mathbb{E}[X^2YZ_{[k]}Z_{[r]}] - \mathbb{E}[X^2Z_{[k]})\mathbb{E}[YZ_{[r]}] = 0 - 0 = 0,$$

$$\text{cov}(X^2Z_{[k]}, X^2Z_{[r]}) = \mathbb{E}[X^4Z_{[k]}Z_{[r]}] - \mathbb{E}[X^2Z_{[k]})\mathbb{E}[X^2Z_{[r]}] = 0 - p_k p_r = -p_k p_r,$$

$$\text{cov}(X^2Z_{[k]}, Y^2Z_{[r]}) = \mathbb{E}[X^2Y^2Z_{[k]}Z_{[r]}] - \mathbb{E}[X^2Z_{[k]})\mathbb{E}[Y^2Z_{[r]}] = 0 - p_k p_r = -p_k p_r,$$

$$\text{cov}(X^2Z_{[k]}, XYZ_{[r]}) = \mathbb{E}[X^3YZ_{[k]}Z_{[r]}] - \mathbb{E}[X^2Z_{[k]})\mathbb{E}[XYZ_{[r]}] = 0 - p_k p_r \rho_r = -p_k p_r \rho_r,$$

$$\text{cov}(Y^2Z_{[k]}, Z_{[r]}) = \mathbb{E}[Y^2Z_{[k]}Z_{[r]}] - \mathbb{E}[Y^2Z_{[k]})\mathbb{E}[Z_{[r]}] = 0 - p_k p_r = -p_k p_r,$$

$$\text{cov}(Y^2Z_{[k]}, XZ_{[r]}) = \mathbb{E}[XY^2Z_{[k]}Z_{[r]}] - \mathbb{E}[Y^2Z_{[k]})\mathbb{E}[XZ_{[r]}] = 0 - 0 = 0,$$

$$\text{cov}(Y^2Z_{[k]}, YZ_{[r]}) = \mathbb{E}[Y^3Z_{[k]}Z_{[r]}] - \mathbb{E}[Y^2Z_{[k]})\mathbb{E}[YZ_{[r]}] = 0 - 0 = 0,$$

$$\begin{aligned}
\text{cov}(Y^2 Z_{[k]}, X^2 Z_{[r]}) &= \mathbb{E}[X^2 Y^2 Z_{[k]} Z_{[r]}] - \mathbb{E}[Y^2 Z_{[k]}] \mathbb{E}[X^2 Z_{[r]}] = 0 - p_k p_r = -p_k p_r, \\
\text{cov}(Y^2 Z_{[k]}, Y^2 Z_{[r]}) &= \mathbb{E}[Y^4 Z_{[k]} Z_{[r]}] - \mathbb{E}[Y^2 Z_{[k]}] \mathbb{E}[Y^2 Z_{[r]}] = 0 - p_k p_r = -p_k p_r, \\
\text{cov}(Y^2 Z_{[k]}, XY Z_{[r]}) &= \mathbb{E}[XY^3 Z_{[k]} Z_{[r]}] - \mathbb{E}[Y^2 Z_{[k]}] \mathbb{E}[XY Z_{[r]}] = 0 - p_k p_r \rho_r = -p_k p_r \rho_r, \\
\text{cov}(XY Z_{[k]}, Z_{[r]}) &= \mathbb{E}[XY Z_{[k]} Z_{[r]}] - \mathbb{E}[XY Z_{[k]}] \mathbb{E}[Z_{[r]}] = 0 - p_k \rho_k p_r = -p_k p_r \rho_k, \\
\text{cov}(XY Z_{[k]}, X Z_{[r]}) &= \mathbb{E}[X^2 Y Z_{[k]} Z_{[r]}] - \mathbb{E}[XY Z_{[k]}] \mathbb{E}[X Z_{[r]}] = 0 - 0 = 0, \\
\text{cov}(XY Z_{[k]}, Y Z_{[r]}) &= \mathbb{E}[XY^2 Z_{[k]} Z_{[r]}] - \mathbb{E}[XY Z_{[k]}] \mathbb{E}[Y Z_{[r]}] = 0 - 0 = 0, \\
\text{cov}(XY Z_{[k]}, X^2 Z_{[r]}) &= \mathbb{E}[X^3 Y Z_{[k]} Z_{[r]}] - \mathbb{E}[XY Z_{[k]}] \mathbb{E}[X^2 Z_{[r]}] = 0 - p_k \rho_k p_r = -p_k p_r \rho_k, \\
\text{cov}(XY Z_{[k]}, Y^2 Z_{[r]}) &= \mathbb{E}[XY^3 Z_{[k]} Z_{[r]}] - \mathbb{E}[XY Z_{[k]}] \mathbb{E}[Y^2 Z_{[r]}] = 0 - p_k \rho_k p_r = -p_k p_r \rho_k, \\
\text{cov}(XY Z_{[k]}, XY Z_{[r]}) &= \mathbb{E}[X^2 Y^2 Z_{[k]} Z_{[r]}] - \mathbb{E}[XY Z_{[k]}] \mathbb{E}[XY Z_{[r]}] = 0 - p_k \rho_k p_r \rho_r = -p_k p_r \rho_k \rho_r.
\end{aligned}$$

That is,

$$\mathbf{\Sigma}_{kr} = \begin{bmatrix} -p_k p_r & 0 & 0 & -p_k p_r & -p_k p_r & -p_k p_r \rho_r \\ 0 & 0 & 0 & 0 & 0 & 0 \\ 0 & 0 & 0 & 0 & 0 & 0 \\ -p_k p_r & 0 & 0 & -p_k p_r & -p_k p_r & -p_k p_r \rho_r \\ -p_k p_r & 0 & 0 & -p_k p_r & -p_k p_r & -p_k p_r \rho_r \\ -p_k p_r \rho_k & 0 & 0 & -p_k p_r \rho_k & -p_k p_r \rho_k & -p_k p_r \rho_k \rho_r \end{bmatrix}.$$

Applying Cramér's Theorem (Ferguson, 1996) to function g (Equation (A.4)) and the joint asymptotic distribution of $\widehat{\boldsymbol{\mu}}$ (Equation (A.5)), we have the joint asymptotic distribution of $\widehat{\boldsymbol{\theta}} = g(\widehat{\boldsymbol{\mu}})$ as

$$\sqrt{n} \left(\widehat{\boldsymbol{\theta}} - \boldsymbol{\theta} \right) \xrightarrow{d} \mathcal{N}(0, \boldsymbol{\Omega}), \tag{A.6}$$

where

$$\boldsymbol{\theta} = g(\boldsymbol{\mu}) = g \begin{pmatrix} p_1 \\ 0 \\ 0 \\ p_1 \\ p_1 \\ p_1 \rho_1 \\ \vdots \\ p_K \\ 0 \\ 0 \\ p_K \\ p_K \\ p_K \\ p_K \rho_K \end{pmatrix} = \begin{pmatrix} p_1 \\ \rho_1 \\ 1 \\ 1 \\ \vdots \\ p_K \\ \rho_K \\ 1 \\ 1 \end{pmatrix},$$

and

$$\boldsymbol{\Omega} = Dg(\boldsymbol{\mu}) \boldsymbol{\Sigma} (Dg(\boldsymbol{\mu}))^\top.$$

Evaluating the Jacobian of g at $\boldsymbol{\mu}$, we have

$$Dg(\boldsymbol{\mu}) = \begin{bmatrix} Dg(\boldsymbol{\mu})_1 & & \\ & \ddots & \\ & & Dg(\boldsymbol{\mu})_K \end{bmatrix},$$

with

$$Dg(\boldsymbol{\mu})_k = \begin{bmatrix} 1 & 0 & 0 & 0 & 0 & 0 \\ -\rho_k/p_k & 0 & 0 & 0 & 0 & 1/p_k \\ -1/p_k & 0 & 0 & 1/p_k & 0 & 0 \\ -1/p_k & 0 & 0 & 0 & 1/p_k & 0 \end{bmatrix}.$$

Hence,

$$\boldsymbol{\Omega} = \begin{bmatrix} \boldsymbol{\Omega}_{11} & \cdots & \boldsymbol{\Omega}_{1K} \\ \vdots & \ddots & \vdots \\ \boldsymbol{\Omega}_{K1} & \cdots & \boldsymbol{\Omega}_{KK} \end{bmatrix}_{(4K) \times (4K)},$$

where for $k = 1, \dots, K$,

$$\begin{aligned} \mathbf{\Omega}_{kk} &= Dg(\boldsymbol{\mu})_k \boldsymbol{\Sigma}_{kk} (Dg(\boldsymbol{\mu})_k)^\top \\ &= \begin{bmatrix} p_k(1-p_k) & 0 & 0 & 0 \\ 0 & \frac{-\rho_k^2 + \mu_{X^2Y^2,k}}{p_k} & \frac{-\rho_k + \mu_{X^3Y,k}}{p_k} & \frac{-\rho_k + \mu_{XY^3,k}}{p_k} \\ 0 & \frac{-\rho_k + \mu_{X^3Y,k}}{p_k} & \frac{-1 + \mu_{X^4,k}}{p_k} & \frac{-1 + \mu_{X^2Y^2,k}}{p_k} \\ 0 & \frac{-\rho_k + \mu_{XY^3,k}}{p_k} & \frac{-1 + \mu_{X^2Y^2,k}}{p_k} & \frac{-1 + \mu_{Y^4,k}}{p_k} \end{bmatrix}, \end{aligned}$$

and for $1 \leq k \neq r \leq K$,

$$\mathbf{\Omega}_{kr} = Dg(\boldsymbol{\mu})_k \boldsymbol{\Sigma}_{kr} (Dg(\boldsymbol{\mu})_r)^\top = \begin{bmatrix} -p_k p_r & 0 & 0 & 0 \\ 0 & 0 & 0 & 0 \\ 0 & 0 & 0 & 0 \\ 0 & 0 & 0 & 0 \end{bmatrix}.$$

With the joint asymptotic distribution of $\widehat{\boldsymbol{\theta}} = (\widehat{p}_1, \widehat{\sigma}_{XY,1}, \widehat{\sigma}_{X,1}^2, \widehat{\sigma}_{Y,1}^2, \dots, \widehat{p}_K, \widehat{\sigma}_{XY,K}, \widehat{\sigma}_{X,K}^2, \widehat{\sigma}_{Y,K}^2)^\top$, our final step is to derive the asymptotic distribution of $R_{\mathcal{G}(S)}^2$.

Given any $\boldsymbol{\eta} = (x_1, y_1, z_1, u_1, \dots, x_K, y_K, z_K, u_K)^\top \in \mathbb{R}^{4K}$, we define a function $h : \mathbb{R}^{4K} \rightarrow \mathbb{R}$ as

$$h(\boldsymbol{\eta}) = \sum_{k=1}^K x_k \frac{y_k^2}{z_k u_k}.$$

Hence,

$$R_{\mathcal{G}(S)}^2 = h(\widehat{\boldsymbol{\theta}}).$$

The gradient of h is

$$\nabla h(\boldsymbol{\eta}) = \left(\frac{y_1^2}{z_1 u_1}, 2x_1 \frac{y_1}{z_1 u_1}, -x_1 \frac{y_1^2}{z_1^2 u_1}, -x_1 \frac{y_1^2}{z_1 u_1^2}, \dots, \frac{y_K^2}{z_K u_K}, 2x_K \frac{y_K}{z_K u_K}, -x_K \frac{y_K^2}{z_K^2 u_K}, -x_K \frac{y_K^2}{z_K u_K^2} \right)^\top.$$

Applying Cramér's Theorem (Ferguson, 1996) to the joint asymptotic distribution of $\widehat{\boldsymbol{\theta}}$ (Equation (A.6)), we have

$$\sqrt{n} \left(R_{\mathcal{G}(S)}^2 - h(\boldsymbol{\theta}) \right) \xrightarrow{d} \mathcal{N} \left(0, (\nabla h(\boldsymbol{\theta}))^\top \boldsymbol{\Omega} \nabla h(\boldsymbol{\theta}) \right).$$

Given $\boldsymbol{\theta} = (p_1, \rho_1, 1, 1, \dots, p_K, \rho_K, 1, 1)^\top$, it is easy to see that

$$h(\boldsymbol{\theta}) = \sum_{k=1}^K p_k \rho_k^2 = \rho_{\mathcal{G}(S)}^2,$$

based on the definition of the population measure $\rho_{G(S)}^2$ in Equation (6).

Evaluating the gradient of h at $\boldsymbol{\theta}$, we have

$$\nabla h(\boldsymbol{\theta}) = \left((\nabla h(\boldsymbol{\theta})_1)^\top, \dots, (\nabla h(\boldsymbol{\theta})_K)^\top \right)^\top, \text{ with } \nabla h(\boldsymbol{\theta})_k = (\rho_k^2, 2p_k\rho_k, -p_k\rho_k^2, -p_k\rho_k^2)^\top.$$

Hence,

$$(\nabla h(\boldsymbol{\theta}))^\top \boldsymbol{\Omega} \nabla h(\boldsymbol{\theta}) = \sum_{k=1}^K \sum_{r=1}^K (\nabla h(\boldsymbol{\theta})_k)^\top \boldsymbol{\Omega}_{kr} \nabla h(\boldsymbol{\theta})_r.$$

For $k = 1, \dots, K$,

$$\begin{aligned} & (\nabla h(\boldsymbol{\theta})_k)^\top \boldsymbol{\Omega}_{kk} \nabla h(\boldsymbol{\theta})_k \\ &= (\rho_k^2, 2p_k\rho_k, -p_k\rho_k^2, -p_k\rho_k^2) \begin{bmatrix} p_k(1-p_k) & 0 & 0 & 0 \\ 0 & \frac{-\rho_k^2 + \mu_{X^2Y^2,k}}{p_k} & \frac{-\rho_k + \mu_{X^3Y,k}}{p_k} & \frac{-\rho_k + \mu_{XY^3,k}}{p_k} \\ 0 & \frac{-\rho_k + \mu_{X^3Y,k}}{p_k} & \frac{-1 + \mu_{X^4,k}}{p_k} & \frac{-1 + \mu_{X^2Y^2,k}}{p_k} \\ 0 & \frac{-\rho_k + \mu_{XY^3,k}}{p_k} & \frac{-1 + \mu_{X^2Y^2,k}}{p_k} & \frac{-1 + \mu_{Y^4,k}}{p_k} \end{bmatrix} \begin{pmatrix} \rho_k^2 \\ 2p_k\rho_k \\ -p_k\rho_k^2 \\ -p_k\rho_k^2 \end{pmatrix} \\ &= p_k \left[\rho_k^4 (\mu_{X^4,k} + 2\mu_{X^2Y^2,k} + \mu_{Y^4,k}) - 4\rho_k^3 (\mu_{X^3Y,k} + \mu_{XY^3,k}) + 4\rho_k^2 \mu_{X^2Y^2,k} \right] + p_k(1-p_k)\rho_k^4 \\ &= A_{k(S)} + B_{k(S)} \text{ as defined in (31)}. \end{aligned}$$

For $1 \leq k \neq r \leq K$,

$$\begin{aligned} & (\nabla h(\boldsymbol{\theta})_k)^\top \boldsymbol{\Omega}_{kr} \nabla h(\boldsymbol{\theta})_r \\ &= (\rho_k^2, 2\rho_k, -\rho_k^2, -\rho_k^2) \begin{bmatrix} -p_k p_r & 0 & 0 & 0 \\ 0 & 0 & 0 & 0 \\ 0 & 0 & 0 & 0 \\ 0 & 0 & 0 & 0 \end{bmatrix} \begin{pmatrix} \rho_r^2 \\ 2\rho_r \\ -\rho_r^2 \\ -\rho_r^2 \end{pmatrix} \\ &= -p_k p_r \rho_k^2 \rho_r^2 \\ &= C_{kr(S)} \text{ as defined in (31)}. \end{aligned}$$

Hence,

$$\begin{aligned}
(\nabla h(\boldsymbol{\theta}))^\top \boldsymbol{\Omega} \nabla h(\boldsymbol{\theta}) &= \sum_{k=1}^K (\nabla h(\boldsymbol{\theta})_k)^\top \boldsymbol{\Omega}_{kk} \nabla h(\boldsymbol{\theta})_k + 2 \sum_{1 \leq k < r \leq K} (\nabla h(\boldsymbol{\theta})_k)^\top \boldsymbol{\Omega}_{kr} \nabla h(\boldsymbol{\theta})_r \\
&= \sum_{k=1}^K (A_{k(\mathcal{S})} + B_{k(\mathcal{S})}) + 2 \sum_{1 \leq k < r \leq K} C_{kr(\mathcal{S})} \\
&= \gamma_{(\mathcal{S})}^2.
\end{aligned}$$

Therefore, the asymptotic distribution of $R_{\mathcal{G}(\mathcal{S})}^2$ is

$$\sqrt{n} \left(R_{\mathcal{G}(\mathcal{S})}^2 - \rho_{\mathcal{G}(\mathcal{S})}^2 \right) \xrightarrow{d} \mathcal{N} \left(0, \gamma_{(\mathcal{S})}^2 \right).$$

□

A.4 Proof of Corollary 3.2

Proof. Following the proof of Theorem 3.1, where we assume without loss of generality that

$$\begin{aligned}
\mu_{X,k} &= \mathbb{E}[X|Z = k] = 0, \\
\mu_{Y,k} &= \mathbb{E}[Y|Z = k] = 0, \\
\sigma_{X,k}^2 &= \text{var}[X|Z = k] = 1, \\
\sigma_{Y,k}^2 &= \text{var}[Y|Z = k] = 1.
\end{aligned}$$

Then in this special case, with the same notations used in the proof of Theorem 3.1, we have

$$(X, Y)|(Z = k) \sim \mathcal{N} \left(\mathbf{0}, \begin{bmatrix} 1 & \rho_k \\ \rho_k & 1 \end{bmatrix} \right),$$

with the following moments

$$\begin{aligned}
\mu_{X^4,k} &= \mathbb{E}[X^4|Z = k] = 3, & \mu_{Y^4,k} &= \mathbb{E}[Y^4|Z = k] = 3, \\
\mu_{X^3Y,k} &= \mathbb{E}[X^3Y|Z = k] = 3\rho_k, & \mu_{XY^3,k} &= \mathbb{E}[XY^3|Z = k] = 3\rho_k, \\
\mu_{X^2Y^2,k} &= \mathbb{E}[X^2Y^2|Z = k] = (1 + 2\rho_k^2).
\end{aligned}$$

Hence,

$$\begin{aligned}
A_k &= p_k \left[\rho_k^4 (\mu_{X^4,k} + 2\mu_{X^2Y^2,k} + \mu_{Y^4,k}) - 4\rho_k^3 (\mu_{X^3Y,k} + \mu_{XY^3,k}) + 4\rho_k^2 \mu_{X^2Y^2,k} \right] \\
&= p_k (8\rho_k^4 + 4\rho_k^6 - 24\rho_k^4 + 8\rho_k^4 + 4\rho_k^2) \\
&= 4p_k \rho_k^2 (1 - \rho_k^2)^2.
\end{aligned}$$

Provided that

$$\begin{aligned} B_k &= p_k(1 - p_k)\rho_k^4, \\ C_{kr} &= -p_k p_r \rho_k^2 \rho_r^2, \quad k \neq r, \end{aligned}$$

the joint asymptotic distribution of $R_{\mathcal{G}(\mathcal{S})}^2$ in (30) becomes (32), which completes the proof. \square

A.5 Proof of Theorem 3.3

Here we adapt the main ideas from the proof of the strong consistency theorem of the K -means clustering algorithm (Pollard et al., 1981). A key technical challenge we need to tackle in this proof is the handling of two types of points, where the *data* type refers to the n data points $(X_1, Y_1)^\top, \dots, (X_n, Y_n)^\top$, and the *center* type corresponds to the K lines $\beta_1 = (a_1, b_1, c_1)^\top, \dots, \beta_K = (a_K, b_K, c_K)^\top$, where $a_k \neq 0$ or $b_k \neq 0$, $k = 1, \dots, K$, as cluster centers. In this proof, without loss of generality, we assume $0 < c_k < \infty$, $k = 1, \dots, K$, because we can always find a vertical shift of the data and the K lines to satisfy this condition. To simplify the following discussion, we define a *center point* $(\eta, \xi)^\top$ as an equivalent representation of a line $\beta = (a, b, c)^\top$, such that

$$\begin{cases} \eta = -ac/(a^2 + b^2) \\ \xi = -bc/(a^2 + b^2) \end{cases} \quad \text{and} \quad \begin{cases} a = -\eta/\sqrt{\eta^2 + \xi^2} \cdot u \\ b = -\xi/\sqrt{\eta^2 + \xi^2} \cdot u \\ c = \sqrt{\eta^2 + \xi^2} \cdot u \end{cases} \quad \text{with } u \neq 0, \quad (\text{A.7})$$

so that $\|(\eta, \xi)^\top\| = d_\perp((0, 0)^\top, \beta)$, where the perpendicular distance $d_\perp(\cdot, *)$ is defined in Equation (7).

We define the distance between a data point $(x, y)^\top$ and a center point $(\eta, \xi)^\top$ not as the usual Euclidean distance but as

$$d'((x, y)^\top, (\eta, \xi)^\top) := d_\perp((x, y)^\top, \beta) = \frac{|-\eta x - \xi y + \eta^2 + \xi^2|}{\sqrt{\eta^2 + \xi^2}}.$$

Note that $d'(\cdot, *)$ is not a metric, and $d'((x, y)^\top, (\eta, \xi)^\top) = \|(x, y)^\top - (\eta, \xi)^\top\|$ if and only if $(x, y)^\top = (0, 0)^\top$.

The result in Lemma 2.1 now translates to

$$d'((x, y)^\top, (\eta, \xi)^\top) \leq \|(x, y)^\top - (x', y')^\top\| + d'((x', y')^\top, (\eta, \xi)^\top). \quad (\text{A.8})$$

For the rest of the proof, we denote the set of K cluster centers using two equivalent representations:

1. $B'_K = \{(\eta_1, \xi_1)^\top, \dots, (\eta_K, \xi_K)^\top\}$, where each cluster center is represented by a center point.
2. $B_K = \{\beta_1, \dots, \beta_K\}$, where each line $\beta_k = (a_k, b_k, c_k)^\top$, where $a_k \neq 0$ or $b_k \neq 0$.

The one-to-one relationship between $(\eta_k, \xi_k)^\top$ and $(a_k, b_k, c_k)^\top$ follows from (A.7). Hence, there is a one-to-one correspondence between B'_K and B_K , and we define

$$\begin{aligned} W'(B'_K, P) &:= \int \min_{(\eta, \xi)^\top \in B'_K} d'^2 \left((x, y)^\top, (\eta, \xi)^\top \right) P \left((dx, dy)^\top \right) \\ &= \int \min_{\beta \in B_K} d_\perp^2 \left((x, y)^\top, \beta \right) P \left((dx, dy)^\top \right) \\ &= W(B_K, P). \end{aligned} \tag{A.9}$$

We define the set of center points to which the origin data point $(0, 0)^\top$ has a distance no greater than $M > 0$ as

$$\mathcal{B}(M) := \left\{ (\eta, \xi)^\top : d' \left((0, 0)^\top, (\eta, \xi)^\top \right) \leq M \right\} = \left\{ (\eta, \xi)^\top : \eta^2 + \xi^2 \leq M^2 \right\},$$

which is a closed ball of radius M and centered at the origin in \mathbb{R}^2 .

The first step consists of finding an $M > 0$ so large that, when n is large enough, at least one center point in $\widehat{B}'_{K(\mathcal{U})} = \left\{ (\widehat{\eta}_1, \widehat{\xi}_1)^\top, \dots, (\widehat{\eta}_K, \widehat{\xi}_K)^\top \right\}$ (the alternative representation of $\widehat{B}_{K(\mathcal{U})} = \left\{ \widehat{\beta}_{1(\mathcal{U})}, \dots, \widehat{\beta}_{K(\mathcal{U})} \right\}$ defined in Equation (20)) is contained in the set $\mathcal{B}(M)$. We will prove this in the following using a counterexample.

- We find an $r > 0$ so that the ball $\mathcal{B}(r) \subset \mathbb{R}^2$ of radius r and centered at the origin has a positive P measure. For the purposes of this first step, it will suffice that M be large enough to make

$$(M - r)^2 P(\mathcal{B}(r)) > \int d'^2 \left((x, y)^\top, (1, 1)^\top \right) P \left((dx, dy)^\top \right), \tag{A.10}$$

(1st requirement on M)

whose right hand side is equal to $\int d_\perp \left((x, y)^\top, (-1, -1, 2)^\top \right)^2 P \left((dx, dy)^\top \right)$, which is finite by (34). Define $B'_0 = \{(1, 1)^\top\}$, a set with one center point. Then (A.10) becomes

$$(M - r)^2 P(\mathcal{B}(r)) > W'(B'_0, P). \tag{A.11}$$

- By the strong law of large numbers (SLLN),

$$\begin{aligned}
W'(B'_0, P_n) &= \int d'^2 \left((x, y)^\top, (1, 1)^\top \right) P_n \left((dx, dy)^\top \right) \\
&\rightarrow \int d'^2 \left((x, y)^\top, (1, 1)^\top \right) P \left((dx, dy)^\top \right) \text{ a.s.} \\
&= W'(B'_0, P).
\end{aligned} \tag{A.12}$$

- If, for infinitely many values of n , no centers in $\widehat{B}'_{K(\mathcal{U})}$ were contained in $\mathcal{B}(M)$, i.e., $\min_{(\eta, \xi)^\top \in \widehat{B}'_{K(\mathcal{U})}} d' \left((0, 0)^\top, (\eta, \xi)^\top \right) > M$, then

$$\limsup_n W'(\widehat{B}'_{K(\mathcal{U})}, P_n) \geq \lim_n (M - r)^2 P_n(\mathcal{B}(r)) = (M - r)^2 P(\mathcal{B}(r)) \text{ a.s.}, \tag{A.13}$$

where the first inequality holds because for any data point $(X_i, Y_i)^\top \in \mathcal{B}(r)$, which has a positive P measure, the following holds by (A.8):

$$\begin{aligned}
\min_{(\eta, \xi)^\top \in B'_n} d' \left((X_i, Y_i)^\top, (\eta, \xi)^\top \right) &\geq \min_{(\eta, \xi)^\top \in B'_n} d' \left((0, 0)^\top, (\eta, \xi)^\top \right) - \left\| (X_i, Y_i)^\top - (0, 0)^\top \right\| \\
&> M - r.
\end{aligned}$$

- Hence by (A.11), (A.12) and (A.13),

$$\limsup_n W'(\widehat{B}'_{K(\mathcal{U})}, P_n) > \lim_n W'(B'_0, P_n), \tag{A.14}$$

which implies that $W(\widehat{B}_{K(\mathcal{U})}, P_n) = W'(\widehat{B}'_{K(\mathcal{U})}, P_n) > W'(B'_0, P_n) = W(B_0, P_n)$ infinitely often, where $B_0 = \{(-1, 2)^\top\}$ is the set of one line corresponding to B'_0 . This contradicts the definition of $\widehat{B}_{K(\mathcal{U})}$ in (20) of Definition 7: $W(\widehat{B}_{K(\mathcal{U})}, P_n) \leq W(B_0, P_n)$ for any set B_0 containing at most K lines. Without loss of generality, we therefore assume that $\widehat{B}'_{K(\mathcal{U})}$ always contains at least one center point in $\mathcal{B}(M)$. We denote one of such center points as $(\widehat{\eta}_1, \widehat{\xi}_1)^\top$.

If $K = 1$, the second step in this proof can be skipped; if $K > 1$, then we will show that, for n large enough, the set $\mathcal{B}(5M)$ contains all the center points in $\widehat{B}'_{K(\mathcal{U})}$.

- For the purposes of an inductive argument, we assume that the conclusions of the theorem are valid when applied to globally optimal clustering with $1, 2, \dots, K - 1$ centers. If $\widehat{B}'_{K(\mathcal{U})}$ were not eventually contained in $\mathcal{B}(5M)$, we could delete the center points in $\widehat{B}'_{K(\mathcal{U})}$ that are

outside of $\mathcal{B}(5M)$ to obtain a set of at most $K - 1$ center points that would reduce $W'(\cdot, P_n)$ below its minimum over all sets of $K - 1$ centers, i.e., $W'(\widehat{B}'_{K-1}(\mathcal{U}), P_n)$, which results in a contradiction.

- To obtain such a contradiction, we need M large enough to ensure that

$$4 \int_{\|(x,y)^\top\| \geq 2M} \left\| (x,y)^\top \right\|^2 P \left((dx, dy)^\top \right) < \epsilon, \quad (\text{A.15})$$

(2nd requirement on M)

where $\epsilon > 0$ is chosen to satisfy $\epsilon < W'(B'_{K-1}(\mathcal{U}), P) - W'(B'_K(\mathcal{U}), P)$, which is positive by the uniqueness condition on $B_k(\mathcal{U})$ and thus $B'_k(\mathcal{U})$.

- Suppose that $\widehat{B}'_{K(\mathcal{U})}$ contains at least one center point outside $\mathcal{B}(5M)$. Denote one of such center points as $(\widehat{\eta}_K, \widehat{\xi}_K)^\top$. What would be the effect on $W'(\cdot, P_n)$ of deleting such center points in $\widehat{B}'_{K(\mathcal{U})}$? At worst, one of the centers that are known to lie in $\mathcal{B}(M)$, e.g., $(\widehat{\eta}_1, \widehat{\xi}_1)^\top$, might have to accept into its own cluster all of the data points presently assigned to cluster centers outside $\mathcal{B}(5M)$. Denote one of these data points as $(X_i, Y_i)^\top$. We argue that $(X_i, Y_i)^\top$ must have a Euclidean distance at least $2M$ from the origin data point $(0, 0)^\top$; otherwise $(X_i, Y_i)^\top$ would have been closer to the cluster center $(\widehat{\eta}_1, \widehat{\xi}_1)^\top$ than to $(\widehat{\eta}_K, \widehat{\xi}_K)^\top$. The reason is as follows. By (A.8),

$$\begin{aligned} d' \left((X_i, Y_i)^\top, (\widehat{\eta}_1, \widehat{\xi}_1)^\top \right) &\leq \left\| (X_i, Y_i)^\top - (0, 0)^\top \right\| + d' \left((0, 0)^\top, (\widehat{\eta}_1, \widehat{\xi}_1)^\top \right) \\ &\leq \left\| (X_i, Y_i)^\top \right\| + M, \\ d' \left((X_i, Y_i)^\top, (\widehat{\eta}_K, \widehat{\xi}_K)^\top \right) &\geq d' \left((0, 0)^\top, (\widehat{\eta}_K, \widehat{\xi}_K)^\top \right) - \left\| (X_i, Y_i)^\top - (0, 0)^\top \right\| \\ &\geq 5M - \left\| (X_i, Y_i)^\top \right\|. \end{aligned}$$

If $\left\| (X_i, Y_i)^\top \right\| < 2M$, then

$$d' \left((X_i, Y_i)^\top, (\widehat{\eta}_1, \widehat{\xi}_1)^\top \right) < 3M < d' \left((X_i, Y_i)^\top, (\widehat{\eta}_K, \widehat{\xi}_K)^\top \right).$$

That is, if $(X_i, Y_i)^\top$ were assigned to the cluster with center $(\widehat{\eta}_K, \widehat{\xi}_K)^\top$, then $\left\| (X_i, Y_i)^\top \right\| \geq 2M$.

- The extra contribution to $W'(\cdot, P_n)$ due to deleting centers outside $\mathcal{B}(5M)$ would therefore be at most

$$\begin{aligned}
& \int_{\|(x,y)^\top\| \geq 2M} d'^2 \left((x, y)^\top, (\hat{\eta}_1, \hat{\xi}_1)^\top \right) P_n \left((dx, dy)^\top \right) \\
& \leq \int_{\|(x,y)^\top\| \geq 2M} \left(\left\| (x, y)^\top - (0, 0)^\top \right\| + d' \left((0, 0)^\top, (\hat{\eta}_1, \hat{\xi}_1)^\top \right) \right)^2 P_n \left((dx, dy)^\top \right) \\
& \leq 4 \int_{\|(x,y)^\top\| \geq 2M} \left\| (x, y)^\top \right\|^2 P_n \left((dx, dy)^\top \right). \tag{A.16}
\end{aligned}$$

- The set $\widehat{B}'_{K(\mathcal{U})}$ obtained by deleting from $\widehat{B}'_{K(\mathcal{U})}$ all centers outside $\mathcal{B}(5M)$ is a candidate for minimizing $W'(\cdot, P_n)$ over sets of $K - 1$ or fewer centers; it is therefore beaten by the optimal set $\widehat{B}'_{K-1(\mathcal{U})}$. Thus

$$\begin{aligned}
W'(\widehat{B}'_{K(\mathcal{U})}, P_n) & \geq W'(\widehat{B}'_{K-1(\mathcal{U})}, P_n) \\
& = W(\widehat{B}_{K-1(\mathcal{U})}, P_n) \\
& \rightarrow W(B_{K-1(\mathcal{U})}, P) = W'(B'_{K-1(\mathcal{U})}, P) \text{ a.s.} \tag{A.17}
\end{aligned}$$

by the inductive hypothesis. If $\widehat{B}'_{K(\mathcal{U})} \not\subseteq \mathcal{B}(5M)$ along some subsequence $\{n_j\}$ of sample sizes, we therefore obtain

$$\begin{aligned}
& W'(B'_{K-1(\mathcal{U})}, P) \\
& \leq \liminf_j W'(\widehat{B}'_{K(\mathcal{U})}, P_{n_j}) \text{ a.s.} \tag{by (A.17)} \\
& \leq \limsup_n \left[W'(\widehat{B}'_{K(\mathcal{U})}, P_n) + 4 \int_{\|(x,y)^\top\| \geq 2M} \left\| (x, y)^\top \right\|^2 P_n \left((dx, dy)^\top \right) \right] \tag{by (A.16)} \\
& \leq \limsup_n W'(B'_{K(\mathcal{U})}, P_n) + 4 \int_{\|(x,y)^\top\| \geq 2M} \left\| (x, y)^\top \right\|^2 P \left((dx, dy)^\top \right) \text{ a.s.} \\
& < W'(B'_{K(\mathcal{U})}, P) + \epsilon \tag{by (A.15)} \\
& < W'(B'_{K-1(\mathcal{U})}, P),
\end{aligned}$$

a contradiction.

We now know that, for n large enough, it suffices to search for $\widehat{B}'_{K(\mathcal{U})}$ among the class of sets $\Xi_K = \{B' \subseteq \mathcal{B}(5M) : |B'| \leq K\}$. For the final requirement on M , we assume it is large enough to ensure that Ξ_K contains $B'_{K(\mathcal{U})}$. Therefore, the function $W'(\cdot, P)$ achieves its unique minimum on

Ξ_K at $B'_{K(\mathcal{U})}$. Under the topology induced by the Hausdorff metric, Ξ_K is compact (this follows from the compactness of $\mathcal{B}(5M)$) and, as is proved in (Pollard et al., 1981), the map $B' \rightarrow W'(B', P)$ is continuous on Ξ_K . The function $W'(\cdot, P)$ therefore enjoys an even stronger minimization property on Ξ_K : given any neighborhood \mathcal{N} of $B'_{K(\mathcal{U})}$, there exists an $\delta > 0$, depending on \mathcal{N} , such that

$$W'(B', P) \geq W'(B'_{K(\mathcal{U})}, P) + \delta, \forall B' \in \Xi_K \setminus \mathcal{N}.$$

The proof can now be completed by an appeal to a uniform SLLN:

$$\sup_{B' \in \Xi_K} |W'(B', P_n) - W'(B', P)| \rightarrow 0 \text{ a.s.}$$

This result is proved in (Pollard et al., 1981). We need to show that $\widehat{B}'_{K(\mathcal{U})}$ is eventually inside the neighborhood \mathcal{N} . It is enough to check that $W'(\widehat{B}'_{K(\mathcal{U})}, P) < W'(B'_{K(\mathcal{U})}, P) + \delta$ eventually. This follows from

$$W'(\widehat{B}'_{K(\mathcal{U})}, P_n) \leq W'(B'_{K(\mathcal{U})}, P_n)$$

and

$$W'(\widehat{B}'_{K(\mathcal{U})}, P_n) - W'(\widehat{B}'_{K(\mathcal{U})}, P) \rightarrow 0 \text{ a.s.}$$

and

$$W'(B'_{K(\mathcal{U})}, P_n) - W'(B'_{K(\mathcal{U})}, P) \rightarrow 0 \text{ a.s.}$$

Therefore, $\widehat{B}'_{K(\mathcal{U})} \rightarrow B'_{K(\mathcal{U})}$ a.s. That is, $\widehat{B}_{K(\mathcal{U})} \rightarrow B_{K(\mathcal{U})}$ a.s.

Similarly, for n large enough,

$$\begin{aligned} W(\widehat{B}_{K(\mathcal{U})}, P_n) &= W'(\widehat{B}'_{K(\mathcal{U})}, P_n) \\ &= \inf\{W'(B', P_n) : B' \in \Xi_K\} \\ &\rightarrow \inf\{W'(B', P) : B' \in \Xi_K\} \\ &= W'(B'_{K(\mathcal{U})}, P) = W(B_{K(\mathcal{U})}, P) \text{ a.s.} \end{aligned}$$

A.6 Proof of Theorem 3.4

Proof. We derive the asymptotic distribution of the unsupervised sample generalized R^2 , $R_{\mathcal{G}(\mathcal{U})}^2$, in this proof. For notation simplicity, we drop the subscript “ (\mathcal{U}) ” in $p_{k(\mathcal{U})}$ in (18), $\rho_{k(\mathcal{U})}^2$ in (19), and

$\widehat{p}_k(\mathcal{U})$, $\widehat{\rho}_k^2(\mathcal{U})$, $\bar{X}_k(\mathcal{U})$, and $\bar{Y}_k(\mathcal{U})$ in Definition 9, following which we have

$$R_{\mathcal{G}(\mathcal{U})}^2 = \sum_{k=1}^K \widehat{p}_k \widehat{\rho}_k^2 = \sum_{k=1}^K \widehat{p}_k \frac{\widehat{\sigma}_{XY,k}^2}{\widehat{\sigma}_{X,k}^2 \widehat{\sigma}_{Y,k}^2}, \quad (\text{A.18})$$

where

$$\begin{aligned} \widehat{p}_k &= \frac{1}{n} \sum_{i=1}^n \mathbb{I} \left(\widehat{Z}_i = k \right), \\ \widehat{\sigma}_{XY,k} &= \frac{1}{n \widehat{p}_k} \sum_{i=1}^n (X_i - \bar{X}_k)(Y_i - \bar{Y}_k) \mathbb{I} \left(\widehat{Z}_i = k \right), \\ \widehat{\sigma}_{X,k}^2 &= \frac{1}{n \widehat{p}_k} \sum_{i=1}^n (X_i - \bar{X}_k)^2 \mathbb{I} \left(\widehat{Z}_i = k \right), \\ \widehat{\sigma}_{Y,k}^2 &= \frac{1}{n \widehat{p}_k} \sum_{i=1}^n (Y_i - \bar{Y}_k)^2 \mathbb{I} \left(\widehat{Z}_i = k \right), \end{aligned}$$

with $\bar{X}_k = \frac{1}{n \widehat{p}_k} \sum_{i=1}^n X_i \mathbb{I} \left(\widehat{Z}_i = k \right)$ and $\bar{Y}_k = \frac{1}{n \widehat{p}_k} \sum_{i=1}^n Y_i \mathbb{I} \left(\widehat{Z}_i = k \right)$.

Similar to the proof of Theorem 3.1, to derive the asymptotic distribution of $R_{\mathcal{G}(\mathcal{U})}^2$, we need to first derive the joint asymptotic distribution of

$$\widehat{\boldsymbol{\theta}} = (\widehat{p}_1, \widehat{\sigma}_{XY,1}, \widehat{\sigma}_{X,1}^2, \widehat{\sigma}_{Y,1}^2, \dots, \widehat{p}_K, \widehat{\sigma}_{XY,K}, \widehat{\sigma}_{X,K}^2, \widehat{\sigma}_{Y,K}^2)^\top \in \mathbb{R}^{4K},$$

which depends on the joint asymptotic distribution of

$$\widehat{\boldsymbol{\mu}} = (M_1, M_{X,1}, M_{Y,1}, M_{X^2,1}, M_{Y^2,1}, M_{XY,1}, \dots, M_K, M_{X,K}, M_{Y,K}, M_{X^2,K}, M_{Y^2,K}, M_{XY,K})^\top \in \mathbb{R}^{6K},$$

where

$$\begin{aligned} M_k &:= \frac{1}{n} \sum_{i=1}^n \mathbb{I} \left(\widehat{Z}_i = k \right), & M_{XY,k} &:= \frac{1}{n} \sum_{i=1}^n X_i Y_i \mathbb{I} \left(\widehat{Z}_i = k \right), \\ M_{X,k} &:= \frac{1}{n} \sum_{i=1}^n X_i \mathbb{I} \left(\widehat{Z}_i = k \right), & M_{X^2,k} &:= \frac{1}{n} \sum_{i=1}^n X_i^2 \mathbb{I} \left(\widehat{Z}_i = k \right), \\ M_{Y,k} &:= \frac{1}{n} \sum_{i=1}^n Y_i \mathbb{I} \left(\widehat{Z}_i = k \right), & M_{Y^2,k} &:= \frac{1}{n} \sum_{i=1}^n Y_i^2 \mathbb{I} \left(\widehat{Z}_i = k \right), \end{aligned}$$

$k = 1, \dots, K$.

To derive the joint asymptotic distribution of $\widehat{\boldsymbol{\mu}}$, we need to resolve the non i.i.d. nature of $(X_1, Y_1, \widehat{Z}_1), \dots, (X_n, Y_n, \widehat{Z}_n)$, which is due to fact that \widehat{Z}_i depends on the K unsupervised sample line centers $\widehat{B}_K(\mathcal{U})$ and thus the whole sample $(X_1, Y_1), \dots, (X_n, Y_n)$. Given the K unsupervised

population line centers $B_{K(\mathcal{U})} = \{\boldsymbol{\beta}_{1(\mathcal{U})}, \dots, \boldsymbol{\beta}_{K(\mathcal{U})}\}$ defined in (14) in Definition 4, we define the (unobservable) realization of \tilde{Z} , defined in (16), based on the sample $(X_1, Y_1), \dots, (X_n, Y_n)$ as

$$\tilde{Z}_i := \arg \min_{k \in \{1, \dots, K\}} d_{\perp} \left((X_i, Y_i)^{\top}, \boldsymbol{\beta}_{k(\mathcal{U})} \right). \quad (\text{A.19})$$

Because $(X_1, Y_1), \dots, (X_n, Y_n)$ are i.i.d. and $B_{K(\mathcal{U})}$ is fixed, we have $(X_1, Y_1, \tilde{Z}_1), \dots, (X_n, Y_n, \tilde{Z}_n)$ as i.i.d. from the joint distribution of (X, Y, \tilde{Z}) .

Define

$$\hat{\boldsymbol{\mu}}^* = (M_1^*, M_{X,1}^*, M_{Y,1}^*, M_{X^2,1}^*, M_{Y^2,1}^*, M_{XY,1}^*, \dots, M_K^*, M_{X,K}^*, M_{Y,K}^*, M_{X^2,K}^*, M_{Y^2,K}^*, M_{XY,K}^*)^{\top} \in \mathbb{R}^{6K},$$

where

$$\begin{aligned} M_k^* &:= \frac{1}{n} \sum_{i=1}^n \mathbb{I}(\tilde{Z}_i = k), & M_{XY,k}^* &:= \frac{1}{n} \sum_{i=1}^n X_i Y_i \mathbb{I}(\tilde{Z}_i = k), \\ M_{X,k}^* &:= \frac{1}{n} \sum_{i=1}^n X_i \mathbb{I}(\tilde{Z}_i = k), & M_{X^2,k}^* &:= \frac{1}{n} \sum_{i=1}^n X_i^2 \mathbb{I}(\tilde{Z}_i = k), \\ M_{Y,k}^* &:= \frac{1}{n} \sum_{i=1}^n Y_i \mathbb{I}(\tilde{Z}_i = k), & M_{Y^2,k}^* &:= \frac{1}{n} \sum_{i=1}^n Y_i^2 \mathbb{I}(\tilde{Z}_i = k), \end{aligned}$$

$k = 1, \dots, K$.

Because of the i.i.d. nature of $(X_1, Y_1, \tilde{Z}_1), \dots, (X_n, Y_n, \tilde{Z}_n)$, following the proof of Theorem 3.1, we can derive the joint asymptotic distribution of $\hat{\boldsymbol{\mu}}^*$, which we denote as

$$\sqrt{n}(\hat{\boldsymbol{\mu}}^* - \boldsymbol{\mu}) \xrightarrow{d} \mathcal{N}(0, \boldsymbol{\Sigma}), \quad (\text{A.20})$$

where $\boldsymbol{\Sigma}$ has the same form as in (A.5), except that all the notations related to Z under the supervised scenario are now related to \tilde{Z} under the current unsupervised scenario.

Next we will derive the asymptotic distribution of $\hat{\boldsymbol{\mu}}$ based on (A.20). By Theorem 3.3, we have (33): $\hat{\boldsymbol{\beta}}_{k(\mathcal{U})} \rightarrow \boldsymbol{\beta}_{k(\mathcal{U})}$ a.s., $k = 1, \dots, K$. By the definitions of $\hat{\tilde{Z}}_i$ (8), which is determined by (X_i, Y_i) and $\hat{B}_{k(\mathcal{U})} = \{\hat{\boldsymbol{\beta}}_{1(\mathcal{U})}, \dots, \hat{\boldsymbol{\beta}}_{K(\mathcal{U})}\}$, and \tilde{Z}_i (A.19), which is determined by (X_i, Y_i) and $B_{k(\mathcal{U})} = \{\boldsymbol{\beta}_{1(\mathcal{U})}, \dots, \boldsymbol{\beta}_{K(\mathcal{U})}\}$, we have

$$\mathbb{I}(\hat{\tilde{Z}}_i = k) - \mathbb{I}(\tilde{Z}_i = k) \xrightarrow{P} 0, \quad \forall i = 1, 2, \dots \quad (\text{A.21})$$

Hence,

$$\begin{aligned}
(M_k - M_k^*) &= \frac{1}{n} \sum_{i=1}^n \left[\mathbb{I} \left(\widehat{Z}_i = k \right) - \mathbb{I} \left(\widetilde{Z}_i = k \right) \right] \xrightarrow{P} 0, \\
(M_{X,k} - M_{X,k}^*) &= \frac{1}{n} \sum_{i=1}^n X_i \left[\mathbb{I} \left(\widehat{Z}_i = k \right) - \mathbb{I} \left(\widetilde{Z}_i = k \right) \right] \xrightarrow{P} 0, \\
(M_{Y,k} - M_{Y,k}^*) &= \frac{1}{n} \sum_{i=1}^n Y_i \left[\mathbb{I} \left(\widehat{Z}_i = k \right) - \mathbb{I} \left(\widetilde{Z}_i = k \right) \right] \xrightarrow{P} 0, \\
(M_{XY,k} - M_{XY,k}^*) &= \frac{1}{n} \sum_{i=1}^n X_i Y_i \left[\mathbb{I} \left(\widehat{Z}_i = k \right) - \mathbb{I} \left(\widetilde{Z}_i = k \right) \right] \xrightarrow{P} 0, \\
(M_{X^2,k} - M_{X^2,k}^*) &= \frac{1}{n} \sum_{i=1}^n X_i^2 \left[\mathbb{I} \left(\widehat{Z}_i = k \right) - \mathbb{I} \left(\widetilde{Z}_i = k \right) \right] \xrightarrow{P} 0, \\
(M_{Y^2,k} - M_{Y^2,k}^*) &= \frac{1}{n} \sum_{i=1}^n Y_i^2 \left[\mathbb{I} \left(\widehat{Z}_i = k \right) - \mathbb{I} \left(\widetilde{Z}_i = k \right) \right] \xrightarrow{P} 0,
\end{aligned}$$

$k = 1, \dots, K$. That is,

$$(\widehat{\boldsymbol{\mu}} - \widehat{\boldsymbol{\mu}}^*) \xrightarrow{P} \mathbf{0} \tag{A.22}$$

Therefore, given (A.20) and (A.22) and by the Slutsky Theorem, we have the asymptotic distribution of $\widehat{\boldsymbol{\mu}}$ as

$$\sqrt{n} (\widehat{\boldsymbol{\mu}} - \boldsymbol{\mu}) \xrightarrow{d} \mathcal{N}(0, \boldsymbol{\Sigma}). \tag{A.23}$$

Then given (A.23) and by applying Cramer's Theorem (Ferguson, 1996), we can derive the joint asymptotic distribution of $\widehat{\boldsymbol{\theta}}$, which we denote as

$$\sqrt{n} (\widehat{\boldsymbol{\theta}} - \boldsymbol{\theta}) \xrightarrow{d} \mathcal{N}(0, \boldsymbol{\Omega}). \tag{A.24}$$

where $\boldsymbol{\Omega}$ has the same form as in (A.6), except that all the notations related to Z under the supervised scenario are now related to \widetilde{Z} under the current unsupervised scenario.

Finally, given (A.24) and by applying Cramer's Theorem (Ferguson, 1996) again, we can derive the asymptotic distribution of $R_{\mathcal{G}(U)}^2$:

$$\sqrt{n} \left(R_{\mathcal{G}(U)}^2 - \rho_{\mathcal{G}(U)}^2 \right) \xrightarrow{d} \mathcal{N} \left(0, \gamma_{(U)}^2 \right), \tag{A.25}$$

where $\gamma_{(U)}^2$ is defined in (37). The detailed derivation steps follow from the proof of Theorem 3.1.

□

A.7 Proof of Corollary 3.5

Proof. Given Theorem 3.4, the proof of Corollary 3.5 follows from the proof of Corollary 3.5 in A.4. □

B. REAL DATASETS

B.1 *Arabidopsis thaliana* gene expression data

In the application of our generalized R^2 measures to *Arabidopsis thaliana* gene expression analysis, we used four public microarray datasets from the AtGenExpress Consortium (www.arabidopsis.org/portals/expression/microarray/ATGenExpress.jsp), summarized in Table A1.

Dataset	Submission Number	Number of Genes	Sample Size
Oxidation	ME00340	22,657	52
Wounding	ME00330	22,657	60
UV-B light	ME00329	22,657	60
Drought	ME00338	22,657	60

Table A1: Four *Arabidopsis thaliana* microarray gene expression datasets from the AtGenExpress Consortium.

Figures A1-A3 shows pairwise scatterplots of the five FMO genes in Figure 1A colored by each of the four index variables: `condition` (oxidation, wounding, UV-B light, and drought), `treatment` (yes and no), `replicate` (1 and 2), and `tissue` (root and shoot). It is clear that only the `tissue` variable serves as a good index variable for linear dependences.

The processed data and the analysis codes are provided in the “Supplementary Data and Codes” file.

B.2 Single-cell RNA sequencing data

In the application of our generalized R^2 measures to studying the relationships of cell-cycle genes, we used a single-cell RNA sequencing dataset that includes 182 embryonic stem cells (ESCs), which was staged for cell cycle phases (G1, G2M, and S) (Buettner et al., 2015). The data accession number is E-MTAB-2512. For data pre-processing, we imputed the data to correct the excess zero

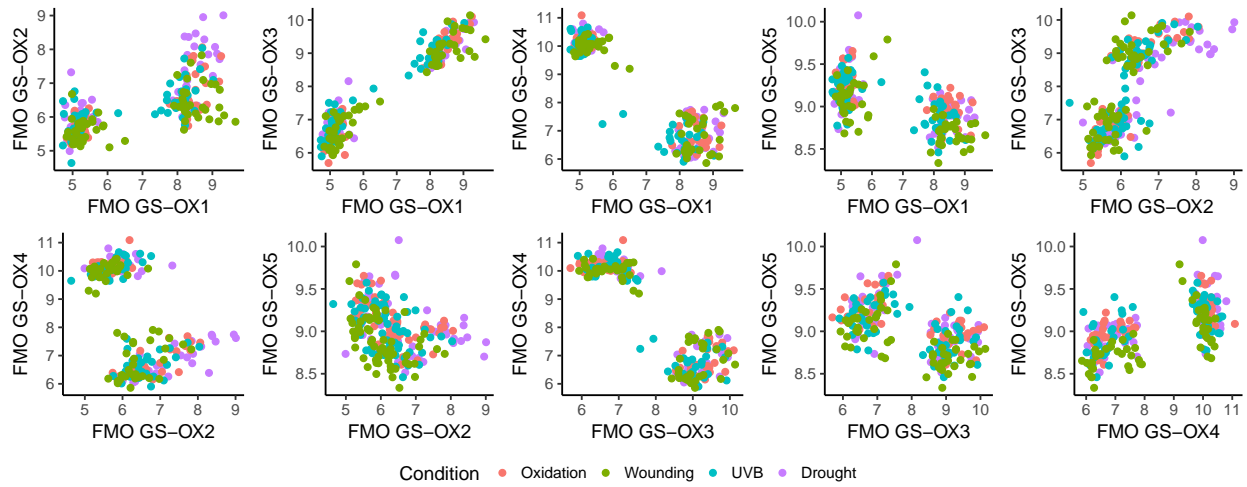


Figure A1: Expression levels of the five Arabidopsis thaliana genes in Figure 1A, with colors marked by the condition variable.

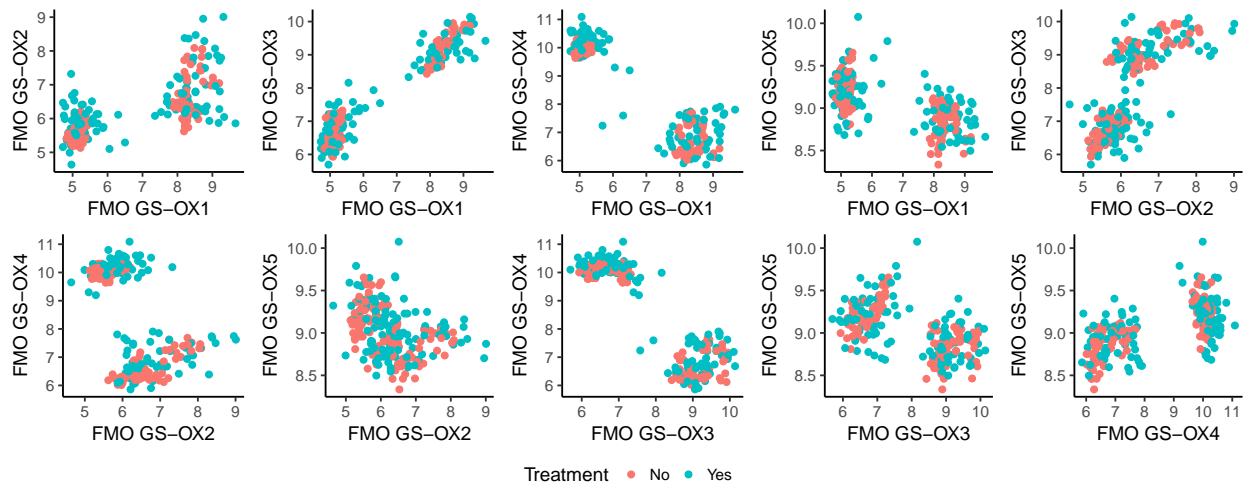


Figure A2: Expression levels of the five Arabidopsis thaliana genes in Figure 1A, with colors marked by the treatment variable.

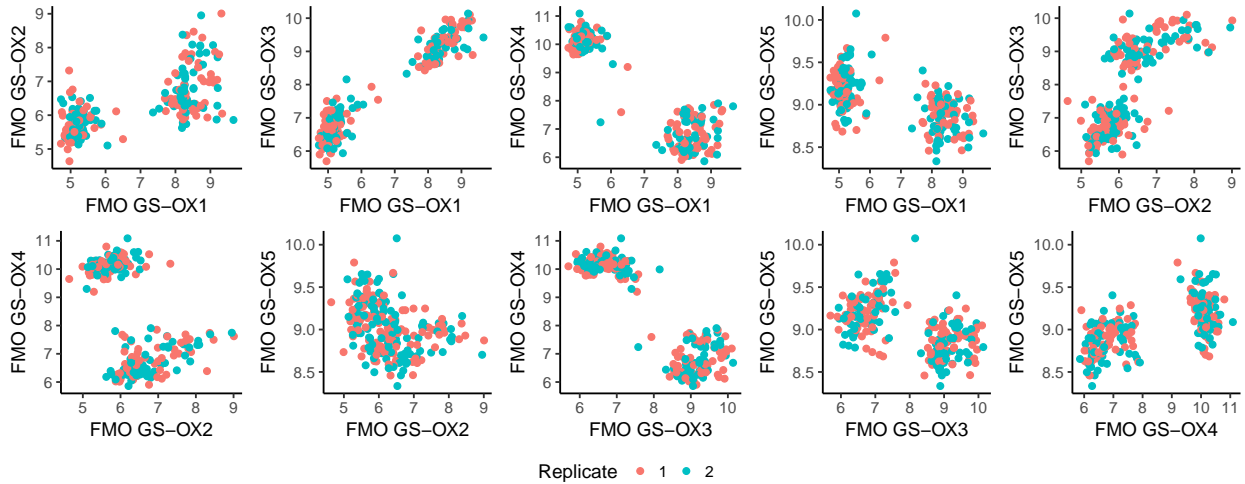


Figure A3: Expression levels of the five *Arabidopsis thaliana* genes in Figure 1A, with colors marked by the `replicate` variable.

values, which are likely false due to technological limitations, using `scImpute v0.0.3` with `Kcluster = 3` and other default parameters (Li and Li, 2018).

The list of cell-cycle genes, the imputed gene expression data, and the analysis codes are provided in the “Supplementary Data and Codes” file.

C. MORE SIMULATION RESULTS

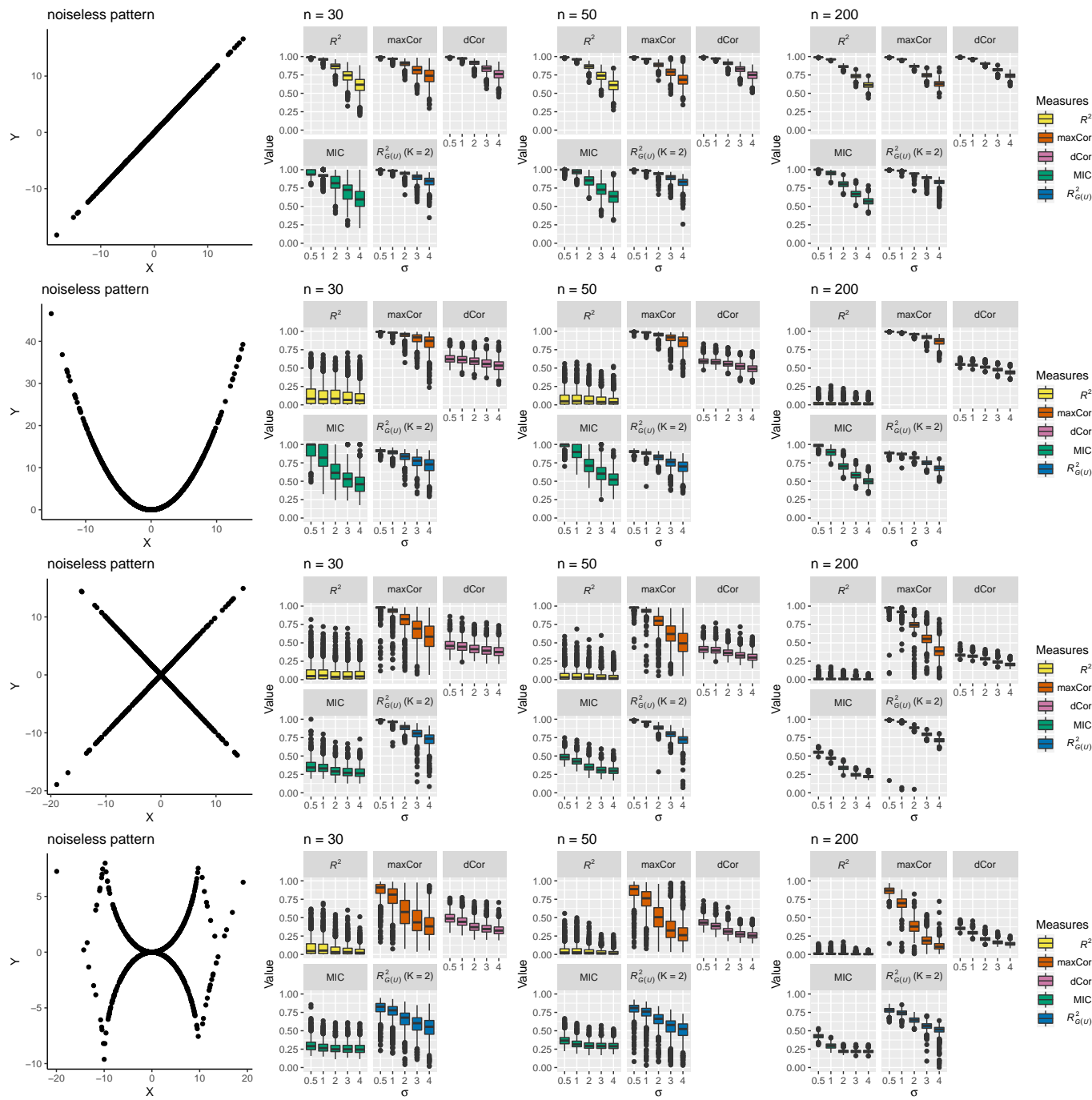


Figure A4: Values of the five measures: squared Pearson correlation (R^2), maximal correlation (maxCor), distance correlation (dCor), maximal information coefficient (MIC), and $R^2_{G(u)}$ with $K = 2$, in 1000 simulations at each sample size n and noise standard deviation σ .